

**Synthesis and Evaluation of Novel 20-HETE formation inhibitors**

by

Ameya Uday Deshpande

B.Pharm, Manipal College of Pharmaceutical Sciences, 2015

Submitted to the Graduate Faculty of  
School of Pharmacy in partial fulfillment  
of the requirements for the degree of  
Master of Science

University of Pittsburgh

2018

UNIVERSITY OF PITTSBURGH

School of Pharmacy

This thesis was presented

by

Ameya Uday Deshpande

It was defended on

July 23, 2018

and approved by

Dr Lee McDermott, Assistant Professor, School of Pharmacy

Dr Prema Iyer, Assistant Professor, School of Pharmacy

Dr Maggie Folan, Director Graduate Program, Pharmaceutical Sciences, School of Pharmacy

Thesis Advisor: Dr Lee McDermott, Assistant Professor, School of Pharmacy

Copyright © by Ameya Uday Deshpande

2018

## Synthesis and Evaluation of Novel 20-HETE formation inhibitors

Ameya Uday Deshpande, B.Pharm

University of Pittsburgh, 2018

20-hydroxyecosatetraenoic acid (20-HETE) is a metabolite of arachidonic acid (AA) formed via CYP4 enzymes and has been shown to have strong vasoconstriction activity in the microvasculature. Epoxyecosatetraenoic acids (EETs) products of the epoxygenation pathway and possess vasodilatory function. Both of these fatty acid metabolites have demonstrated opposite effects in the microvasculature. 20-HETE has been studied *in-vitro* and *in-vivo* with results suggesting a role in secondary brain injury after subarachnoid hemorrhage (SAH) or cardiac arrest (CA). Several molecules, which target the formation of 20-HETE, have been studied and reported in literature such as 1-ABT, 17-ODYA and others. There has been no clinical translation for any of them due to their physicochemical properties, potency and selectivity. Over 15 years ago Taisho disclosed two molecules, both showing excellent potency and selectivity towards 20-HETE-formation inhibition over EET formation. However, these compounds were marred by chemical instability at low pH, poor solubility and a shockingly low  $t_{1/2}$ . Currently, there are no CYP4 inhibitors in the clinic for the purpose of neuroprotection. Through scaffold hopping of compound **8**, a 20-HETE formation inhibitor with poor metabolic stability, novel leads UPMP00010/19 were designed in McDermott lab. These leads have improved stability when compared to compound **8**. Our aim is to further optimize these leads by the synthesis of derivatives with physicochemical properties appropriate for compounds that must act in the brain. As a part of greater optimization effort, we synthesized 24 UPMP00010/19 derivatives and these compounds are the focus of this work. Compounds generated were tested

against a panel of enzymes, which include human liver microsomes (HLM), recombinant CYP4F2 (rCYP4F2), rat liver microsomes (RLM) and rat kidney microsomes (RKM) in the lab of Dr. Samuel Poloyac at the University of Pittsburgh. Compounds with promising potency were taken for further evaluation, which included determination of intrinsic clearance, kinetic solubility and CNS permeability potential. Compounds **21a** showed promising potency ( $IC_{50}=73nM$ ), good HLM stability (92% parent molecule remaining at 30 mins) and high CNS permeability potential (efflux ratio=0.803). Compound **21c** is equipotent ( $IC_{50}=79nM$ ) to **21a** and has good HLM stability (92% parent molecule remaining at 30 mins). **21a** showed very little inhibition of EET formation at the highest concentration tested (3.1% @ 50,000nM). Compounds **21f** and **21h** are particularly attractive molecules as these molecules have excellent results in single point titrations in both human and rat enzyme systems.

Keywords: 20-HETE, Cardiac arrest, subarachnoid hemorrhage, Vasoconstriction, Scaffold-hopping, human liver microsomes, rat liver microsomes, rat kidney microsomes CNS permeability, Kinetic solubility, HLM stability.

## TABLE OF CONTENTS

<b>PREFACE.....</b>	<b>X</b>
<b>1.0 INTRODUCTION.....</b>	<b>1</b>
<b>1.1 EICOSANOIDS AND CYP-450S.....</b>	<b>1</b>
<b>1.2 20-HETE AND EETS: BIOLOGICAL FUNCTION .....</b>	<b>2</b>
<b>1.3 20-HETE AND EETS FORMATION IN THE BRAIN.....</b>	<b>3</b>
<b>1.4 SUBARACHNOID HEMORRHAGE AND 20-HETE .....</b>	<b>4</b>
<b>1.5 CARDIAC ARREST AND 20-HETE .....</b>	<b>5</b>
<b>1.6 20-HETE FORMATION INHIBITORS AND ANTAGONISTS.....</b>	<b>7</b>
<b>1.7 PROPERTIES OF CNS DRUGS .....</b>	<b>10</b>
<b>1.8 20-HETE FORMATION INHIBITORS UPMP00010 AND UPMP00019... </b>	<b>11</b>
<b>2.0 CHEMISTRY .....</b>	<b>16</b>
<b>3.0 RESULTS AND DISCUSSION .....</b>	<b>22</b>
<b>3.1 20-HETE FORMATION INHIBITION IN HLM, RCYP4F2, RLM AND RKM.....</b>	<b>23</b>
<b>3.1.1 DERIVATIVES WITH SIMPLE SUBSTITUENT ON PHENYL MOIETY .....</b>	<b>23</b>
<b>3.1.2 EFFECT OF METHYL SUBSTITUTION ON PYRAZOLE AND EFFECT OF S AS HETEROATOM LINKER.....</b>	<b>26</b>

3.2	KINETIC SOLUBILITY OF POTENT COMPOUNDS.....	27
3.3	HLM STABILITY OF POTENT ANALOGS .....	28
3.4	ASSESSMENT OF CNS PERMEABILITY OF SELECTED COMPOUNDS.....	29
3.5	INHIBITION OF EPOXYGENASE PATHWAY .....	30
4.0	CONCLUSION AND FUTURE DIRECTIONS .....	32
5.0	EXPERIMENTAL SECTION .....	34
5.1	INSTRUMENTATION AND REAGENTS .....	34
5.2	GENERAL PROCEDURE-SYNTHESIS OF N-BOC-4-ARYL DIHYDROPYRIDINE.....	35
5.3	GENERAL PROCEDURE-SYNTHESIS OF N-BOC-4-ARYL PIPERIDINES .....	36
5.4	GENERAL PROCEDURE-SYNTHESIS OF 4-ARYL PIPERIDINES .....	36
5.5	GENERAL PROCEDURE-SYNTHESIS OF 4-ARYL-1-(1H-PYRAZOLE- 5-YL, 4YL) PIPERIDINE, 1-(3-METHYL-1H-PYRAZOLE-4-YL)-4-PHENYL PIPERIDINE, 1-(5-METHYL-1H-PYRAZOLE-3-YL)-4-PHENYL PIPERIDINE, 4- (PHENYLTHIO)-1-(1H-PYRAZOL-5-YL, 4-YL) PIPERIDINE AND 4- (PHENYLSULFONYL)-1-(1H-PYRAZOL-5-YL, 4-YL) PIPERIDINE .....	37
5.6	DATA FOR EACH ANALOG .....	38
APPENDIX A .....		66
APPENDIX B .....		69
BIBLIOGRAPHY .....		118

## LIST OF TABLES

Table 1: Physicochemical properties seen in CNS drugs .....	11
Table 2: Properties of compounds 8, UPMP00010 and UPMP00019.....	15
Table 3: Key physicochemical properties and assay results for novel inhibitors .....	24
Table 4: Potencies of compounds 21e, 20f, 21f and 21h in RLM and RKM .....	26
Table 5: Kinetic solubility of potent compounds.....	28
Table 6: MDR1-MDCK assay results.....	30
Table 7: Inhibition of epoxygenase pathway by 20a and 21a.....	31



## LIST OF FIGURES

Figure 1: AA metabolism pathway .....	2
Figure 2: 20-HETE formation inhibitors/ antagonists .....	9
Figure 3: Rationale for design of Compound 8 and lead UPMP00010 .....	13
Figure 4: Rationale for design of lead UPMP00019 (a) Tautomers of HET0016 (b) Tautomers of UPMP00010 (c) Tautomers of UPMP00019 .....	14
Figure 5: Points of variation on UPMP00010 and potential modifications .....	16
Figure 6: Synthesis of 20a-i, 21a-i, 25a and 26a.....	18
Figure 7: Synthesis of 32a-b and 33a-b .....	20
Figure 8: Inhibitors previously generated in McDermott lab and their IC <sub>50</sub> in HLM.....	23
Figure 9: HLM stability of potent compounds at 30 mins.....	29

## PREFACE

I would like to thank the University of Pittsburgh, School of Pharmacy for granting me the opportunity to pursue my studies. I would like to sincerely thank my advisor Dr. Lee McDermott for giving me an opportunity to be a part of this project. His powerful questioning got me a better hold of the concepts in chemistry as it made me think and dive deeper into the subject. He showed me a streamlined way of dealing with concepts. I must confess, his striving for perfection pushed me hard and I am sure this would help me in the future! I thank Dr. Prema Iyer for patiently teaching me all the pertinent laboratory skills including setting up reactions, work-ups, column chromatography, NMR, IR and LC-MS. She also kept encouraging me in my endeavor in synthesizing molecules for the project. She has been a great sounding board for me all through the work. I would like to thank Dr. Samuel Poloyac for taking the time to help understand the bigger picture, elucidate for me the importance and relevance of this project. I would like to thank Chenxiao Tang and Andrew Haddad for meticulously testing the molecules synthesized by me. I would also like to thank Dr. Larry Verneti for diligently carrying out solubility studies for the molecules synthesized by me.

I would like to thank Dr. Maggie Folan, Lori Altenbough and all graduate students for their kind support during the course of my study. Lastly, I can't thank my parents so very much for believing in me and encouraging me in my quest towards my masters here in the US.

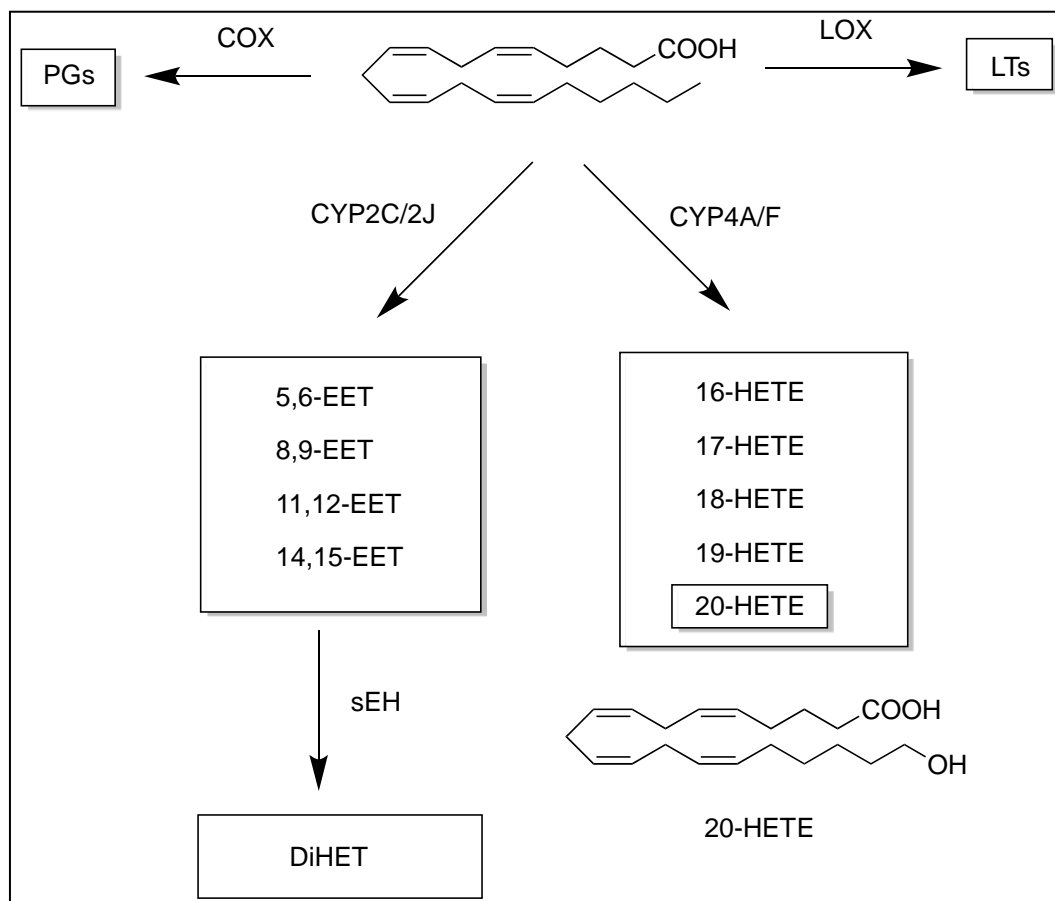


## 1.0 INTRODUCTION

### 1.1 EICOSANOIDS AND CYP-450S

Arachidonic acid (AA), a 20-carbon polyunsaturated fatty acid, is synthesized from linoleic acid in humans<sup>1</sup> and released from the cell membrane by a cytosolic enzyme phospholipase A<sub>2</sub><sup>2</sup>. It is metabolized by three enzymatic routes: cyclooxygenases (COX), lipoxygenases (LOX) and cytochrome P-450s (CYPs). In the COX pathway AA is converted to prostaglandins (PGs) and thromboxanes (TXAs). In the LOX pathway AA is converted to leukotrienes (LTs)<sup>3</sup>. CYP families of enzymes are known as hemoproteins as they contain heme as a co-factor in their catalytic domain<sup>4</sup>. These enzymes are commonly associated with the cell membranes of the endoplasmic reticulum or mitochondria. CYPs like CYP3A4, CYP2D6, and others are critical metabolizing enzymes, which have been characterized in different parts of the body like liver, kidney, and lungs among others and play a role in the metabolic fate of endogenous and exogenous molecules<sup>5</sup>. They catalyze the oxidation of their substrates in the presence of oxygen and NADPH<sup>6</sup>. CYP4s metabolize AA by oxidation of carbon close to the terminal carbon and CYP2s metabolize AA by epoxidation of allylic carbons. The first metabolic route yields 16-, 17-, 18-, 19- and 20-hydroxyecosatetraenoic acid (HETE)<sup>7</sup> whereas epoxidation of AA acid across allylic carbons produces 5,6-, 8,9-, 11,12- and 14,15-epoxyecosatetraenoic acid (EETs)<sup>8</sup>. Recombinant human forms of the enzymes CYP4F3B, CYP4F2, and CYP4A11 have been

shown to have a high catalytic activity of metabolism of AA to 20-HETE<sup>9</sup>. Figure 1 illustrates the metabolic pathways of AA.



**Figure 1: AA metabolism pathway**

## 1.2 20-HETE AND EETS: BIOLOGICAL FUNCTION

The hydroxylation pathway of AA has been well studied. 20-HETE is a major metabolite of AA in liver, kidney, brain and other organs<sup>10</sup>. The majority of 20-HETE formation has been attributed to the CYP4A and CYP4F families<sup>10</sup>. Powell et al. demonstrated in human liver and kidney microsomes that CYP4A11 and CYP4F2 are key enzymes for 20-HETE formation<sup>11</sup>.

Similarly, human recombinant CYP4F3B exhibited a high catalytic activity towards the formation of 20-HETE, when incubated with AA<sup>12</sup>. 20-HETE has been shown to have powerful vasoconstriction activity in renal arteries<sup>10</sup> via inhibition of large conductance calcium-activated potassium channels, resulting in vascular smooth muscle contraction<sup>13</sup>. 20-HETE mediated vasoconstriction is associated with decrease in cerebral blood flow (CBF) and contributes to acute and delayed cerebral vasospasm<sup>14</sup>. EETs, on the other hand, are vasodilator-signaling molecules that have been shown to produce opposite effects to that of 20-HETE. Their formation is linked to AA metabolism by the CYP2J and CYP2C families<sup>15,16,17</sup>. EETs activate large conductance calcium-activated potassium channel and cause vasodilation by hyperpolarization of vascular smooth muscles in renal and cerebral arteries<sup>10,18,19</sup>. EETs can be further metabolized to dihydroxyecosatetraenoic acid (DiHETs) by soluble epoxide hydroxylase (sEH), which has lower vasodilating activity as compared to EETs<sup>2</sup>.

### **1.3 20-HETE AND EETS FORMATION IN THE BRAIN**

Previous studies have reported CYP2C, CYP2J, CYP4F, and CYP4A to be highly expressed in the brain<sup>20,21</sup>. Rat brain arteriolar CYPs incubated with AA catalyzed its conversion to 20-HETE and EETs<sup>22</sup>. 20-HETE has been shown to affect the cerebral blood flow (CBF), and there is a correlation between the levels of 20-HETE and the corresponding increase in transmural pressure<sup>22</sup>. Transformation of radiolabeled AA to 5,6-EETs and 15,16-EETs was observed in rat brain slices<sup>23</sup>. 5,6-EETs when applied to cerebral arteries topically cause approximately 28% vasodilation<sup>23</sup>. 20-HETE and EETs have been detected in human CSF<sup>24</sup> and they have opposite roles in microvascular blood flow regulation. In a review by Huang et al, 20-HETE formation

inhibition and inhibition of EET conversion to DiHET were identified as viable targets to manage ischemic and hemorrhagic stroke mediated brain damage<sup>25</sup>.

#### **1.4 SUBARACHNOID HEMORRHAGE AND 20-HETE**

According to the American Association of Stroke, approximately 795,000 strokes occur in the US every year, with 60% occurring outside of hospital settings<sup>26</sup>. There are two major types of stroke: ischemic (which comprises 87% of total stroke events) and hemorrhagic (which comprises the remaining 13%). Ischemic stroke occurs when there is a decrease in blood flow due to clot formation in the cerebral arteries or when a clot travels through the arteries and reaches the brain. Hemorrhagic stroke refers to an event where bleeding into the brain occurs due to rupturing of a diseased blood vessel or an aneurysm.

Aneurysmal subarachnoid hemorrhage (aSAH) is a type of hemorrhagic stroke and accounts for 30,000 cases associated with aneurysms every year resulting in a significant number of fatalities and morbidity<sup>27</sup>. Early brain injury (EBI) occurs within 72 hours of initial ictus<sup>28</sup>. After SAH, several events occur: increased intracranial pressure (ICP), edema, and increased blood-brain barrier permeability<sup>28</sup>. Uncontrolled increase in ICP can lead to an increased risk of patient mortality<sup>29</sup>.

Vasospasm, a narrowing of cerebral blood vessels has been observed in a majority of SAH patients via angiography<sup>27</sup> and commonly occurs between the 3<sup>rd</sup> and 14<sup>th</sup>-day, post SAH event is a common cause of morbidity<sup>27</sup>. A study in patients with SAH elucidated that increase in ICP was associated with vasospasm detected via transcranial doppler sonography<sup>30</sup>. Association

of vasospasm with a decrease in CBF and cerebral perfusion was also established in a study involving patients suffering from SAH<sup>31</sup>.

Delayed cerebral ischemia (DCI) refers to neurological deficits following the EBI phase<sup>32</sup>. DCI was earlier thought to have a causal relationship with vasospasm. Vasospasm, even though it shows an association with DCI, does not appear to be the only cause of it. This was observed in a clinical trial where an endothelin-1 receptor antagonist did not result in a significant decrease in DCI even though it reduced moderate to severe vasospasm<sup>33</sup>.

In a study conducted in SAH patients, an elevated level of 20-HETE was found in cerebrospinal fluid (CSF)<sup>34</sup>. A study conducted in aSAH patients, suggests that increased levels of 20-HETE are a determinant of severity of injury and DCI<sup>35</sup>. In a study in rats, it was shown that levels of 20-HETE increase following SAH and pretreatment with HET0016, a 20-HETE-formation inhibitor, attenuated the decrease in CBF following SAH<sup>36</sup>. In another rat study, pretreatment with TS-011, a 20-HETE-formation inhibitor had similar outcomes<sup>37</sup>. These studies in humans and animals suggest that inhibition of 20-HETE formation in the clinical setting may improve outcomes.

## **1.5 CARDIAC ARREST AND 20-HETE**

Cardiac arrest (CA) refers to an event when the heart loses its ability to pump sufficient supply to the body. Several comorbid conditions associated with cardiac arrest include atherosclerosis, obesity, coronary heart disease, diabetes, and others. CA leads to a drastic decrease in blood flow to multiple organ systems with the brain being susceptible, as it requires a constant supply of oxygen and glucose to maintain function. A significant time lapse between



cardiac arrest and resuscitation will essentially translate into a neuronal insult. Following resuscitation, there is an alteration in cerebral blood flow<sup>38</sup>. There is a short phase of global hyperemia followed by a phase of reduced blood flow that may last for hours or even days post-resuscitation<sup>38</sup>. This extended periods of reduced blood flow, termed delayed hypoperfusion, is associated with poor neurocognitive outcomes after resuscitation<sup>39</sup>.

A multitude of events occur after the restoration of CBF and reperfusion after resuscitation from CA. There is excitotoxicity due to the release of glutamate that causes neuronal depolarization leading to loss of calcium homeostasis<sup>40</sup>. Increased reactive oxygen species (ROS), mitochondrial dysfunction and activation of apoptosis also occur<sup>41</sup>. These events have been shown to be contributing factors to secondary brain injury after reperfusion after CA<sup>42,43</sup>.

Rat models of CA suggest that after resuscitation levels of 20-HETE increase in the cortical and subcortical region of the brain<sup>44</sup>. As mentioned, 20-HETE is a vasoconstrictor, and an increase in 20-HETE levels decrease CBF leading to hypoperfusion, and secondary brain injury. Administration of HET0016, a 20-HETE-formation inhibitor, has been shown to improve cerebral perfusion and reduce neurological deficits in rats after CA<sup>44</sup>. Treatment with HET0016 also showed neuroprotection in a neonatal piglet CA model<sup>45</sup>.

The available data suggest that, as in SAH, targeting 20-HETE formation may be an effective strategy for mitigating secondary brain injury after CA.

## 1.6 20-HETE FORMATION INHIBITORS AND ANTAGONISTS

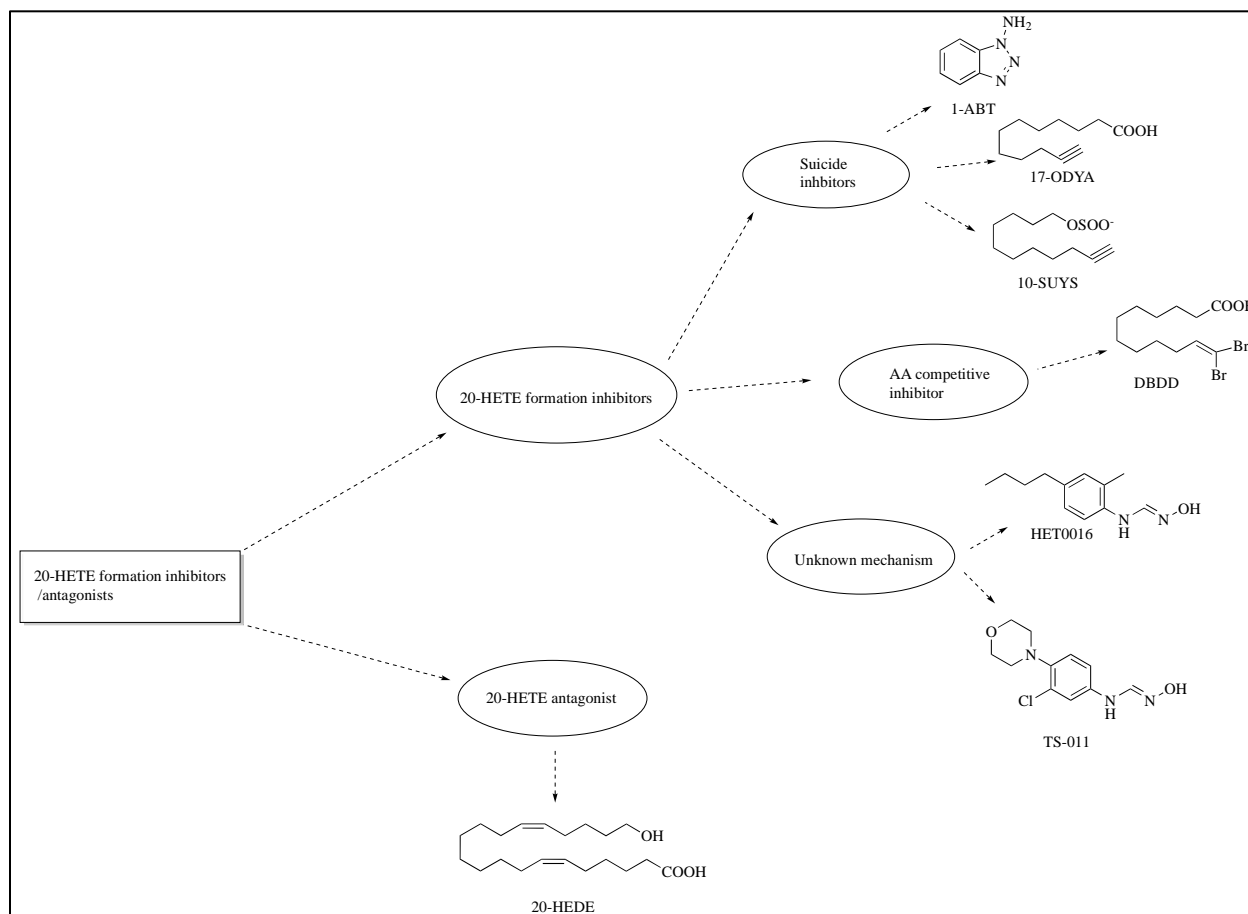
Much research has been carried out to identify molecules that can inhibit the 20-HETE formation or antagonize its action. Structures of selected inhibitors are represented in Figure 2. 1-aminobenzotriazole (1-ABT), a suicide inhibitor, which alkylates heme residue via a benzyne metabolite<sup>46</sup>, was shown to inhibit renal arachidonic acid metabolism to 20-HETE in spontaneously hypertensive rats<sup>47</sup>. Octadec-17-ynoic acid (17-ODYA) inhibited the formation of 20-HETE, EETs and DiHETs in rat renal microsomes with an  $IC_{50}$  100nM<sup>48</sup>. Undec-10-yn-1-yl sulfate (10-SUYS) also inhibited the formation of 20-HETE in rat renal microsomes<sup>49</sup>. 12,12-dibromododec-11-enoic acid (DBDD), a competitive inhibitor of arachidonic acid, showed inhibition of 20-HETE formation in rat renal microsome with an  $IC_{50}$  of 2 $\mu$ M<sup>50</sup>. Lastly, (6Z, 15Z)-20-hydroxyicosa-6, 15-dienoic acid (20-HEDE), a competitive inhibitor of 20-HETE, attenuated its activity when tested *in-vitro* on isolated cerebral arteries<sup>51</sup>. These compounds have several drawbacks. 1-ABT inhibits the formation of both 20-HETE, EETs and also inhibits important xenobiotic metabolizing enzyme, hence lacks selectivity. Compounds 17-ODYA, 10-SUYS, and DBDD based on their structure, have physicochemical liabilities such as high lipophilicity, increased number of rotatable bonds and low CNS penetration. Additionally, these compounds have low potency and some of them lack selectivity towards the inhibition of hydroxylation pathway over the epoxidation pathway.

Taisho Pharmaceuticals was first to disclose two molecules with formamidine moieties HET0016 and TS-011, with promising activities. These compounds have demonstrated good potency and selectivity towards inhibition of formation of 20-HETE over EETs. For example, HET0016 has been reported to have an  $IC_{50}$  value of 8.9nM against 20-HETE formation in human renal microsomal enzymes while its  $IC_{50}$  against recombinant xenobiotic metabolizing

enzymes CYP2C9, CYP2D6 and CYP3A4 is reported to be 3.3, 83.9 and 71.0 $\mu$ M respectively<sup>52</sup>. Its inhibition of EET formation, in rat renal microsomes, was reported to have an IC<sub>50</sub> of 2800nM<sup>53</sup>. As discussed earlier, HET0016 was shown to afford neuroprotection in animal models of SAH and CA<sup>36,44,45</sup>. HET0016, although it displays great potency and selectivity towards 20-HETE formation inhibition, was shown to have a short T<sub>1/2</sub> (< 60 minutes) in rats, poor solubility, and poor stability at a relatively low pH required for increasing its solubility<sup>54,55</sup>.

The second compound, TS-011, containing a morpholine group instead of an n-butyl group seen in HET0016 also showed excellent activity and selectivity towards inhibition of 20-HETE formation. It was shown to have an IC<sub>50</sub> of 9.19nM against 20-HETE formation in rat renal microsomes, no effects on EET formation or the activities of CYP2C9, CYP2C19, CYP2D6 and CYP3A4 up to a concentration of 100 $\mu$ M<sup>37</sup>. TS-011 has better solubility than HET0016, but unfortunately an even shorter T<sub>1/2</sub> (< 10 mins)<sup>37</sup>.

DDMS and DPMS are two compounds, which bear structural similarity to DBDD and can be viewed as its derivatives. However, they have low potencies IC<sub>50</sub> of 2 $\mu$ M and 31 $\mu$ M against 20-HETE formation in rat renal microsomes and have similar physicochemical liabilities as DBDD<sup>50</sup>.



**Figure 2: 20-HETE formation inhibitors/ antagonists (1) 1-ABT: 1-aminobenzotriazole; (2) 17-ODYA: octadec-17-ynoic acid; (3) 10-SUYS: undec-10-yn-1-yl sulfate; (4) DBDD: 12,12-dibromododec-11-enoic acid; (5) HET0016: *N*-(4-butyl-2-methylphenyl)-*N'*-hydroxyformimidamide; (6) TS-011: *N'*-hydroxy-*N*-(4-morpholinophenyl) formimidamide; (7) 20-HEDE: (6*Z*,15*Z*)-20-hydroxyicosa-6,15-dienoic acid**

None of the available inhibitors have reached the clinical trials. This is not surprising as available agents have physicochemical and pharmacological limitations that make them unsuitable for clinical advancement as neuroprotectants. In that regard, for success in the clinic, the design of novel 20-HETE formation inhibitors must overcome the liabilities of current inhibitors, and take into account the physicochemical properties often seen in well absorbed and CNS active drugs.

## 1.7 PROPERTIES OF CNS DRUGS

Drug-like properties refer to the physicochemical characteristics of molecules, which would allow for their proper absorption, distribution, metabolism, and elimination (ADME). Lipinski described the 'rule of 5' after carefully assessing physicochemical properties and activities of a dataset of select compounds from the World Drug Index (WDI) which contains over 50,000 drugs either in the market or clinical trials. According to the rule of 5, for oral absorption, a compound's molecular weight should be less than 500 Daltons, its number of hydrogen bond donor (HBD) atoms (OH and NH) should no more than 5, its number of hydrogen bond acceptor (HBA) atoms should be no more than 10 (O and N) and its partition coefficient (log P) should be not greater than 5<sup>56</sup>. Aside from the properties mentioned above, some additional properties and factors influence oral absorption. According to the Veber rule, compounds with 10 or fewer rotatable bonds and polar surface area no greater than 140 Å<sup>2</sup> have a better prediction of oral absorption. To be effective as neuroprotectants, 20-HETE formation inhibitors must be able to cross the blood-brain barrier (BBB), the interface between the brain and its periphery. The BBB is a physical, transport, metabolic and immunologic barrier, which allows passage of select molecules by passive diffusion or active transport<sup>57</sup>. An article by Pajouhesh et al. compiled various literature studies that aimed to understand physicochemical properties of drugs and their co-relation with good CNS permeability<sup>58</sup>. The studies compiled suggest that good CNS permeability is often associated with the common physicochemical properties and value ranges shown in Table 1.

**Table 1: Physicochemical properties seen in CNS drugs**

Partition co-efficient (Log P)	< 5
Molecular weight (M.W)	< 450
Polar Surface Area (PSA)	< 70 Å <sup>2</sup>
Number of rotatable bonds (NRB)	< 8
Hydrogen bond donors (HBD)	< 3
Hydrogen bond acceptors (HBA)	< 7

The key objective in our lab is the design and optimization of novel 20-HETE formation inhibitors, which show selective and effective inhibition of 20-HETE formation and which, by design, have physicochemical properties that will allow them to cross the BBB.

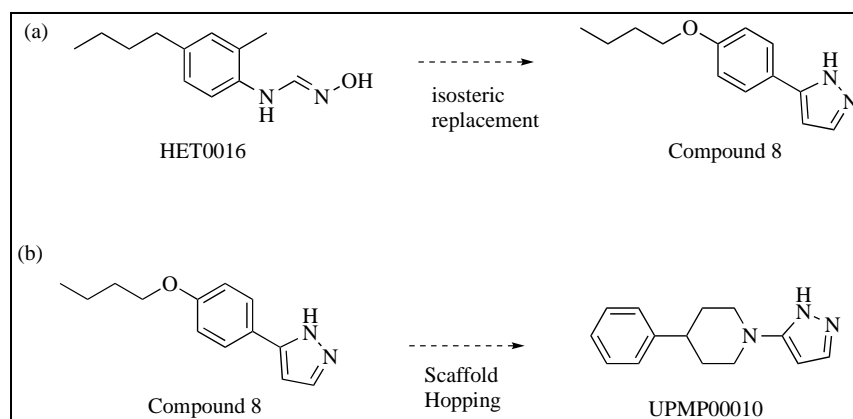
## **1.8 20-HETE FORMATION INHIBITORS UPMP00010 AND UPMP00019**

As discussed in section 1.6, HET0016 is a potent 20-HETE-formation inhibitor disclosed by Taisho pharmaceuticals. Although it has good potency and selectivity, it had a short half-life ( $T_{1/2} < 60$  minutes), which has been attributed to its formamidine moiety. According to X-rays of formamidine containing molecules, formamidines can be internally hydrogen bonded and hence, can exist in cis-configuration that resembles 1,3-azoles<sup>59</sup>. As mentioned earlier, HET0016 also has poor solubility in neutral pH. Under acidic pH, its solubility can be improved but to the detriment of its stability<sup>55</sup>. At a pH of 4, 56% of the compound is degraded within 24 hours<sup>55</sup>. In an attempt to mitigate these limitations, scientists at Taisho Pharmaceuticals initiated a search for an isosteric replacement for the formamidine group<sup>55</sup>. They replaced the formamidine group with

imidazole, pyridine, and pyrazole, among other heterocycles. Some of the analogs generated in this effort showed good activity towards inhibition of 20-HETE formation in human renal microsomes but they also inhibited xenobiotic CYPs<sup>55</sup>. Compound **8**, shown in Figure 3, was one of the compounds generated in this effort. This compound contained pyrazole as a replacement for the formamidine moiety, and was shown to have very good selectivity and potency toward inhibition of formation of 20-HETE formation with an IC<sub>50</sub> of 23nM in human renal microsomes<sup>55</sup>. This compound was stable in acidic pH and more soluble than HET0016 as a freebase or a mesylate salt<sup>55</sup>. Despite this improvement, compound **8** suffers from high intrinsic clearance. Stability testing in Dr. Samuel Poloyac's lab at the University of Pittsburgh showed that upon incubation with human liver microsomes for 30 mins, only 35% of the parent compound remained. Despite its shortcomings, compound **8** was viewed as an attractive starting point for a new scaffold design in Dr. McDermott's lab, where lead compound UPMP00010 was designed via scaffold hopping.

Scaffold hopping is an approach used in medicinal chemistry to design new scaffolds by using molecules with proven biological potential as a template. Through scaffold hopping, entirely new compound structures are generated that are dissimilar from the parent compound, but with the ability to maintain similar interactions as the parent in 3D space.<sup>60</sup> This technique has been historically used to improve physicochemical properties of compounds along with their potencies. Scaffold hopping of compound **8** to lead compound UPMP00010 involved replacement of the aliphatic tail in **8** with an aromatic phenyl and the replacement of the benzene ring in **8** with a piperidine moiety (Figure 3). This latter replacement was thought to be beneficial for solubility since it could alter pKa of the pyrazole group and yield non-planar compounds that

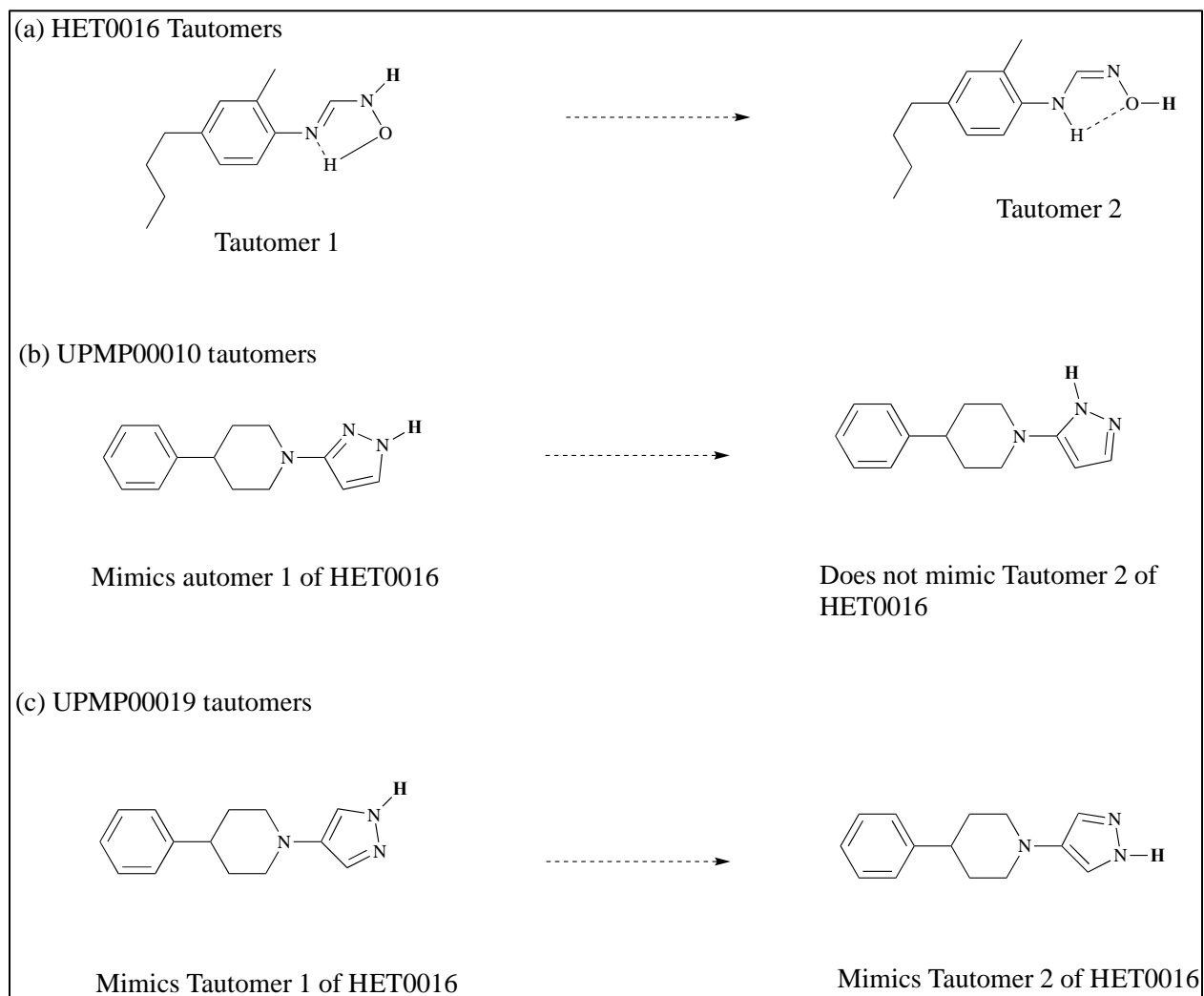
may not pack well in a crystal lattice. UPMP00010 has good potency ( $IC_{50}=443\mu M$ ), excellent solubility and better intrinsic clearance, in comparison to compound **8** (Table 2).



**Figure 3: Rationale for design of Compound 8 and lead UPMP00010**

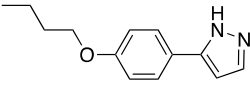
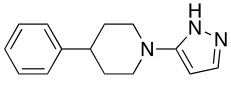
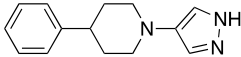
In an attempt to improve potency by better mimicking the tautomeric forms of HET0016 (Figure 4), the point of connection of the phenylpiperidine and pyrazole moieties of UPMP00010 was shifted from the 3<sup>rd</sup> to 4<sup>th</sup> position to produce lead compound UPMP00019. UPMP00019 has much-improved potency towards inhibition of 20-HETE formation in human liver microsomes ( $IC_{50}=187\mu M$ ) than UPMP00010 ( $443\mu M$ ). Also, like UPMP00010, it has excellent metabolic stability. UPMP00010 and UPMP00019 both have physicochemical property values well within the range desirable (Table 2) for CNS acting compounds.





**Figure 4: Rationale for design of lead UPMP00019 (a) Tautomers of HET0016 (b) Tautomers of UPMP00010 (c) Tautomers of UPMP00019**

**Table 2: Properties of compounds 8, UPMP00010 and UPMP00019**

Compound	Structure	Log P	PSA	M.W	Kinetic solubility ( $\mu\text{M}$ )	HLM stability
8		3.0	37.9	216.28	333	35%
UPMP00010		2.7	31.9	227.31	>600	91%
UPMP00019		2.7	31.9	227.31	121	100%

This thesis describes our efforts to expand and understand structural activity relationships (SAR) around the lead compounds UPMP00010/19.

## 2.0 CHEMISTRY

### UPMP00010/19 points of variation and synthesis of derivatives

UPMP00010/19 have 4 points of variation that are structural elements that can be changed in the pursuit of novel derivatives (Figure 5).

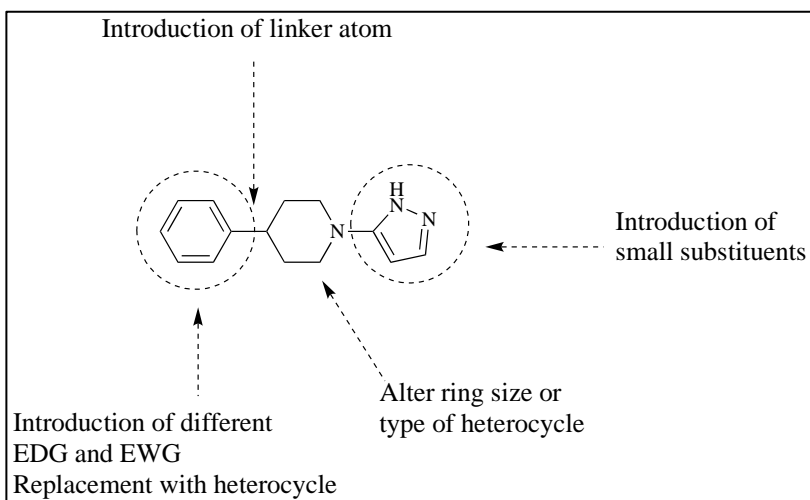
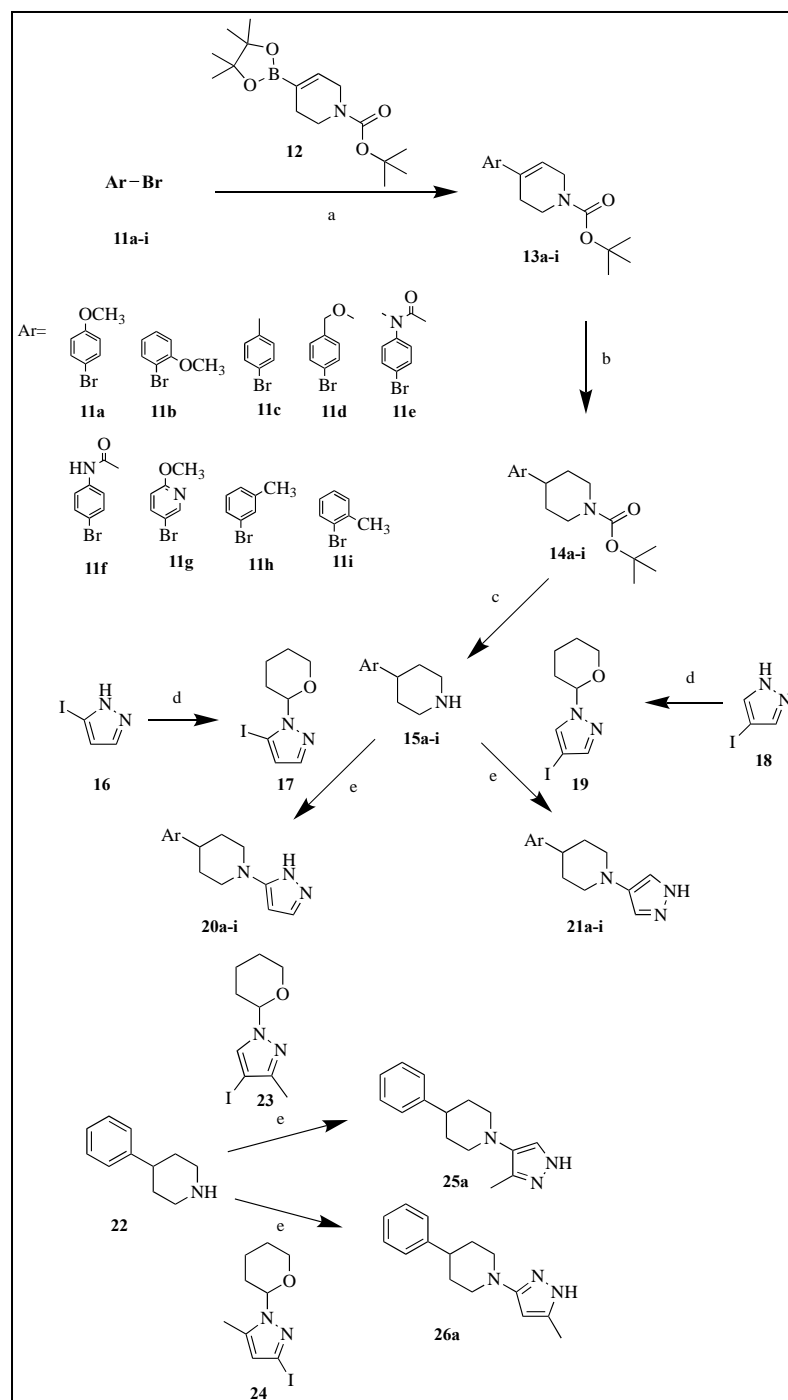


Figure 5: Points of variation on UPMP00010 and potential modifications

It is evident from the Figure 5 that available points of variation allow for the synthesis of a high number of putative derivatives. This work is focused on the synthesis of a subset of the available possibilities. The modifications on a UPMP00010/19 structure that were made in this work are:

- 1) Introduction of electron donating groups [EDG:  $-\text{OCH}_3$ ,  $-\text{CH}_3$ ,  $\text{NHCOCH}_3$ ,  $\text{N}(\text{Me})\text{COCH}_3$ ] and the introduction of a methoxy methyl ( $-\text{CH}_2\text{OCH}_3$ ) group on the phenyl ring;
- 2) Replacement of the phenyl ring with an N-atom containing heterocyclic ring (pyridine);
- 3) Introduction of a small substituent on the pyrazole ring ( $-\text{CH}_3$ );
- 4) Introduction of heteroatom linker (S);

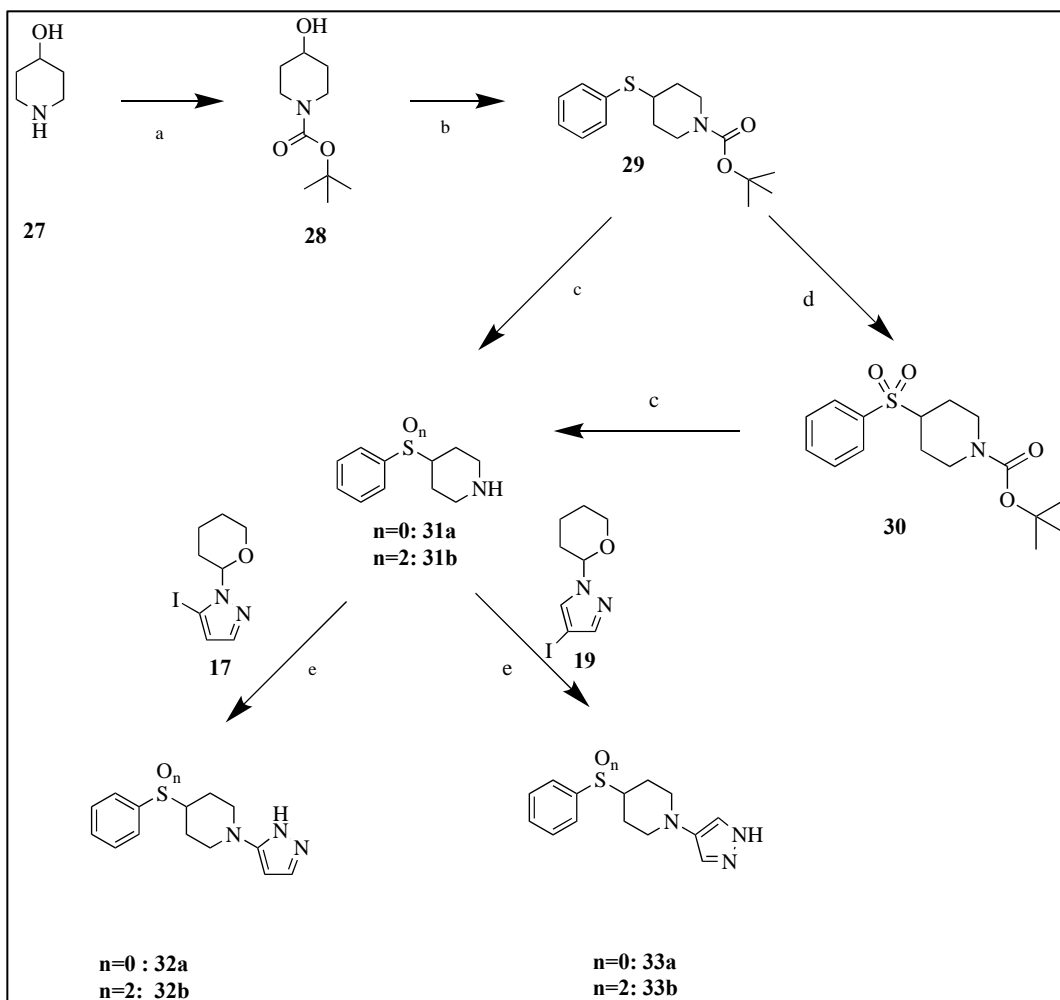
Table 3 and Figures 6 and 7 show derivatives synthesized in this work and the synthetic routes followed to obtain them.



**Figure 6: Synthesis of 20a-i, 21a-i, 25a and 26a - Reagents and conditions (a) PdCl<sub>2</sub>(dppf), K<sub>2</sub>CO<sub>3</sub>, DMF, 80°C (b) 10% Pd/C, H<sub>2</sub>, 1 atm (c) 4N HCl in dioxane (d) PTSA.H<sub>2</sub>O, 3,4-dihydro-2H-pyran (e) CuI, K<sub>2</sub>CO<sub>3</sub>, L-proline, DMSO, 90°C, then 4N HCl in dioxane**

Compounds **20a-i**, **21a-i**, **25a** and **26a** were synthesized via the CuI/proline coupling of aryl piperidines **15a-i** and **22** with THP protected iodopyrazoles **17**, **19**, **23** and **24** followed by THP deprotection of the corresponding coupling products with 4N HCl in dioxane<sup>61,62</sup> (Figure 6).

The 4-arylpiperidines **15a-i** used in these couplings were synthesized in a 3 step sequence that involved Suzuki coupling of commercially available boronate **12** with aryl bromides **11a-i** to afford intermediates **13a-i**, a H<sub>2</sub> Pd/C double bond reduction and then BOC deprotection with 4N HCl in dioxane<sup>63</sup>. THP protected 3-iodo and 4-iodopyrazoles **17** and **19** were synthesized via THP protection of commercially available iodopyrazoles **16** and **18** using 0.1 equivalents of PTSA.H<sub>2</sub>O and 1.2 equivalents of 3,4-dihydro-2H-pyran. THP protected 4-iodo-3-methyl and 3-iodo-5-methyl pyrazoles **23** and **24** were prepared in the same manner as **17** and **19**.



**Figure 7: Synthesis of 32a-b and 33a-b, Reagents and conditions (a) Boc<sub>2</sub>O, DCM (b) MsCl, Et<sub>3</sub>N, DMF, Ph-SH, K<sub>2</sub>CO<sub>3</sub>, DMF (c) 4N HCl in dioxane (d) mCPBA, DCM (e) CuI, K<sub>2</sub>CO<sub>3</sub>, L-proline, DMSO, 90°C, then 4N HCl in dioxane**

Synthesis of **32a-b** and **33a-b** was started with 4-hydroxy-N-BOC piperidine (**28**), which was prepared according to literature from 4-hydroxy piperidine and di-tert-butyl carbonate. Treatment of **28** with mesyl chloride to obtain the corresponding mesylate intermediate, followed by treatment with thiobenzene that led to the 4-thiobenzene-N-BOC protected piperidine intermediate **29**<sup>64</sup>. This N-BOC protected intermediate was then subjected to BOC-deprotection to obtain **31a**. Compound **31a** was coupled with THP protected 3-iodo and 4-iodopyrazoles **17**

and **19** via CuI/proline coupling to obtain the corresponding coupling intermediates, which were then subjected to THP deprotection by 4N HCl in dioxane to afford **32a** and **33a**.

Oxidation of intermediate **29** with meta-chloroperbenzoic acid in methylene chloride for 2 hours, afforded sulfone **30**<sup>65</sup>. Intermediate **30** was subjected to BOC deprotection to obtain piperidine derivative **31b**. **31b** was then converted to compounds **32b** and **33b** in the same manner as the sulfides **32a** and **33a**.



### 3.0 RESULTS AND DISCUSSION

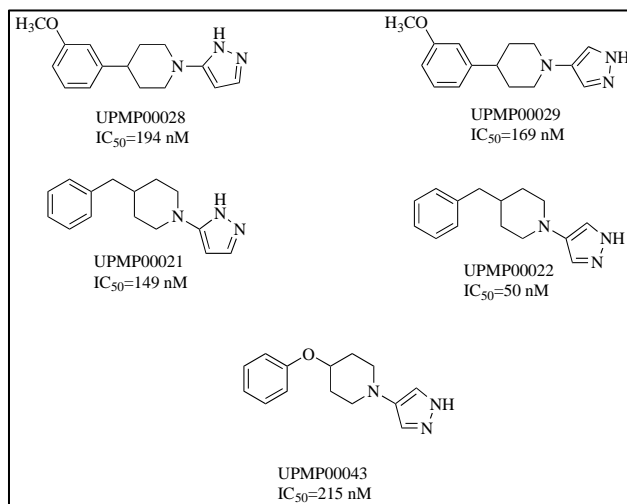
The potential of our molecules towards inhibition of 20-HETE formation was tested *in-vitro* in the lab of Dr. Samuel Poloyac at the University of Pittsburgh. As the first screen, compounds were tested for 20-HETE formation inhibition at 500nM concentration in human liver microsomes (HLM), human recombinant CYP4F2 (rCYP4F2), rat liver microsomes (RLM) and rat kidney microsomes (RKM). The objective of testing against rCYP4F2 as well as human and rat microsomal preparations was to have a better assessment of the activity of our compounds and to understand possible interspecies potency variabilities and their drivers.

Compounds which could inhibit 20-HETE formation by 50% or greater at 500nM concentration in HLM or rCYP4F2 assay were considered further for IC<sub>50</sub> determination and/or kinetic solubility measurement. Promising compounds were then considered for epoxygenase pathway inhibition (EET formation inhibition) assessment, and/or assessment for BBB penetration potential in an MDR-1-MDCK assay.

### 3.1 20-HETE FORMATION INHIBITION IN HLM, RCYP4F2, RLM AND RKM

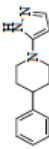
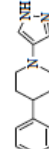
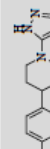
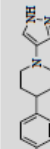
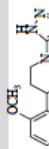
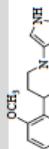
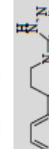







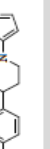
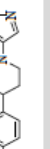
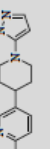
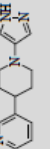

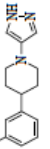


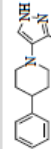
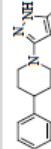
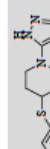
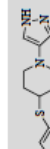
#### 3.1.1 DERIVATIVES WITH SIMPLE SUBSTITUENT ON PHENYL MOIETY

Previous work in our lab showed that compounds UPMP00028/29, which have a simple meta-methoxy substitution (OMe) had good potency against 20-HETE formation (Figure 8). To expand the SAR around these compounds we prepared compounds **20a**, **21a**, **20b**, and **21b**, which had methoxy substituent in the para and ortho positions. As seen in table 3, **20a** and **21a** showed greater than 50% inhibition of 20-HETE formation in HLM at 500nM and their IC<sub>50</sub> were better than the IC<sub>50</sub> of the leads UPMP00010/19 and the IC<sub>50</sub> of UPMP00028/29 (Table 3, Figure 8). Compounds **20b** and **21b** had little to no activity in HLM and rCYP4F2 assay.



**Figure 8: Inhibitors previously generated in McDermott lab and their IC<sub>50</sub> in HLM**

**Table 3: Key physicochemical properties and assay results for novel inhibitors**

No	Structure	M.W	Log P	PSA	HLM	rCYP4F2 IC50 (nM)	No	Structure	M.W	Log P	PSA	HLM	rCYP4F2 IC50 (nM)
10		227.31	2.7	31.9	47.4	ND	19		227.31	2.7	31.9	78.8	ND
20a		257.33	2.59	41.15	72.3	41.4	21a		257.33	2.5	41.15	73.1	67.7
20b		257.33	3.09	41.15	8.8	2	21b		257.33	2.5	41.15	0	0
20c		241.33	3.26	31.92	67.4	70.8	21c		241.33	3.17	31.92	73.8	79.9
20d		271.36	3.13	41.15	56.4	67.8	21d		271.36	2.53	41.15	71.7	81.7
20e		298.38	1.85	53.23	20	14	21e		298.38	1.76	52.23	75	58
20f		284.36	1.98	61.02	60	55	21f		284.36	1.89	61.02	86	95
20g		258.32	1.97	54.04	35	44	21g		258.32	1.88	54.04	59	67
20h		241.33	3.26	31.92	72	69	21h		241.33	3.17	31.92	80	86
20i		241.33	3.26	31.92	20	20	21i		241.33	3.17	31.92	46	61
25a		241.33	2.79	31.92	0	31.9	26a		241.33	3.45	31.92	0	22.3
32a		259.37	2.71	31.91	6	22.7	33a		259.37	2.62	31.92	65.8	75.9
32b		291.37	1.43	66.06	32	0	33b		291.37	1.37	66.06	5	28

M.W- Molecular weight, Log P- Partition coefficient; PSA- Polar surface area; HLM-% inhibition in Human liver microsomes @ 500 nM; rCYP4F2- % inhibition in recombinant CYP4F2 @ 500 nM; IC50 (nM)- in HLM; ND- Not done; TBD-To be determined; 10-lead UPMP00010; 19-lead UPMP00010

To ascertain the effects of a simple methyl substituent, compounds **20c**, **21c**, **20h-i**, and **21h-i** were prepared. Compounds **20c** and **21c** are practically equipotent with their methoxy counterparts (Table 3, HLM IC<sub>50</sub> 110nM and 79nM respectively). The currently available data (20-HETE formation inhibition at 500nM) for **20h-i** and **21h-i** suggests that methyl group in the meta position does not seem to affect potency, while methyl group in ortho position appears to reduce potency.

Extending the methoxy group of **20a** and **21a** away from the phenyl ring moiety by one carbon (Table 3, compounds **20d** and **21d**) lowers potency, as compared to their parent compounds.

Compounds **20g** and **21g** were prepared in order to assess the effect of substituting a carbon next to OMe group in **20a** and **21a** with a N-atom. However, the result available at this time (% inhibition of 20-HETE formation, Table 3) suggests that this substitution does not offer overall improvement in potency.

As a means to expand and understand the SAR further, we pursued the synthesis of compounds **20e-f** and **21e-f** that contain an acetamide group at the para position of phenyl moiety. The available data seems to suggest that acetamide substitution is tolerated with the exception of compound **20e**. Compounds **21e** and **21f** show good potency (Table 3). The available data (Table 3) shows that compounds **20f** and **21f** are far better in the single point titration (HLM and rCYP4F2) in comparison to **21e**.

The data in Table 3 suggests that there is a potency trend associated with the connection location of aryl piperidine moiety with the pyrazole ring. A pairwise comparison between derivatives with the same arylpiperidine moieties overall, suggests that 4-pyrazole derivatives are generally more potent than the 3-pyrazole derivatives.

Aside from testing in HLM and rCYP4F2 derivatives, **20a-i** and **21a-i** were assessed for their activity in RLM and RKM at the concentration of 500nM. This testing showed that most derivatives in the set had little to no activity for inhibition of 20-HETE formation in these preparations. Exceptions were compounds **21e**, **20f**, **21f** and **21h**, which had activity in both human and rat microsomal preparations (Tables 3 and 4).

**Table 4: Potencies of compounds 21e, 20f, 21f and 21h in RLM and RKM**

No	% Inhibition in RLM at 500nM	% Inhibition in RKM at 500nM
<b>21e</b>	52	43
<b>20f</b>	38	7
<b>21f</b>	37	40
<b>21h</b>	44	36

### **3.1.2 EFFECT OF METHYL SUBSTITUTION ON PYRAZOLE AND EFFECT OF S AS HETEROATOM LINKER**

Compounds **25a** and **26a** were made in order to assess the effects of small methyl substitution on pyrazole ring on activity. Testing of these compounds in HLM and rCYP4F2 showed that such substitution is quite unfavorable for activity (Table 3).

Data from our lab suggest that UPMP00010/19 derivatives with a methylene linker between the phenyl and the piperidine moiety have improved potency than their parent compounds for 20-HETE formation inhibition in HLM (Figure 8). Data from our lab also

suggests that replacement of methylene with oxygen leads to a reduction in potency (Figure 8). To assess the effect of a sulfur atom on the activity, compounds **32a** and **33a** that have a sulfide linker were made (Table 3). Among these compounds, **33a** showed good 20-HETE formation inhibition in rCYP4F2 and HLM and had an IC<sub>50</sub> of 98nM (Table 3). Replacement of a sulfide linker with a sulfone in molecules **32b** and **33b** on the other hand was detrimental to activity (Table 3). Compounds **25a** and **26a** were also tested in rat microsomal incubates where they showed little to no potency towards inhibition of 20-HETE formation.

### 3.2 KINETIC SOLUBILITY OF POTENT COMPOUNDS

Kinetic solubility measurements of potent compounds were determined by Dr. Larry Verneti at the University of Pittsburgh Drug Discovery Institute. Kinetic solubility involves the addition of DMSO solution of the compound in small increments to an aqueous buffer until the limit of solubility is reached and a precipitate is formed. It determines the concentration preceding the concentration at which precipitation occurs<sup>66</sup>. Kinetic solubility for our potent molecules is shown in Table 5. Solubility data in the table points to the fact that a number of our potent compounds have superior solubility than compound **8** (Table 5). For example, Compounds **20e**, **20f**, **21e**, **21h** and **21i** have a high solubility as their maximum solubility is above 600μM, which is significantly higher than compound **8** (Table 5). Compounds **21g** and **21f** have a solubility of 391μM and 481.8μM, which are also greater than the maximum solubility of compound **8**.

**Table 5: Kinetic solubility of potent compounds**

No	Maximum solubility ( $\mu\text{M}$ )	No	Maximum solubility ( $\mu\text{M}$ )
<b>20a</b>	106	<b>21f</b>	481.8
<b>20c</b>	166	<b>21g</b>	391
<b>20e</b>	> 600	<b>21h</b>	> 600
<b>20f</b>	> 600	<b>21i</b>	> 600
<b>21a</b>	35	<b>33a</b>	96
<b>21c</b>	85	<b>8</b>	333
<b>21e</b>	> 600		

### 3.3 HLM STABILITY OF POTENT ANALOGS

HLM stability provides information about a compound's intrinsic clearance. HLM stability data and assays are extensively used by medicinal chemists during the optimization of leads and provide them with insights on how structural changes on the lead impact their elimination<sup>67</sup>.

A set of derivatives prepared, selected on the basis of  $\text{IC}_{50}$  potency, were tested for metabolic stability in HLM at the lab of Dr. Samuel Poloyac. The result of this testing is shown in Figure 9 and indicate that these compounds have a high metabolic stability than their comparator compound **8** and maintain excellent stability profile of leads UPMP00010/19.

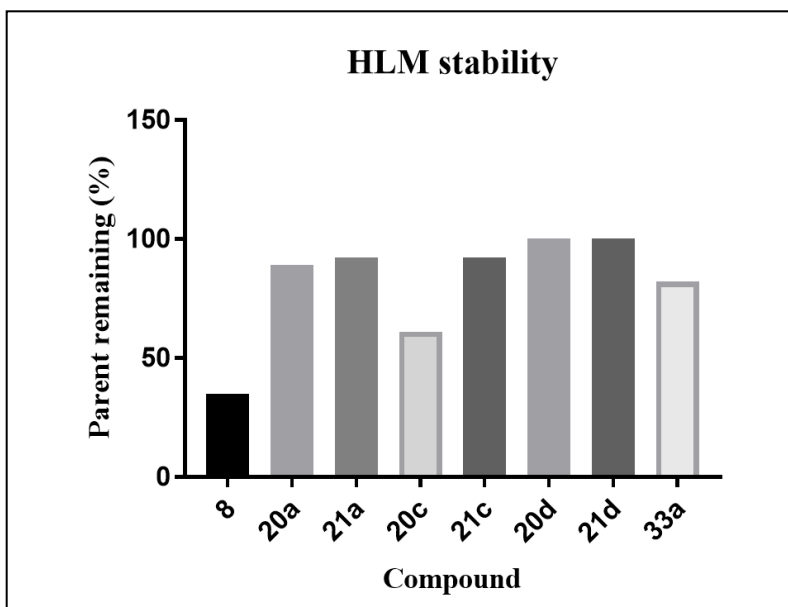


Figure 9: HLM stability of potent compounds at 30 mins

### 3.4 ASSESSMENT OF CNS PERMEABILITY OF SELECTED COMPOUNDS

As discussed in section 1.7, we aim to identify compounds that can cross BBB and are able to inhibit 20-HETE formation in the brain for use as neuroprotectants. The MDR1-MDCK assay is a validated *in-vitro* assay used to evaluate the potential of molecules to penetrate across the BBB<sup>68</sup>. It involves a trans-well system made of a monolayer of Madine Canine Darby kidney cells, which overexpress P-gp<sup>68</sup>, an efflux transporter expressed extensively in the brain<sup>69</sup>. This assay measures effective permeability, which is the movement of molecules from the apical to basolateral side ( $P_{A-B}$ ) of the cells and vice versa ( $P_{B-A}$ ). Effective permeability values are used to calculate efflux ratio ( $P_{B-A} / P_{A-B}$ ). An efflux ratio below 3 implies that the molecule possesses good CNS permeability potential. This assay was done in a contract research organization AMRI. Number and choice of compounds was influenced by the assay cost and the ability of



compounds to potently inhibit 20-HETE formation in humans and/or rat microsomal preparations. High solubility was also a factor of choice. These considerations led us to select compounds **21a**, **21e** and **21h** for MDR1-MDCK assay.

Assay results are documented in Table 6; they show that compounds **21a**, **21e** and **21h** have high effective permeability ( $P_{A-B}$ ) and low efflux indicating excellent CNS permeability potential (Table 6).

**Table 6: MDR1-MDCK assay results**

No	$P_{A-B}$ ( $10^{-6}$ cm/sec)	$P_{B-A}$ ( $10^{-6}$ cm/sec)	Efflux ratio
<b>21a</b>	32	25.70	0.803
<b>21e</b>	18.4	40.2	2.2
<b>21h</b>	60.1	48.6	0.8

### 3.5 INHIBITION OF EPOXYGENASE PATHWAY

We have discussed in the background that EETs and 20-HETE have opposite effect on microvasculature<sup>10</sup>. 20-HETE formation inhibitors should not attenuate EET mediated vasodilation and must have selectivity for 20-HETE formation inhibition vs. inhibition of EET formation by epoxygenase. Selectivity (EET formation inhibition) assessment of all the potent inhibitors we synthesized during this work is currently underway in the lab of Dr. Samuel Poloyac. At this time, EET formation inhibition is only available for compounds **20a** and **21a** and is shown in Table 7. Comparison of 20-HETE formation inhibition data for these compounds

(Table 3) with the data for EET formation inhibition, points to the fact that **20a** and **21a** are highly selective compounds towards 20-HETE formation inhibitions (Table 7).

**Table 7: Inhibition of epoxygenase pathway by 20a and 21a**

Compound	EET formation inhibition
<b>20a</b>	No inhibition upto 25,000nM
<b>21a</b>	3.1% @ 50,000nM

## 4.0 CONCLUSION AND FUTURE DIRECTIONS

The objective of this work was to expand the SAR around the lead molecules UPMP00010/19. We described analogs of UPMP00010/19 that have a simple substitution on aryl ring and pyrazole and contain a heteroatom linker between the phenyl ring and aliphatic piperidine. Our efforts led to the synthesis of 24 analogs that by design, had physicochemical properties appropriate for CNS acting compounds. Several of the compounds synthesized showed good activity against the 20-HETE formation. For example, compounds **20a**, **21a**, **20c**, **21c**, **21e**, **21f**, **21h**, and **33a** showed good potency in human microsomal preparations and rCYP4F2. Compounds **21e**, **20f**, **21f** and **21h** also showed potency against 20-HETE formation in rat microsomal systems. This is particularly important. The broader goal in our lab of this project is to identify a preclinical candidate with clinical translation potential. A number of compounds synthesized in this series had better kinetic solubility than comparator molecule **8**. HLM stability available for potent molecules also indicates better intrinsic clearance as compared to compound **8**. All compounds selected for CNS permeability assessment showed excellent CNS permeability potential.

Completion of IC<sub>50</sub> determination as well as determination of HLM stability data for potent compounds would further increase our understanding of the SAR around UPMP00010/19 scaffold and the set of compounds synthesized in this work. Some of the molecules show inhibition of 20-HETE formation in HLM and rat microsomal systems whereas others are able to

inhibit 20-HETE formation only in human systems. A future direction would be to understand the reason for this by synthesis of more analogs and computational experiments. Further exploration of SAR around leads UPMP00010/19 by the introduction of electron withdrawing substituents and di-substitution on the phenyl ring is required. Furthermore, the generation of derivatives based on UPMP00022 is another important avenue to further the overall goal of this project.

## 5.0 EXPERIMENTAL SECTION

### 5.1 INSTRUMENTATION AND REAGENTS

<sup>1</sup>H nuclear magnetic resonance spectra (NMR) was recorded using Bruker avance III 400 MHz spectrometer. Mass spectra (MS) under electron spray ionization condition (ESI) were obtained using Shimadzu UFLC/Applied Biosystems 2000 MS mass spectrometer. Infrared spectra were obtained using Bruker alpha Attenuated total reflectance (ATR) spectrometer. Purifications of compounds with column chromatography were carried out using Teledyne ISCO combiflash Rx instrument. The following chemicals were obtained from commercial sources and used for synthesizing molecules: *tert*-butyl 4-(4,4,5,5-tetramethyl-1,3,2-dioxaborolan-2-yl)-3,6-dihydropyridine-1(2*H*)-carboxylate, potassium carbonate, [1,1'-Bis(Diphenylphosphino)ferrocene]dichloropalladium [PdCl<sub>2</sub>(dppf)], 4-methoxybromobenzene, 2-methoxybromobenzene, 4-methylbromobenzene, 3-methylbromobenzene, 2-methylbromobenzene, 4-bromobenzylbromide, 4-aminobromobenzene, 5-bromo-2-methoxypyridine, Palladium over charcoal (Pd/C, 10%), 4N hydrochloric acid in dioxane, 4-phenylpiperidine, 3-iodopyrazole, 4-iodopyrazole, 4-iodo-3-methyl-1*H*-pyrazole, 3-iodo-5-methyl-1*H*-pyrazole, P-toluene sulfonic acid monohydrate (PTSA.H<sub>2</sub>O), 3,4-dihydro-2*H*-pyran, acetic anhydride, methyl iodide, sodium hydride, sodium metal, 4-hydroxypiperidine, di-*tert*-butyl carbonate, mesyl chloride, thiobenzene, *m*-chloroperbenzoic acid, copper-I-iodide and L-

proline. Following solvents were used for dichloromethane (DCM), Ethyl acetate (EtOAc), methanol (MeOH), tetrahydrofuran (THF), Dimethylformamide (DMF), Dimethylsulfoxide (DMSO), ethyl ether and dioxane.

## 5.2 GENERAL PROCEDURE-SYNTHESIS OF N-BOC-4-ARYL DIHYDROPYRIDINE

A mixture of desired bromobenzene **11a-i** (1eq), *tert*-butyl 4-(4,4,5,5-tetramethyl-1,3,2-dioxaborolan-2-yl)-3,6-dihydropyridine-1(2*H*)-carboxylate **12** (1eq) and potassium carbonate 3eq was taken in DMF. Argon gas was bubbled through DMF for 10 mins. Followed addition of PdCl<sub>2</sub>(dppf) 0.01 eq and the reaction mixture was sealed and heated at 80 °C until the consumption of limiting reagents deemed complete by TLC. DMF evaporated under a slow stream of air at 80 °C and the resultant residue partitioned between water and EtOAc. The aqueous layer was efficiently extracted with EtOAc, dried using sodium sulfate and concentrated to obtain crude residue. The obtained residue was then purified by silica gel column chromatography to get N-Boc-4-aryl dihydropyridines (**13a-i**).

### 5.3 GENERAL PROCEDURE-SYNTHESIS OF N-BOC-4-ARYL PIPERIDINES

A slurry of N-BOC-4-aryl-dehydropiperidine **13a-i** and Pd/C (0.1 eq, based on Pd content) was hydrogenated under 1 atm of H<sub>2</sub>. Reaction mixture filtered through a pad of celite and the resultant filtrate concentrated to obtain 4-aryl-N-BOC-piperidines (**14a-i**).

### 5.4 GENERAL PROCEDURE-SYNTHESIS OF 4-ARYL PIPERIDINES

A mixture of desired N-BOC-4-aryl piperidines (**14a-i**) was dissolved in 4N HCl in dioxane at room temperature. After stirring overnight, the volatiles were evaporated, and the resultant salt was partitioned between saturated sodium bicarbonate and EtOAc. The aqueous layer was extracted with EtOAc until TLC detected no product in the organic extract. The combined organic layer was dried using sodium sulfate and concentrated to get corresponding piperidine derivatives (**15a-i**).

**5.5 GENERAL PROCEDURE-SYNTHESIS OF 4-ARYL-1-(1H-PYRAZOLE-5-YL, 4YL) PIPERIDINE, 1-(3-METHYL-1H-PYRAZOLE-4-YL)-4-PHENYL PIPERIDINE, 1-(5-METHYL-1H-PYRAZOLE-3-YL)-4-PHENYL PIPERIDINE, 4-(PHENYLTHIO)-1-(1H-PYRAZOL-5-YL, 4-YL) PIPERIDINE AND 4-(PHENYLSULFONYL)-1-(1H-PYRAZOL-5-YL, 4-YL) PIPERIDINE**

A mixture of desired THP protected pyrazole (**17**, **19**, **23** and **24**) (1 eq), piperidine derivatives (**15a-i**, **31a**, **31b** and **22**), copper-I-iodide (0.2 eq), L-proline (0.4 eq) and potassium carbonate (5 eq) in DMSO was stirred at 90 °C until TLC indicated consumption of starting material. DMSO was then evaporated and the residue was partitioned between ammonium chloride and EtOAc. The aqueous layer was extracted well with small portions of EtOAc until indicated no product in the organic extract. The combined organic layer was dried using sodium sulfate and concentrated to a residue that was chromatographed with a silica gel column chromatography. THP protected intermediate obtained from this purification, without further characterization was dissolved in 4N HCl in dioxane at room temperature and stirred until TLC indicated the consumption of starting material. The volatiles were then evaporated, and the residue was partitioned between saturated sodium bicarbonate and EtOAc. The aqueous layer was extracted with small portions of EtOAc until TLC indicated no product in the organic extract. The combined organic layer was dried using sodium sulfate and concentrated to get a residue which was purified by silica gel column chromatography, and/or precipitation out of DCM with an excess of hexanes to obtain final products (**20a-i**, **21a-i**, **25a**, **26a**, **32a-b** and **33a-b**).



## 5.6 DATA FOR EACH ANALOG

### Synthesis of *tert*-butyl 4-(4-methoxyphenyl)-3,6-dihydropyridine-1(2*H*)-carboxylate (13a)

Synthesized by following general procedure 5.2. Crude residue was chromatographed by a silica gel using EtOAc in hexane gradient to obtain 787 mg of colorless liquid (53% Yield). [0-50% Hex:EtOAc]

<sup>1</sup>HNMR- (400 MHz, CDCl<sub>3</sub>)  $\delta$  1.49 (s, 9H); 2.50 (bs, 2H); 3.62 (t, J=6.0 Hz, 2H); 3.81 (s, 3H); 4.03-4.08 (m, 2H); 5.93 (s, 1H); 6.88 (d, J=8.8 Hz, 2H); 7.31 (d, J=8.8 Hz, 2H).

### Synthesis of *tert*-butyl 4-(2-methoxyphenyl)-3,6-dihydropyridine-1(2*H*)-carboxylate (13b)

Synthesized by following general procedure 5.2. Crude residue was chromatographed by silica gel using EtOAc in hex gradient to obtain 1.68 g of colorless liquid (72% Yield). [0-100% Hex:EtOAc]

<sup>1</sup>HNMR - (400 MHz, CDCl<sub>3</sub>)  $\delta$  1.49 (s, 9H); 2.5 (apparent bs, 2H); 3.59 (apparent t, 2H); 3.81 (s, 3H); 4.04 (s, 2H); 5.75 (s, 1H); 6.85-6.96 (m, 2H); 7.14 (dd,  $J_1=1.6$  Hz,  $J_2=7.6$  Hz, 1H); 7.22-7.26 (m, 1H).

ATIR (cm<sup>-1</sup>)-2973, 2931, 2834, 1689, 1596, 1489, 1453, 1413, 1363, 1335, 1291, 1270, 1235, 1161, 1108, 1051, 1025, 972, 937, 863, 826, 793, 750, 691, 629.

LC-MS– (ESI)  $m/z$  ratio for  $C_{17}H_{23}NO_3$  Calculated (289.38); Observed ( $M+1=290.7$ ).

### Synthesis of *tert*-butyl 4-(*p*-tolyl)-3,6-dihydropyridine-1(2*H*)-carboxylate (13c)

Synthesized by following general procedure 5.2. Crude residue obtained was chromatographed by silic gel using EtOAc in hexane gradient to obtain mg of colorless liquid. [0-50% Hex: EtOAc]

$^1\text{HNMR}$  - (400 MHz,  $\text{CDCl}_3$ )  $\delta$  1.49 (s, 9H); 2.34 (s, 3H); 2.51 (apparent bs, 2H); 3.63 (apparent t, 2H); 4.06 (apparent s, 2H); 5.99 (s, 1H); 7.14 (d,  $J=7.6$  Hz, 2H); 7.27 (d,  $J=8$  Hz, 2H).

### Synthesis of *tert*-butyl 4-(4-(methoxymethyl)phenyl)-3,6-dihydropyridine-1(2*H*)-carboxylate (13d)

Prep of 11d was done using procedure known in literature<sup>70</sup>.

$^1\text{HNMR}$  - (400 MHz,  $\text{CDCl}_3$ )  $\delta$  3.38 (s, 3H); 4.41 (s, 2H); 7.21 (d,  $J=8.8$  Hz, 2H); 7.47 (d,  $J=8$  Hz, 2H).

Synthesized by following general procedure 5.2. Crude residue was chromatographed by silica gel using EtOAc in hexane gradient to obtain 2.06 g of pale liquid (88% Yield).

$^1\text{HNMR}$  - (400 MHz,  $\text{CDCl}_3$ )  $\delta$  1.49 (s, 9H); 2.52 (s, 2H); 3.39 (s, 3H); 3.63 (apparent t,  $J=6$  Hz, 2H); 4.07 (apparent q,  $J=6$  Hz, 2H); 4.45 (s, 2H); 6.04 (s, 1H); 7.30 (d,  $J=8.4$  Hz, 2H); 7.36 (d,  $J=8.4$  Hz, 2H).

ATIR ( $\text{cm}^{-1}$ ) - 2975, 2926, 2893, 2821, 1689, 1513, 1476, 1451, 1415, 1363, 1337, 1309, 1288, 1235, 1163, 1106, 1059, 1018, 986, 968, 936, 920, 863, 801, 768, 679, 625.

LC-MS– (ESI)  $m/z$  ratio for  $C_{18}H_{25}NO_3$  Calculated (303.40); Observed.

**Synthesis of *tert*-butyl 4-(4-(*N*-methylacetamido)phenyl)-3,6-dihydropyridine-1(2*H*)-carboxylate (13e)**

Synthesis of 11e was done according to the procedure known in literature.<sup>71</sup>

<sup>1</sup>HNMR - (400 MHz,  $CDCl_3$ )  $\delta$  1.87 (s, 3H); 3.24 (s, 3H); 7.07 (d,  $J=8.0$  Hz, 2H); 7.54 (d,  $J=8.4$  Hz, 2H).

Synthesized by following general procedure 5.2. Crude residue obtained was chromatographed by silica gel using EtOAc in hexane gradient to obtain 981 mg of pale yellow solid (82% Yield).

[0-100% Hex:EtOAc]

<sup>1</sup>HNMR - (400 MHz,  $CDCl_3$ )  $\delta$  1.49 (s, 9H); 1.88 (s, 3H); 2.53 (bs, 2H); 3.26 (s, 3H); 3.66 (apparent distorted t,  $J=4.8$  Hz, 2H); 4.09 (bs, 2H); 6.08 (bs, 1H); 7.15 (d,  $J=7.6$  Hz, 2H); 7.41 (d,  $J=8.4$  Hz, 2H).

ATIR ( $cm^{-1}$ ) – 3036, 2974, 2929, 2867, 2839, 1690, 1655, 1603, 1510, 1416, 1376, 1364, 1288, 1236, 1162, 1111, 1085, 1060, 1036, 1016, 971, 920, 861, 813, 769, 728.67, 644, 631.

LC-MS– (ESI)  $m/z$  ratio for  $C_{19}H_{26}N_2O_3$  Calculated (330.43); Observed ( $M+1=331.4$ )

**Synthesis of *tert*-butyl 4-(4-acetamidophenyl)-3,6-dihydropyridine-1(2*H*)-carboxylate (13f)**

11f was prepared according to the procedure known in the literature.

<sup>1</sup>HNMR - (400 MHz,  $CDCl_3$ )  $\delta$  2.17 (s, 3H), 7.38-7.43 (m, 4H).

Synthesized by following general procedure 5.2. Crude residue obtained was chromatographed by silica gel using EtOAc in hexane gradient to obtain 1.12 g of pale yellow solid (77% Yield).

[0-100% Hex:EtOAc]

<sup>1</sup>HNMR - (400 MHz, CDCl<sub>3</sub>) δ 1.49 (s, 9H); 2.18 (s, 3H); 2.49 (bs, 2H); 3.62 (t, *J*=5.6 Hz, 2H); 4.05 (bs, 2H); 5.99 (bs, 1H); 7.23 (s, 1H); 7.32 (d, *J*=8.8 Hz, 2H); 7.46 (d, *J*=8.8 Hz, 2H); 7.60 (s, 1H).

ATIR (cm<sup>-1</sup>) – 3302, 3266, 3212, 3178, 3103, 3061, 3049, 2986, 2970, 2931, 2861, 2844, 1691, 1659, 1642, 1593, 1529, 1512, 1478, 1460, 1430, 1410, 1361, 1340, 1310, 1287, 1243, 1164, 1114, 1061, 1037, 1025, 1007, 997, 980, 964, 929, 861, 847, 825, 809, 767, 722, 697.

LC-MS– (ESI) *m/z* ratio for C<sub>18</sub>H<sub>24</sub>N<sub>2</sub>O<sub>3</sub> Calculated (316.40); Observed (M+1=317.4).

### **Synthesis of *tert*-butyl 4-(*m*-tolyl)-3,6-dihydropyridine-1(2*H*)-carboxylate (13h)**

Synthesized by following general procedure 5.2. Crude residue obtained was chromatographed by silica gel using EtOAc in hexane gradient to obtain 1.09 g of colorless liquid (68% Yield). [0-

35% Hex:EtOAc]

<sup>1</sup>HNMR - (400 MHz, CDCl<sub>3</sub>) δ 1.49 (s, 9H); 2.36 (s, 3H); 2.52 (m, 2H); 3.63 (apparent t, *J*=5.6 Hz, 2H); 4.07 (apparent s, 2H); 6.01 (s, 1H); 7.07 (d, *J*=7.2 Hz, 1H); 7.15-7.25 (m, 3H).

ATIR (cm<sup>-1</sup>)- 3004, 2974, 2927, 2862, 2836, 1690, 1604, 1583, 1478, 1451, 1414, 1363, 1337, 1290, 1236, 1161, 1110, 1060, 1039, 984, 949, 901, 865, 822, 783, 764, 695, 634.

LC-MS– (ESI) *m/z* ratio for C<sub>17</sub>H<sub>23</sub>NO<sub>2</sub> Calculated (273.38); Observed [M-H<sup>+</sup>=272.4].

### Synthesis of *tert*-butyl 4-(*o*-tolyl)-3,6-dihydropyridine-1(2*H*)-carboxylate (13i)

Synthesized by following general procedure 5.2. Crude residue was chromatographed by silica gel using EtOAc in hexane gradient to obtain 1.043 g of clear liquid (70% Yield). [0-20% Hex:EtOAc]

<sup>1</sup>HNMR - (400 MHz, CDCl<sub>3</sub>)  $\delta$  1.50 (s, 9H); 2.79 (s, 3H); 2.31-2.38 (m, 2H); 3.62 (t,  $J=5.6$  Hz, 2H); 4.03 (apparent q,  $J=2.4$  Hz, 2H); 5.55 (bs, 1H); 7.04-7.10 (m, 1H); 7.11-7.20 (m, 3H).

ATIR (cm<sup>-1</sup>) – 3057, 3008, 2974, 2928, 2860, 2837, 1962, 1478, 1452, 1411, 1364, 1335, 1282, 1234, 1163, 1108, 1055, 1022, 971, 936, 863, 827, 797, 752, 725, 688, 632.

LC-MS– (ESI)  $m/z$  ratio for C<sub>17</sub>H<sub>25</sub>NO<sub>2</sub> Calculated (273.38); Observed (M-*tert* butyl+1=218.2).

### Synthesis of *tert*-butyl 4-(4-methoxyphenyl)piperidine-1-carboxylate (14a)

Synthesized by following the general procedure 5.3 to obtain a 433 mg of colorless liquid (86% yield).

<sup>1</sup>HNMR - (400 MHz, CDCl<sub>3</sub>)  $\delta$  1.48 (s, 9H); 1.51-1.63 (m, 2H); 1.79 (apparent d,  $J=12.8$  Hz, 2H); 2.59 (tt,  $J=12$  Hz, 3.6 Hz, 1H); 2.78 (apparent t,  $J=12.4$  Hz, 2H); 3.79 (s, 3H); 4.22 (apparent bs, 2H); 6.85 (d,  $J=8.8$  Hz, 2H); 7.12 (d,  $J=8.4$  Hz, 2H).

ATIR (cm<sup>-1</sup>)- 2974, 2932, 2848, 1686, 1610, 1582, 1512, 1443, 1420, 1364, 1323, 1283, 1245, 1228, 1160, 1122, 1035, 1016, 986, 941, 885, 861, 827, 804, 764, 638.

### Synthesis of *tert*-butyl 4-(2-methoxyphenyl)piperidine-1-carboxylate (14b)

Synthesized by following the general procedure 5.3 to obtain 1.63 g of colorless liquid (96% Yield).

<sup>1</sup>HNMR - (400 MHz, CDCl<sub>3</sub>)  $\delta$  1.48 (s, 9H); 1.60 (ddd,  $J_1=16$  Hz,  $J_2=12$  Hz,  $J_3=3.6$  Hz, 2H); 1.79 (apparent d, 2H); 2.82 (apparent t, 2H); 3.08 (tt,  $J_1=15.6$  Hz,  $J_2=3.6$  Hz, 1H); 3.83 (s, 3H); 4.21-4.25 (apparent bs, 2H); 6.86 (d,  $J=8$  Hz, 1H); 6.93 (t,  $J=7.6$  Hz, 1H); 7.12-7.23 (m, 2H).

ATIR (cm<sup>-1</sup>)- 3065, 2973, 2933, 2849, 1686, 1600, 1585, 1492, 1462, 1418, 1364, 1327, 1286, 1231, 1159, 1127, 1108, 1053, 1012, 985, 941, 926, 862, 826, 801, 750, 649, 623.

### Synthesis of *tert*-butyl 4-(*p*-tolyl)piperidine-1-carboxylate (14c)

Synthesized by following general procedure 5.3 to obtain 748 mg colorless liquid (94% Yield).

<sup>1</sup>HNMR - (400 MHz, CDCl<sub>3</sub>)  $\delta$  1.48 (s, 9H); 1.56-1.64 (m, 2H); 1.80 (apparent d,  $J=13.2$  Hz, 2H); 2.32 (s, 3H); 2.60 (tt,  $J=12$  Hz, 3.6 Hz, 1H); 2.79 (td,  $J=13.2$  Hz, 2.4 Hz, 2H); 4.21-4.25 (m, 2H); 7.06-7.15 (m, 4H).

### Synthesis of *tert*-butyl 4-(4-(methoxymethyl)phenyl)piperidine-1-carboxylate (14d)

Synthesized by following general procedure 5.3 to obtain 1.40 g of colorless liquid (97% Yield).

<sup>1</sup>HNMR - (400 MHz, CDCl<sub>3</sub>)  $\delta$  1.48 (s, 9H); 1.56-1.1.67 (m, 2H); 1.76-1.84 (apparent bd,  $J=12.8$  Hz, 2H); 2.64 (tt,  $J=3.2$  Hz, 12.4 Hz, 1H); 2.76-2.82 (m, 2H), 3.39 (s, 3H); 4.24 (apparent d,  $J=13.6$  Hz, 2H); 4.24 (s, 2H); 7.18 (d,  $J=8$  Hz, 2H); 7.27 (d,  $J=8$  Hz, 2H).

### Synthesis of *tert*-butyl 4-(4-(*N*-methylacetamido)phenyl)piperidine-1-carboxylate (14e)

Synthesized by following the general procedure 5.3 to obtain 961 mg of white solid (97% Yield).

<sup>1</sup>HNMR - (400 MHz, CDCl<sub>3</sub>) δ 1.48 (s, 9H); 1.55-1.68 (m, 2H); 1.79-1.89 (s merged with apparent d, 5H); 2.69 (tt, *J*=12.4 Hz, 3.6 Hz, 1H); 2.81 (apparent t, *J*=11.6 Hz, 2H); 3.25 (s, 3H); 4.25 (bs, 2H); 7.12 (d, *J*=8 Hz, 2H); 7.23 (d, *J*=8.4 Hz, 2H).

ATIR (cm<sup>-1</sup>) – 2974, 2932, 2852, 1686, 1657, 1606, 1509, 1418, 1364, 1350, 1323, 1293, 1275, 1230, 1161, 1123, 1084, 1013, 976, 921, 884, 797, 768, 730, 644, 627.

LC-MS– (ESI) *m/z* ratio for Calculated (332.44); Observed (M+1=333.4).

### Synthesis of *tert*-butyl 4-(4-acetamidophenyl)piperidine-1-carboxylate (14f)

Synthesized by following general procedure 5.3 to obtain 1.08 g of white solid (98% Yield).

<sup>1</sup>HNMR - (400 MHz, CDCl<sub>3</sub>) δ 1.48 (s, 9H); 1.50-1.65 (m, 2H); 1.8 (apparent d, *J*=12.4 Hz, 2H); 2.17 (s, 3H); 2.57-2.66 (m, 1H); 2.80 (apparent t, *J*=, 2H); 4.22-4.24 (m, 2H); 7.19 (d overlapping with s, *J*=8.4 Hz, 3H); 7.42 (d, *J*=8 Hz, 2H).

ATIR (cm<sup>-1</sup>)-3311, 3280, 3223, 3193, 3120, 3068, 2994, 2977, 2915, 2882, 2866, 1699, 1659, 1600, 1535, 1515, 1479, 1463, 1446, 1425, 1410, 1362, 1335, 1312, 1292, 1270, 1256, 1230, 1167, 1122, 1083, 1016, 991, 969, 941, 890, 861, 850, 831, 789, 768, 738, 676, 651, 634.

LC-MS– (ESI) *m/z* ratio for C<sub>18</sub>H<sub>26</sub>N<sub>2</sub>O<sub>3</sub> calculated (318.42); observed (M+1=319.7).

### Synthesis of *tert*-butyl 4-(6-methoxy-pyridin-3-yl)piperidine-1-carboxylate (14g)

Synthesized by following general procedure 5.3 and reduction by general procedure 3.2 to obtain 786 mg of clear liquid (89% Yield).

<sup>1</sup>HNMR - (400 MHz, CDCl<sub>3</sub>) δ 1.48 (s, 9H); 1.53-1.66 (m, 2H); 1.78 (apparent d, *J*=12.8 Hz, 2H); 2.61 (tt, *J*=12.0 Hz, 3.6 Hz, 1H); 2.65-2.84 (bm, 2H); 3.91 (s, 3H); 4.24 (apparent bs, 2H); 6.70 (d, *J*=8.8 Hz, 1H); 7.41 (dd, *J*=8.4 Hz, 2.4 Hz, 1H); 8.0 (d, *J*=2.4 Hz, 1H).

ATIR (cm<sup>-1</sup>)- 2974, 2933, 2849, 1686, 1605, 1572, 1493, 1463, 1445, 1420, 1396, 1363, 1282, 1255, 1229, 1160, 1115, 1018, 986, 940, 918, 885, 861, 828, 768, 640, 620.

LC-MS– (ESI) *m/z* ratio for C<sub>16</sub>H<sub>24</sub>N<sub>2</sub>O<sub>3</sub> Calculated (292.38); Observed (M+1=293.6).

### Synthesis of *tert*-butyl 4-(*m*-tolyl)piperidine-1-carboxylate (14h)

Synthesized by following the general procedure 5.3 to obtain 1.04 g of clear liquid (95% Yield).

<sup>1</sup>HNMR - (400 MHz, CDCl<sub>3</sub>) δ 1.48 (s, 9H); 1.55-1.68 (m, 2H); 1.79 (d, *J*=12.0 Hz, 2H); 2.34 (s, 3H); 2.60 (tt, *J*=12.4 Hz, 3.2 Hz, 1H); 2.78 (td, *J*=13.2 Hz, 3.2 Hz, 2H); 4.23 (apparent d, *J*=13.2 Hz, 2H); 6.97-7.04 (m, 3H); 7.18-7.22 (distorted t, *J*=8.0 Hz, 1H).

ATIR (cm<sup>-1</sup>)- 3005, 2974, 2930, 2851, 1687, 1607, 1589, 1477, 1446, 1419, 1364, 1315, 1279, 1242, 1158, 1118, 1091, 1072, 1023, 985, 927, 897, 866, 813, 783, 766, 701, 655, 629.

LC-MS– (ESI) *m/z* ratio for C<sub>17</sub>H<sub>25</sub>NO<sub>2</sub> Calculated (275.39); Observed (M-*tert* butyl+1=220.3).



### Synthesis of *tert*-butyl 4-(*o*-tolyl)piperidine-1-carboxylate (14i)

Synthesized by following the general procedure 5.3 to obtain 960 mg of clear liquid (91% Yield).

<sup>1</sup>HNMR - (400 MHz, CDCl<sub>3</sub>) δ 1.49 (s, 9H); 1.6 (ddd, *J*=20.4 Hz, 11.6 Hz, 7.2 Hz, 2H); 1.79 (apparent d, *J*=2.8 Hz, 2H); 2.35 (s, 3H); 2.76-2.90 (m, 3H); 4.26 (apparent bs, 2H); 7.07-7.28 (m, 4H).

ATIR (cm<sup>-1</sup>) – 3062, 3005, 2973, 2932, 2851, 1687, 1489, 1478, 1460, 1417, 1364, 1320, 1278, 1229, 1160, 1126, 1105, 1071, 1052, 1012, 985, 932, 885, 861, 827, 806, 750, 724, 645, 626.

LC-MS– (ESI) *m/z* ratio for C<sub>17</sub>H<sub>25</sub>NO<sub>2</sub> Calculated (275.39); Observed (M-*tert* butyl+1=220.2).

### Synthesis of 4-(4-methoxyphenyl)piperidine (15a)

Synthesized by following general procedure 5.4 to obtain 321 mg of yellow viscous liquid (100% Yield).

<sup>1</sup>HNMR - (400 MHz, CDCl<sub>3</sub>) δ 1.61 (ddd, *J*=16 Hz, 12.4 Hz, 3.6 Hz, 2H); 1.81 (apparent d, *J*=13.6 Hz, 2H); 2.56 (tt, *J*=3.6 Hz, 12 Hz, 1H); 2.73 (td, *J*=2.4 Hz, 12.4 Hz, 2H); 3.18 (apparent d, *J*=12 Hz, 2H); 3.79 (s, 3H); 6.85 (d, *J*=8.4 Hz, 2H); 7.14 (d, *J*=8.8 Hz, 2H).

### Synthesis of 4-(2-methoxyphenyl)piperidine (15b)

Synthesized by following general procedure 5.4 to obtain mg of light brown solid (100% Yield).

<sup>1</sup>HNMR - (400 MHz, DMSO-*d*<sub>6</sub>) δ 1.44-1.57 (m, 2H), 1.60-1.66 (m, 2H); 2.58-2.68 (m, 2H); 2.93-3.01 (m, 1H); 3.03-3.08 (m, 2H); 3.77 (s, 3H); 6.86-6.96 (m, 2H); 7.12-7.20 (m, 2H).

ATIR (cm<sup>-1</sup>)- 3283, 3066, 3002, 2931, 2844, 2729, 1599, 1584, 1491, 1461, 1433, 1363, 1339, 1303, 1290, 1257, 1257, 1235, 1191, 1160, 1141, 1106.97, 1094, 1055, 1026, 1007, 957, 928, 898, 865, 809, 793, 753, 630.

LC-MS- (ESI) *m/z* ratio for C<sub>12</sub>H<sub>17</sub>NO Calculated (191.13); Observed (M+1=192; M+2H<sup>+</sup>=193.3).

### Synthesis of 4-(*p*-tolyl)piperidine (15c)

Synthesized by following the general procedure 5.4 to obtain 269 mg of yellow liquid (100% Yield).

<sup>1</sup>HNMR - (400 MHz, CDCl<sub>3</sub>) δ 1.75 (ddd, *J*<sub>1</sub>=25.2 Hz, 13.2 Hz, 3.6 Hz, 2H); 1.85-1.90 (apparent d, 2H); 2.32 (s, 3H); 2.61 (tt, *J*=12 Hz, 4 Hz, 1H); 2.79 (td, 12 Hz, 2.8 Hz, 2H); 3.25-3.31 (m, 2H); 7.12 (bs, 4H).

### Synthesis of 4-(4-(methoxymethyl)phenyl)piperidine (15d)

Synthesized by following the general procedure 5.4 to obtain 872 mg of pale yellow solid (95% Yield).

<sup>1</sup>HNMR - (400 MHz, CDCl<sub>3</sub>) δ 1.66-1.80 (m, 2H); 1.86 (apparent distorted d, *J*=12.4 Hz); 1.59-2.69 (m, 1H); 2.73-2.84 (m, 2H); 3.26 (apparent d, *J*=12 Hz, 2H); 3.39 (s, 3H); 4.24 (s, 2H); 7.21 (distorted d, *J*=8 Hz, 2H); 7.28 (distorted d, *J*=8 Hz, 2H).

### Synthesis of *N*-methyl-*N*-(4-(piperidin-4-yl)phenyl)acetamide (15e)

Synthesized by following the general procedure 5.4 to obtain 199 mg of yellow solid (100% Yield).

<sup>1</sup>HNMR - (400 MHz, CDCl<sub>3</sub>) δ 1.59-1.73 (m merged with water, 2H); 1.83-1.91 (s merged with apparent d, 5H); 2.67 (tt, *J*=13.6 Hz, 4 Hz, 1H); 2.78 (td, *J*=12.4 Hz, 2.4 Hz, 2H); 3.23 (apparent d, *J*=11.6 Hz, 2H); 3.27 (s, 3H); 7.13 (d, *J*=8.4 Hz, 2H); 7.28 (d, *J*=8.4 Hz, 2H)

### Synthesis of *N*-(4-(piperidin-4-yl)phenyl)acetamide (15f)

Synthesized by following general procedure 5.4 to obtain 87 mg of pale yellow solid (51% Yield).

<sup>1</sup>HNMR - (400 MHz, CDCl<sub>3</sub>) δ 1.54-1.66 (m, 2H); 1.80 (distorted apparent d, *J*=12.8 Hz, 2H); 2.16 (s, 3H); 2.54-2.63 (m, 1H); 2.73 (apparent t, 2H); 3.188 (apparent d, *J*=10 Hz, 2H); 7.13 (s, 1H); 7.17 (d, *J*=8 Hz, 2H); 7.41 (d, *J*=8.4 Hz, 2H).

### Synthesis of 2-methoxy-5-(piperidin-4-yl)pyridine (15g)

Synthesized by following the general procedure 5.4 to obtain 160 mg yellow solid (58% Yield).

<sup>1</sup>HNMR - (400 MHz, CDCl<sub>3</sub>) δ 1.54-1.68 (m, 2H); 1.79 (apparent d, *J*=13.6 Hz, 2H); 2.57 (tt, *J*=12.4 Hz, 3.6 Hz, 1H); 2.74 (td, *J*=12.0 Hz, 3.6 Hz, 2H); 3.18-3.21 (m, 2H); 3.91 (s, 3H); 6.69 (d, *J*=8.4 Hz, 1H); 7.43 (dd, *J*=8.4 Hz, 2.4 Hz, 1H); 8.05 (d, *J*=2.4 Hz, 1H).

### Synthesis of 4-(*m*-tolyl)piperidine (15h)

Synthesized by following the general procedure 5.4 to obtain 292 mg of yellow liquid (89% Yield).

<sup>1</sup>HNMR - (400 MHz, CDCl<sub>3</sub>)  $\delta$  1.60-1.74 (m, 2H); 1.83 (apparent bd,  $J=12.8$  Hz, 2H); 2.33 (s, 3H); 2.60 (tt,  $J=12$  Hz, 3.6 Hz, 1H); 2.78 (td,  $J=12.0$  Hz, 2.0 Hz, 2H); 3.22 (apparent bd,  $J=12.0$  Hz, 2H); 6.90-7.64 (m, 3H); 7.18-7.22 (t,  $J=7.2$  Hz, 1H).

### Synthesis of 4-(*o*-tolyl)piperidine (15i)

Synthesized by following the general procedure 5.4 to obtain 299 mg of yellow liquid (98% Yield).

<sup>1</sup>HNMR - (400 MHz, CDCl<sub>3</sub>)  $\delta$  1.57-1.80 (m, 4H); 2.35 (s, 3H); 2.72-2.90 (m, 3H); 3.21 (apparent d,  $J=12$  Hz, 2H); 7.06-7.25 (m, 4H).

### Synthesis of 4-(4-methoxyphenyl)-1-(1*H*-pyrazol-5-yl)piperidine (20a)

Synthesized by following general procedure 5.5 to obtain 18 mg of white solid (22% Yield).

<sup>1</sup>HNMR- (400 MHz, CDCl<sub>3</sub>)  $\delta$  1.78-1.95 (m, 4H); 2.56-2.66 (m, 1H); 2.85 (apparent t,  $J=12$  Hz, 2H); 3.80 (s, 3H); 3.85 (apparent d,  $J=11.6$  Hz, 2H); 5.80 (s, 1H); 6.86 (d,  $J=7.6$  Hz, 2H); 7.17 (d,  $J=7.2$  Hz, 2H); 7.42 (s, 1H).

ATIR ( $\text{cm}^{-1}$ )- 3247, 3138, 3124, 2999, 2972, 2932, 2914, 2820, 1608, 1579, 1547, 1509, 1482, 1459, 1439, 1380, 1323, 1313, 1285, 1237, 1197, 1176, 1152, 1107, 1088, 1064.65, 1016, 983, 940, 923, 903, 864, 825, 805, 763, 709, 676, 636.

LC-MS- (ESI)  $m/z$  ratio for  $\text{C}_{15}\text{H}_{19}\text{N}_3\text{O}$  Calculated (257.34); Observed ( $\text{M}+1=258.4$ ,  $\text{M}+2\text{H}=259.7$ ).

### **Synthesis of 4-(2-methoxyphenyl)-1-(1H-pyrazol-5-yl)piperidine (20b)**

Synthesized by following general procedure 5.5. Crude residue was chromatographed by silica gel using EtOAc in hexane gradient to obtain 75 mg of yellow solid (43.35% Yield). [0-100% Hex:EtOAc]

$^1\text{H}$ NMR - (400 MHz,  $\text{DMSO}-d_6$ )  $\delta$  1.67-1.82 (m, 4H); 2.60-2.71 (apparent t,  $J=9.6$  Hz, 2H); 2.90-3.05 (m, 1H); 3.70-3.85 (m, 5H); 5.70 (s, 1H); 6.85-6.99 (m, 2H); 7.15-7.20 (m, 2H); 7.44 (s, 1H); 11.76 (s, 1H).

ATIR ( $\text{cm}^{-1}$ )- 3172, 3074, 2933, 2808, 2751, 1598, 1582, 1539, 1489, 1461, 1383.51, 1317, 1288, 1232, 1191, 1170, 1154, 1122, 1086, 1052, 1019, 982, 926, 904.59, 866, 777, 734, 620.

LC-MS- (ESI)  $m/z$  ratio for  $\text{C}_{15}\text{H}_{19}\text{N}_3\text{O}$  Calculated (257.34); Observed ( $\text{M}+1=258.3$ ).

### **Synthesis of 1-(1H-pyrazol-5-yl)-4-(p-tolyl)piperidine (20c)**

Synthesized by following the general procedure 5.5. Crude obtained was chromatographed by silica gel using EtOAc in hexane gradient to obtain 28 mg of white solid (55% Yield). [0-100% Hex: EtOAc]

<sup>1</sup>HNMR - (400 MHz, CDCl<sub>3</sub>) δ 1.62-1.81 (m, 4H); 2.26 (s, 3H); 2.57 (tt, *J*=12 Hz, 3.6 Hz, 1H); 2.62-2.72 (apparent td, 2H); 3.70-3.77 (apparent bd, *J*=11.6 Hz, 2H); 5.71 (s, 1H); 7.06-7.16 (apparent q, *J*=8 Hz, 4H); 7.44 (s, 1H); 11.76 (bs, 1H).

ATIR (cm<sup>-1</sup>)- 3142, 3045, 3000, 2963, 2921, 2870, 2856, 2839, 2698, 1536, 1513, 1481, 1454, 1441, 1359, 1344, 1318, 1304, 1280, 1258, 1235, 1183, 1154, 1124, 1102, 1080, 1047, 1005, 978, 927, 904, 857, 813, 801, 764, 724, 699.

LC-MS– (ESI) *m/z* ratio for C<sub>15</sub>H<sub>19</sub>N<sub>3</sub> Calculated (241.34); Observed (M+1=242.1).

### Synthesis of 4-(4-(methoxymethyl)phenyl)-1-(1*H*-pyrazol-5-yl)piperidine (20d)

Synthesized by following the general procedure 5.5. Crude residue obtained was chromatographed by silica gel using EtOAc in hexane gradient to obtain 78 mg of colorless fluffy solid (57% Yield).

<sup>1</sup>HNMR - (400 MHz, CDCl<sub>3</sub>) δ 1.69-1.85 (m, 4H); 2.60-2.73 (m, 3H); 3.27 (s, 3H); 3.75 (apparent d, *J*=10.8 Hz, 2H); 4.36 (s, 2H); 5.71 (s, 1H); 7.24 (s, 4H); 7.44 (s, 1H).

ATIR (cm<sup>-1</sup>)- 3273, 3116, 3039, 2992, 2933, 2867, 2812.82, 1537, 1512, 1477, 1456, 1437, 1383, 1365, 1324, 1311.89, 1282, 1270, 1258, 1233.18, 1208, 1182, 1152, 1086.81, 1067, 1033, 1014, 982, 907, 866, 838, 820, 750, 718, 676, 643, 617.

LC-MS– (ESI) *m/z* ratio for C<sub>16</sub>H<sub>21</sub>N<sub>3</sub>O Calculated (271.17); Observed (M+1=272.5).

### Synthesis of *N*-(4-(1-(1*H*-pyrazol-5-yl)piperidin-4-yl)phenyl)-*N*-methylacetamide (20e)

Synthesized by following the general procedure 5.5. Crude residue obtained was chromatographed by silica gel using EtOH in DCM gradient to obtain 6 mg pale yellow solid of solid (14% Yield). [0-10% DCM:EtOH]

<sup>1</sup>HNMR - (400 MHz, CDCl<sub>3</sub>)  $\delta$  1.80-1.98 (m, 7H); 2.64-2.75 (m, 1H); 2.82-2.91 (m, 2H); 3.25 (s, 3H); 3.87 (apparent d,  $J=12.8$  Hz, 2H); 5.81 (s, 1H); 7.12 (d,  $J=8$  Hz, 2H); 7.28 (d,  $J=8.4$  Hz, 2H); 7.43 (s, 1H).

ATIR (cm<sup>-1</sup>) 3301, 3241, 3225, 2962, 2941, 2919, 2846, 2810, 2746.38, 2697, 1636, 1605, 1534, 1508, 1457, 1447, 1427, 1378, 1357, 1293.64, 1271, 1252, 1230, 1199, 1166, 1150, 1136, 1089, 1060, 1037, 10167, 977, 919, 903, 866, 843, 743, 681, 626, 603.

LC-MS- (ESI)  $m/z$  ratio for C<sub>17</sub>H<sub>22</sub>N<sub>4</sub>O Calculated (298.39); Observed (M+1= 299.7; M+Na=321.7).

### Synthesis of *N*-(4-(1-(1*H*-pyrazol-5-yl)piperidin-4-yl)phenyl)acetamide (20f)

Synthesized by following the general procedure 5.5. Crude residue obtained was chromatographed by silica gel using EtOH in DCM gradient to obtain 39 mg of pale yellow solid (43% Yield). [0-10% DCM:EtOH]

<sup>1</sup>HNMR - (400 MHz, MeOD)  $\delta$  1.78-1.91 (m, 4H); 2.11 (s, 3H); 2.60-2.79 (m, 1H); 2.82 (td,  $J=12.4$  Hz, 3.2 Hz, 2H); 3.79 (apparent d,  $J=12.4$  Hz, 2H); 5.81 (d,  $J=2.4$  Hz, 1H); 7.20 (d,  $J=8.4$  Hz, 2H); 7.43-7.49 (m, 3H).

ATIR (cm<sup>-1</sup>)- 3244, 3187, 3144, 3116, 3055, 2947, 2922, 2849, 2818, 2750, 1659, 1599, 1572, 1536, 1511, 1478, 1460, 1407, 1370, 1314, 1291, 1261, 1200, 1153, 1120, 1102, 1061, 1039, 1015, 989, 948, 923, 905, 867, 845, 794, 762, 721, 671, 660, 609.

LC-MS– (ESI) *m/z* ratio for C<sub>16</sub>H<sub>20</sub>N<sub>4</sub>O calculated (284.36); observed (M+1=285.4).

### **Synthesis of 5-(1-(1*H*-pyrazol-5-yl)piperidin-4-yl)-2-methoxypyridine (20g)**

Synthesized by following the general procedure 5.5. Crude obtained was chromatographed by silica gel using EtOAc in hexane gradient to obtain 9 mg of white solid (43% Yield).

[0-100% Hex: EtOAc]

<sup>1</sup>HNMR - (400 MHz, CDCl<sub>3</sub>) δ 1.76-1.92 (m, 4H); 2.56-2.66 (m, 1H); 2.81-2.88 (m, 2H); 3.89 (apparent bd, *J*=12.0 Hz, 2H); 3.92 (s, 3H); 5.80 (s, 1H); 6.70 (d, *J*=8.4 Hz, 1H); 7.42 (s, 1H); 7.46 (dd, *J*=8.8 Hz, 2.4 Hz, 2H); 8.04 (bs, 1H).

ATIR (cm<sup>-1</sup>)- 3234, 3143, 3128, 3047, 3013, 2975, 2938, 2918, 2847, 3013, 2975, 2938, 2918, 2847, 2819, 2751, 1736, 1671, 1603, 1569, 1551, 1492, 1460, 1443, 1396, 1383, 1360, 1322, 1297, 1280, 1254, 1239, 1201, 1174, 1155, 1133, 1113, 1093, 1066, 1027, 1012, 984, 925, 905, 869, 835, 810, 758, 707, 677, 638, 605.

LC-MS– (ESI) *m/z* ratio for C<sub>14</sub>H<sub>18</sub>N<sub>4</sub>O Calculated (258.33); Observed (M+1=259.3).



### Synthesis of 1-(1*H*-pyrazol-5-yl)-4-(*m*-tolyl)piperidine (20h)

Synthesized by following the general procedure 5.5. Crude residue obtained was chromatographed by silica gel using EtOH in hexane gradient to obtain mg of white solid (% Yield). [0-10% Hex:EtOH]

<sup>1</sup>HNMR - (400 MHz, CDCl<sub>3</sub>) δ 1.84-1.93 (m, 4H); 2.34 (s, 3H); 2.57-2.67 (m, 1H); 2.87 (apparent t, *J*=11.6 Hz, 2H); 3.86 (apparent d, *J*=12.4 Hz, 2H); 5.79 (s, 1H); 7.00-7.08 (m, 3H); 7.17-7.25 (m, 1H); 7.42 (s, 1H).

ATIR (cm<sup>-1</sup>) – 3175, 3020, 2920, 2810, 2751, 2701, 1606, 1577, 1538, 1484, 1462, 1444, 1383, 1338, 1314, 1282, 1258, 1227, 1153, 1101, 1040, 1026, 982, 926, 908, 854, 783, 730, 700, 646.

LC-MS– (ESI) *m/z* ratio for C<sub>15</sub>H<sub>19</sub>N<sub>3</sub> Calculated (241.16); Observed (*M*+1=242.3).

### Synthesis of 1-(1*H*-pyrazol-5-yl)-4-(*o*-tolyl)piperidine (20i)

Synthesized by following the general procedure 5.5. Crude residue obtained was chromatographed by silica gel using EtOAc in DCM gradient to obtain 16 mg of slightly pale colorless liquid (10% Yield). [0-50% DCM:EtOAc]

<sup>1</sup>HNMR - (400 MHz, CDCl<sub>3</sub>) δ 1.82-1.93 (m, 4H); 2.38 (s, 3H); 2.82-2.93 (m, 3H); 3.88 (apparent d, *J*=12.4 Hz, 2H); 5.82 (s, 1H); 7.07-7.28 (m, 4H); 7.43 (s, 1H).

ATIR (cm<sup>-1</sup>) – 3410, 3173, 3066, 3017, 2934, 2849, 2808, 2751, 2705, 1577, 1539, 1483, 1461, 1445, 1383, 1314, 1280, 1253, 1237, 1180, 1153, 1122, 1100, 1066, 1040, 1018, 983, 925, 905, 866, 779, 724, 645, 624.

LC-MS– (ESI)  $m/z$  ratio for  $C_{15}H_{19}N_3$  Calculated (241.16); Observed ( $M+1=242.3$ ).

### **Synthesis of 4-(4-methoxyphenyl)-1-(1*H*-pyrazol-4-yl)piperidine (21a)**

Synthesized by following general procedure 5.5 to obtain 33 mg of pale white solid (35% Yield).

$^1\text{H NMR}$  - (400 MHz,  $\text{CDCl}_3$ )  $\delta$  1.86-1.96 (m, 4H); 2.50-2.62 (m, 1H); 2.63-2.73 (m, 2H); 3.48 (apparent d,  $J=11.6$  Hz, 2H); 3.80 (s, 3H); 6.87 (d,  $J=8.8$  Hz, 2H); 7.17 (d,  $J=8.4$  Hz, 2H); 7.29 (s, 2H).

ATIR ( $\text{cm}^{-1}$ )- 3256, 3119, 3104, 3076, 2945, 2910, 2874, 2835, 2801, 1610, 1578, 1510, 1461, 1443, 1387, 1359, 1336, 1312, 1286, 1249, 1226, 1181, 1129, 1104, 1027, 990, 951, 932, 903, 861, 836, 804, 766, 744, 696, 653, 637, 618.

LC-MS– (ESI)  $m/z$  ratio for  $C_{15}H_{19}N_3O$  Calculated (257.34); Observed ( $M+1=258.5$ ).

### **Synthesis of 4-(2-methoxyphenyl)-1-(1*H*-pyrazol-4-yl)piperidine (21b)**

Synthesized by following the general procedure 5.5. Crude residue chromatographed using silica gel by EtOAc in Hexane gradient to obtain 101 mg of Light Pink solid (62% Yield).

$^1\text{H NMR}$  - (400 MHz,  $\text{CDCl}_3$ )  $\delta$  1.85-1.95 (m, 4H); 2.65-2.77 (m, 2H); 2.99-3.11 (m, 1H); 3.44-3.51 (m, 2H); 3.84 (s, 3H); 6.88 (d,  $J=8.4$  Hz, 1H); 6.95 (t,  $J=7.6$  Hz, 1H); 7.16-7.25 (m, 2H); 7.28 (s, 2H).

ATIR ( $\text{cm}^{-1}$ )- 3142, 3117, 3094, 3067, 22936, 2920, 2839, 2784, 2750, 2667, 1598, 1572, 1532, 1490, 1461, 1381, 1363, 1323, 1288, 1235, 1191, 1171, 1102.06, 1088, 1053, 1024, 992.38, 950, 906, 859, 780, 751, 735, 707, 664, 623.

LC-MS– (ESI)  $m/z$  ratio for  $C_{15}H_{19}N_3O$  Calculated (257.34); Observed ( $M+1=258.3$ ).

### Synthesis of 1-(1*H*-pyrazol-4-yl)-4-(*p*-tolyl)piperidine (21c)

Synthesized by following the general procedure 5.5. Crude residue was chromatographed by silica gel using EtOAc in hexane gradient to obtain white solid (10% Yield). [0-100% Hex:EtOAc]

$^1\text{H NMR}$  - (400 MHz,  $\text{CDCl}_3$ )  $\delta$  1.88-1.97 (m, 2H); 2.33 (s, 3H); 2.51-2.63 (m, 1H); 2.63-2.73 (m, 2H); 3.45-3.52 (m, 2H); 7.10-7.19 (m, 4H); 7.28 (s, 2H).

ATIR ( $\text{cm}^{-1}$ )- 3160, 3114, 3054, 3022, 2936, 2917, 2846, 2809, 2758, 2674.04, 2323, 2114, 2011, 1987, 1955, 1905, 1873, 1734, 1685, 1677, 1639, 1573, 1512, 1460, 1440, 1388, 1357, 1333, 1320, 1279, 1268, 1245, 1229, 1211, 1199, 1181, 1137, 1096, 1037, 1026, 990, 945, 904, 834, 809, 781.15, 763, 720, 698, 661, 649, 614.

LC-MS– (ESI)  $m/z$  ratio for  $C_{15}H_{19}N_3$  Calculated (241.34); Observed ( $M+1=242.1$ ).

### Synthesis of 4-(4-(methoxymethyl)phenyl)-1-(1*H*-pyrazol-4-yl)piperidine (21d)

Synthesized by following the general procedure 5.5. Crude residue obtained was chromatographed by silica gel using EtOAc in hexane gradient to obtain 9 mg of white solid (21% Yield). [0-100% Hex: EtOAc]

$^1\text{H NMR}$  - (400 MHz,  $\text{DMSO } d_6$ )  $\delta$  1.71-1.81 (m, 4H); 2.56-2.61 (m, 3H); 3.27 (s, 3H); 3.42 (apparent d,  $J=11.6$  Hz, 2H); 7.25-7.27 (m, 6H); 12.20 (bs, 1H).

ATIR ( $\text{cm}^{-1}$ ) - 3140, 3119, 2917, 2816.14, 2672, 1734, 1664, 1610, 1573, 1513, 1462, 1444, 1419, 1384, 1359, 1323, 1359, 1323, 1262, 1230, 1191, 1138, 1092, 1041, 1026, 989, 949, 903, 819, 772, 698, 657, 619.

LC-MS– (ESI)  $m/z$  ratio for  $\text{C}_{16}\text{H}_{21}\text{N}_3\text{O}$  Calculated (271.17); Observed ( $\text{M}+1=272.5$ ).

### Synthesis of *N*-(4-(1-(1*H*-pyrazol-4-yl)piperidin-4-yl)phenyl)-*N*-methylacetamide (21e)

Synthesized by following the general procedure 5.5. Crude residue obtained was chromatographed by silica gel using EtOH in DCM gradient to obtain 13 mg of pale yellow solid (26% Yield). [0-20% DCM:EtOH]

$^1\text{H}$ NMR - (400 MHz,  $\text{DMSO-}d_6$ )  $\delta$  1.70-1.90 (m, 7H); 2.53-2.56 (m, 2H); 2.56-2.67 (m, 1H); 3.12 (s, 3H); 3.43 (apparent d,  $J=11.8$  Hz, 2H); 7.22-7.27 (s overlapping with d, 4H); 7.33-7.35 (d,  $J=7.2$  Hz, 2H); 12.21 (bs, 1H).

$^1\text{H}$ NMR - (400 MHz,  $\text{CDCl}_3$ )  $\delta$  - 1.90 (s, 3H), 1.93-2.11 (m, 4H); 2.63-2.75 (m, 1H); 2.82 (apparent t, 2H); 3.28 (s, 3H); 3.56 (apparent d,  $J=11.6$  Hz, 2H); 7.14 (d,  $J=6.8$  Hz, 2H); 7.32 (d,  $J=8$  Hz, 2H); 7.39 (s, 2H).

ATIR ( $\text{cm}^{-1}$ ) - 3215, 3065, 2940, 2851, 2810, 2755, 2669, 1629, 1602, 1574, 1510, 1464, 1443, 1386, 1353, 1295, 1274, 1259, 1245, 1229, 1199, 1139, 1118, 1083, 1036, 1026, 991, 978, 930, 904, 846, 783, 748, 720, 689, 656, 602.

LC-MS– (ESI)  $m/z$  ratio for  $\text{C}_{17}\text{H}_{22}\text{N}_4\text{O}$  Calculated (298.39); Observed ( $\text{M}+1=299.7$ ,  $\text{M}+\text{Na}=321.7$ ).

### Synthesis of *N*-(4-(1-(1*H*-pyrazol-4-yl)piperidin-4-yl)phenyl)acetamide (21f)

Synthesized by following the general procedure 5.5. Crude residue obtained was chromatographed by silica gel using MeOH in DCM gradient to obtain 33 mg of yellow solid (35% Yield). [0-20% DCM:MeOH]

<sup>1</sup>HNMR - (400 MHz, CDCl<sub>3</sub>) δ 1.86-1.96 (m, 2H); 2.18 (s, 3H); 2.54-2.64 (m, 1H); 2.64-2.73 (m, 2H); 3.47-3.49 (m, 2H); 7.09 (bs, 1H); 7.21 (d, *J*=8.0 Hz, 2H); 7.27 (s, 2H); 7.43 (d, *J*=8.0 Hz, 2H).

ATIR (cm<sup>-1</sup>)- 3329, 3142, 3123, 3073, 2943, 2919, 2871, 2845, 2810, 2662, 1660, 1612, 1593, 1578, 1514, 1464, 1447, 1407, 1385, 1360, 1315, 1285, 1256, 1222, 1191, 1131, 1102, 1092, 1040, 1027, 990, 967, 950, 903, 863, 838, 822, 773, 701, 652, 619.

LC-MS– (ESI) *m/z* ratio for C<sub>16</sub>H<sub>20</sub>N<sub>4</sub>O Calculated (284.36); Observed (M+1=285.4).

### **Synthesis of 5-(1-(1*H*-pyrazol-4-yl)piperidin-4-yl)-2-methoxypyridine (21g)**

Synthesized by following the general procedure 5.5. Crude obtained was chromatographed by silica gel using EtOAc in hexane gradient to obtain 13 mg of white solid (42% Yield). [0-100% Hex:EtOAc]

<sup>1</sup>HNMR - (400 MHz, CDCl<sub>3</sub>) δ 1.86-1.94 (m, 4H); 2.52-2.62 (m, 1H); 2.63-2.73 (m, 2H); 3.46-3.52 (m, 2H); 3.92 (s, 3H); 6.71 (d, *J*=8.8 Hz, 1H); 7.28 (bs, 2H); 7.47 (dd, *J*=8.4 Hz, 2.4 Hz, 8.05 (d, *J*=2.0 Hz, 1H).

ATIR (cm<sup>-1</sup>)- 2936, 2852, 2807, 2753, 1621, 1578, 1512, 1464, 1443, 1430, 1398, 1387, 1372, 1324, 1296, 1267, 1247, 1215, 1199, 1177, 1149, 1128, 1101, 1079, 1058, 1039, 1024, 1000, 976, 952, 938, 911, 895, 874, 845, 822, 791, 752, 718, 665, 630.

LC-MS– (ESI) *m/z* ratio for C<sub>14</sub>H<sub>18</sub>N<sub>4</sub>O Calculated (258.33); Observed (M+1=259.4).

### Synthesis of 1-(1*H*-pyrazol-4-yl)-4-(*m*-tolyl)piperidine (21h)

Synthesized by following the general procedure 5.5. Crude obtained was chromatographed by silica gel using EtOAc in hexane gradient to obtain 14 mg of yellow solid (39% Yield). [0-100% Hex:EtOAc]

<sup>1</sup>HNMR - (400 MHz, CDCl<sub>3</sub>) δ 1.88-2.00 (m, 4H); 2.35 (s, 3H); 2.51-2.63 (m, 1H); 2.64-2.73 (m, 2H); 3.45-3.52 (m, 2H); 7.01-7.08 (m, 3H); 7.22 (t, *J*=7.2 Hz, 1H); 7.28 (s, 2H).

ATIR (cm<sup>-1</sup>)-3142, 3119, 3075, 3019, 2933, 2873, 2844, 2811, 2758, 2673, 1605, 1573, 1523, 1487, 1462, 1443, 1387, 1360, 1316, 1279, 1247, 1219, 1180, 1163, 1143, 1108, 1038, 989, 948, 930, 888, 876, 839, 771, 700, 663, 651, 617.

LC-MS– (ESI) *m/z* ratio for C<sub>15</sub>H<sub>19</sub>N<sub>3</sub> Calculated (241.16); Observed (M+1=242.3).

### Synthesis of Compound 1-(1*H*-pyrazol-4-yl)-4-(*o*-tolyl)piperidine (21i)

Synthesized by following the general procedure 5.5. Crude residue obtained was chromatographed by silica gel using EtOAc in hexane gradient to obtain 15 mg of white solid (52% Yield). [0-100% Hex:EtOAc]

<sup>1</sup>HNMR - (400 MHz, CDCl<sub>3</sub>) δ 1.82-2.01 (m, 4H); 2.36 (s, 3H); 2.71 (td, *J*=11.6 Hz, 2.4 Hz); 2.76-2.87 (m, 1H); 3.51 (apparent d, *J*=11.2 Hz, 2H); 7.08-7.24 (m, 4H); 7.28 (s, 2H).

ATIR (cm<sup>-1</sup>) – 3165, 3144, 3121, 3103, 3077, 2977, 2954, 2918, 2877, 2838, 1662, 1578, 1533, 1488, 1462, 1445, 1430, 1387, 1360, 1334, 1322, 1293, 1284, 1263, 1235, 1182, 1143, 1120, 1099, 1054, 1037, 990, 937, 902, 862, 823, 782, 749, 725, 702, 660, 623.

LC-MS– (ESI)  $m/z$  ratio for  $C_{15}H_{19}N_3$  Calculated (241.16); Observed ( $M+1=242.3$ ).

### **Synthesis of 4-iodo-3-methyl-1-(tetrahydro-2*H*-pyran-2-yl)-1*H*-pyrazole (23)**

Synthesis was done by procedure known in literature. Crude residue obtained was chromatographed by silica gel using ethyl ether in hexane gradient to obtain 305 mg of colorless liquid (72% Yield). [0-20% Hex:Ethyl ether]

$^1\text{H NMR}$  - (400 MHz,  $\text{CDCl}_3$ )  $\delta$  1.58-1.72 (m, 3H); 1.97-2.07 (m, 3H); 2.25 (s, 3H); 3.67 (td,  $J=11.2$  Hz, 2.8 Hz, 1H); 4.01-4.09 (m, 1H); 5.27 (distorted dd,  $J=9.2$  Hz, 1H); 7.57 (s, 1H).

ATIR ( $\text{cm}^{-1}$ ) – 3121, 2940, 2851, 2735, 1515, 1439, 1377, 1344, 1318, 1277, 1259, 1245, 1202, 1179, 1148, 1081, 1058, 1039, 980, 936, 909, 875, 844, 791, 764, 681, 658, 624.

LC-MS– (ESI)  $m/z$  ratio for  $C_9H_{13}IN_2O$  Calculated (292.12); Observed ( $M+1=293.3$ ).

### **Synthesis of 3-iodo-5-methyl-1-(tetrahydro-2*H*-pyran-2-yl)-1*H*-pyrazole (24)**

Synthesis was done by procedure known in literature. Crude residue obtained was chromatographed by silica gel using EtOAc in hexane gradient to obtain mg of yellow pale liquid (99% Yield). [0-30% Hex:EtOAc]

$^1\text{H NMR}$  - (400 MHz,  $\text{CDCl}_3$ )  $\delta$  1.53-1.75 (m, 3H); 1.89-1.98 (m, 1H); 2.06-2.13 (m, 1H); 2.32 (s, 3H); 2.36-2.50 (m, 1H); 3.62 (distorted td,  $J=11.2$  Hz, 2.8 Hz, 1H); 3.98-4.04 (m, 1H); 5.21 (dd,  $J=10$  Hz, 2.8 Hz, 1H); 6.19 (s, 1H).

ATIR ( $\text{cm}^{-1}$ ) – 3119, 3059, 2992, 2951, 2926, 2849, 2731, 1534, 1465, 1455, 1418, 1385, 1324, 1313, 1282, 1247, 1202, 1177, 1147, 1111, 1079, 1056, 1039, 1001, 989, 942, 912, 876, 845, 824, 798, 670, 646.

LC-MS– (ESI)  $m/z$  ratio for  $\text{C}_9\text{H}_{13}\text{N}_2\text{O}$  Calculated (292.12); Observed ( $M+1=293.3$ ).

### Synthesis of 1-(3-methyl-1*H*-pyrazol-4-yl)-4-phenylpiperidine (25a)

Synthesized by following the general procedure 5.5. Crude residue obtained was chromatographed by silica gel using EtOAc in hexane gradient to obtain 38 mg of white solid (42% Yield). [0-100% Hex:EtOAc]

$^1\text{H}$ NMR - (400 MHz,  $\text{DMSO-}d_6$ )  $\delta$  1.76-1.83 (m, 4H); 2.12 (s, 3H); 2.54-2.62 (m, 3H); 3.17 (apparent d,  $J=11.2$  Hz, 2H); 7.15-7.22 (m, 1H); 7.27-7.35 (m, 5H); 12.01 (bs, 1H).

ATIR ( $\text{cm}^{-1}$ )- 3224, 3078, 3019, 2936, 2915, 2797, 2738, 2662, 1596, 1563, 1507, 1490, 1460, 1449, 1438, 1426, 1383, 1300, 1271, 1248, 1208, 1173, 1158, 1136, 1102, 1063, 1031, 1013, 983, 942, 909, 852, 793, 758, 700, 664, 616.

LC-MS– (ESI)  $m/z$  ratio for  $\text{C}_{15}\text{H}_{19}\text{N}_3$  Calculated (241.34), Observed ( $M+1=242.5$ ).

### Synthesis of 1-(5-methyl-1*H*-pyrazol-3-yl)-4-phenylpiperidine (26a)



Synthesized by following the general procedure 5.5. Crude residue obtained was chromatographed by silica gel using EtOAc in hexane gradient to obtain 62 mg of white solid (79% Yield). [0-100% Hex:EtOAc]

<sup>1</sup>HNMR - (600 MHz, CDCl<sub>3</sub>) δ 1.64-1.982 (m, 4H); 2.12 (s, 3H); 2.55-2.68 (m, 2H); 3.7 (apparent d, *J*=11.2 Hz, 2H); 5.47 (s, 1H); 7.17-7.20 (m, 1H); 7.24-7.31 (m, 4H); 11.43 (bs, 1H).

ATIR (cm<sup>-1</sup>)- 3188, 3133, 3107, 3060, 3021, 2947, 2917, 2878, 2820, 2752, 2711, 1570, 1492, 1462, 1439, 1385, 1350, 1289, 1247, 1194, 1173, 1118, 1103, 1056, 1033, 1018, 988, 945, 910, 871, 809, 761, 740, 720, 699, 660, 611.

LC-MS– (ESI) *m/z* ratio for C<sub>15</sub>H<sub>19</sub>N<sub>3</sub> Calculated (241.34), Observed (*M*+1=242.5).

### **Synthesis of *tert*-butyl 4-(phenylsulfonyl)piperidine-1-carboxylate (30)**

Synthesized by procedure known in literature. It was then subjected to oxidation by mCPBA to obtain 306 mg of white solid (97% Yield).

<sup>1</sup>HNMR - (400 MHz, CDCl<sub>3</sub>) δ 1.43 (s, 9H); 1.56-1.67 (m, 2H); 1.97 (apparent d, *J*=13.2 Hz, 2H); 2.65-2.68 (m, 2H); 3.03 (tt, *J*=12 Hz, 3.6 Hz, 1H); 4.19-4.27 (m, 2H); 7.58 (apparent distorted t, *J*=7.6 Hz, 2H); 7.68 (apparent distorted t, *J*=7.2 Hz, 1H); 7.87 (d, *J*=7.2 Hz, 2H).

### **Synthesis of 4-(phenylsulfonyl)piperidine (31b)**

Synthesized by following the general procedure 5.4 to obtain 158 mg of pale yellow solid (75% Yield).

<sup>1</sup>HNMR - (400 MHz, CDCl<sub>3</sub>)  $\delta$  1.51-1.63 (m, 2H); 2.00 (apparent d,  $J=12.8$  Hz, 2H); 2.56 (td,  $J=12.4$  Hz, 2.4 Hz, 2H); 3.02 (tt,  $J=12.4$  Hz, 3.2 Hz, 1H); 3.12-3.22 (m, 2H); 7.57- (apparent distorted t,  $J=7.6$  Hz, 2H); 7.66 (apparent distorted t,  $J=7.6$  Hz, 1H); 7.87 (d,  $J=7.2$  Hz, 2H).

### Synthesis of 4-(phenylthio)-1-(1*H*-pyrazol-5-yl)piperidine (32a)

Synthesized by following the general procedure 5.5. Crude residue obtained was chromatographed by silica gel using EtOAc in hexane gradient to obtain 24 mg of pale yellow liquid (34% Yield). [0-100% Hex:EtOAc]

<sup>1</sup>HNMR - (400 MHz, DMSO-*d*<sub>6</sub>)  $\delta$  1.50-1.59 (m, 2H); 1.94 (apparent d,  $J=13.2$  Hz, 2H); 2.76 (apparent t,  $J=12.4$  Hz, 2H); 3.34-3.42 (m, 1H); 3.53-3.58 (m, 2H); 5.68 (s, 1H); 7.22-7.30 (m, 1H); 7.35 (t,  $J=8$  Hz, 2H); 7.39-7.46 (m, 3H); 11.76 (bs, 1H).

ATIR (cm<sup>-1</sup>)- 3174, 3072, 3055, 2942, 2813, 1952, 1871, 1581, 1538, 1478, 1462, 1437, 1382, 1346, 1317, 1267, 1247, 1209, 1150, 1089, 1066, 1039, 1017, 986, 925, 898, 855, 735, 689.

LC-MS– (ESI)  $m/z$  ratio for C<sub>14</sub>H<sub>17</sub>N<sub>3</sub>S Calculated (259.37), Observed (M+1=260.5).

### Synthesis of 4-(phenylsulfonyl)-1-(1*H*-pyrazol-5-yl)piperidine (32b)

Synthesized by following the general procedure 5.5. Crude residue obtained was chromatographed by silica gel using EtOAc in Hexane gradient to obtain 40 mg of pale yellow solid (63% Yield). [0-100% Hex:EtOAc]

<sup>1</sup>HNMR - (400 MHz, CDCl<sub>3</sub>) δ 1.83 (ddd, *J*=16.8 Hz, 12.4 Hz, 4.4 Hz, 2H); 2.09 (apparent d, *J*=13.2 Hz, 2H); 2.72 (td, *J*=12.4 Hz, 2.4 Hz, 2H); 3.05 (tt, *J*=12 Hz, 3.6 Hz, 1H); 3.86 (apparent d, *J*=12.4 Hz, 2H); 5.72 (d, *J*=2.4 Hz, 1H); 7.39 (d, *J*=2.8 Hz, 1H); 7.58 (distorted t, *J*=7.2 Hz, 2H); 7.64-7.68 (m, 1H); 7.90 (apparent d, *J*=7.2 Hz, 2H).

ATIR (cm<sup>-1</sup>) 3161, 3128, 3066, 3029, 2960, 2943, 2839, 2765, 2719, 2662, 1989, 1902, 1819, 1776, 1709, 1605, 1588, 1537, 1497, 1479, 1466, 1447, 1388, 1314, 1283, 1254, 1229, 1198, 1182, 1136, 1101, 1085, 1071, 1036, 1019, 981, 927, 903, 863, 809, 753, 723, 688.

LC-MS- (ESI) *m/z* ratio for C<sub>14</sub>H<sub>17</sub>N<sub>3</sub>O<sub>2</sub>S Calculated (291.37); Observed (M+1=292.6).

#### **Synthesis 4-(phenylthio)-1-(1*H*-pyrazol-4-yl)piperidine (33a )**

Synthesized by following the general procedure 5.5. Crude residue was chromatographed by silica gel using EtOAc in hexane gradient to obtain 31 mg of pale yellowish white solid (61% Yield). [0-100% Hex:EtOAc]

<sup>1</sup>HNMR - (400 MHz, DMSO-*d*<sub>6</sub>) 1.60 (ddd, *J*=23.6 Hz, 10.8 Hz, 3.6 Hz, 2H); 1.92-1.98 (m, 2H); 2.59 (apparent t, *J*=9.6 Hz, 2H); 3.20-3.38 (m, 3H); 7.22-7.28 (s overlapping with m, 3H); 7.30-7.37 (m, 2H); 7.40-7.42 (m, 2H), 12.29 (bs, 1H).

ATIR (cm<sup>-1</sup>)- 3290, 3116, 3056, 3015, 2945, 2743, 2691, 2660, 1578, 1566, 1490, 1472, 1436, 1377, 1360, 1340, 1264, 1250, 1230, 1200, 1174, 1141, 1127, 1090, 1069, 1027, 987, 932, 894, 848, 793, 748, 740, 690, 665, 618.

LC-MS– (ESI)  $m/z$  ratio for  $C_{14}H_{17}N_3S$  Calculated (259.37), Observed ( $M+1=260.5$ )

### Synthesis of Compound 4-(phenylsulfonyl)-1-(1*H*-pyrazol-4-yl)piperidine (33b)

Synthesized by following the general procedure 5.5. Crude residue obtained was chromatographed by silica gel using EtOAc in hexane gradient to obtain 7 mg of pale yellow solid (39% Yield). [0-100% Hex:EtOAc]

$^1\text{H NMR}$  - (400 MHz,  $\text{CDCl}_3$ )  $\delta$  1.80-1.93 (m, 2H); 2.09 (apparent d,  $J=18.8$  Hz, 2H); 2.49-2.58 (m, 2H); 2.99 (tt,  $J=12.4$  Hz, 2.8 Hz, 1H); 3.43 (apparent d,  $J=11.6$  Hz, 2H); 7.20 (s, 2H); 7.55-7.62 (m, 2H); 7.59-7.71 (m, 1H); 7.89 (d,  $J=8$  Hz, 2H).

ATIR ( $\text{cm}^{-1}$ ) - 3134, 3114, 3064, 2948, 2841, 1573, 1455, 1446, 1393, 1381, 1366, 1341, 1306, 1274, 1242, 1219, 1173, 1142, 1086, 1033, 992, 924, 893, 859, 779, 756, 725, 706, 689, 665, 620.

LC-MS– (ESI)  $m/z$  ratio for  $C_{14}H_{17}N_3O_2S$  Calculated (291.37); Observed ( $M+1=292.6$ ).

## APPENDIX A

### ABBREVIATIONS

AA - Arachidonic acid

ADME – Absorption, Distribution, Metabolism, Elimination

ATR- Attenuated total reflectance

BBB – the Blood-brain barrier

Boc<sub>2</sub>O- Di-*tert*-butyl carbonate

COX – Cyclooxygenase

CA – Cardiac arrest

CYPs – Cytochrome P-450s

CBF – Cerebral blood flow

DiHETs – Dihydroxy eicosatetraenoic acid

DCI – Diffused cerebral ischemia

DBDD – 12,12-dibromododec-11-enoic acid

DDMS - N-methylsulfonyl-12,12-dibromododec-11-enamide

DPMS - N-methylsulfonyl-15,15-dibromopentadec-14-enamide

DMSO- Dimethyl sulfoxide

DMF-Dimethylformamide

DCM- Dichloromethane

EET – Epoxyecosatetraenoic acid

EBI – Early brain injury

ESI-Electron spray ionisation

EtOAc- Ethyl acetate

Et<sub>3</sub>N- triethylamine

HEDE - (6Z,15Z)-20-hydroxyicosa-6,15-dienoic acid

HBD – Hydrogen bond donors

HBA – Hydrogen bond acceptors

HCl- hydrochloric acid

HLM- Human liver microsomes

ICP – Intracranial pressure

IR- Infrared spectroscopy

LT – Leukotrienes

LOX – Lipoxygenases

MsCl- Mesityl chloride

MS- Mass spectroscopy

NRB - Number of rotatable bonds

NMR- Nuclear magnetic resonance spectroscopy

PdCl<sub>2</sub>(dppf)- [1,1'-Bis(Diphenylphosphino)ferrocene]dichloropalladium(II)

PSA – Polar surface area

PTSA.H<sub>2</sub>O-Para-toluene sulfonic acid monohydrate

PG – Prostaglandins

PKC – Protein kinase

PhSH- thiophenol

mCPBA- meta-chloroperbenzoic acid

RLM- Rat liver microsomes

RKM- Rat kidney microsomes

rCYP4F2- Recombinant CYP4F2

SAR- Structural activity relationship

SAH – Subarachnoid hemorrhage

sEH – Soluble epoxide hydrolase

TXA – Thromboxane

THF- Tetrahydrofuran

THP- Tetrahydropyran

WDI – World drug index

20-HETE – 20-hydroxyecosatetraenoic acid

1-ABT – 1-aminobenzotriazole

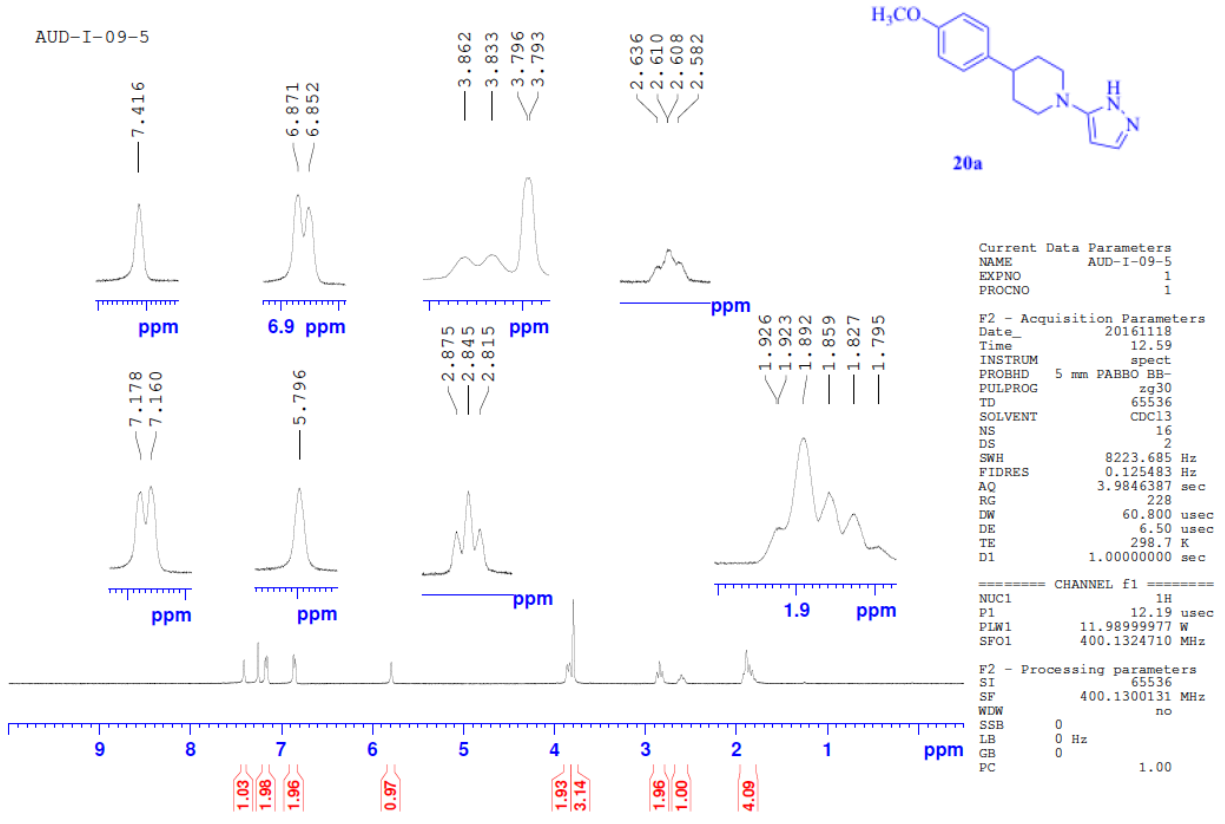
17-ODYA - octadec-17-ynoic acid

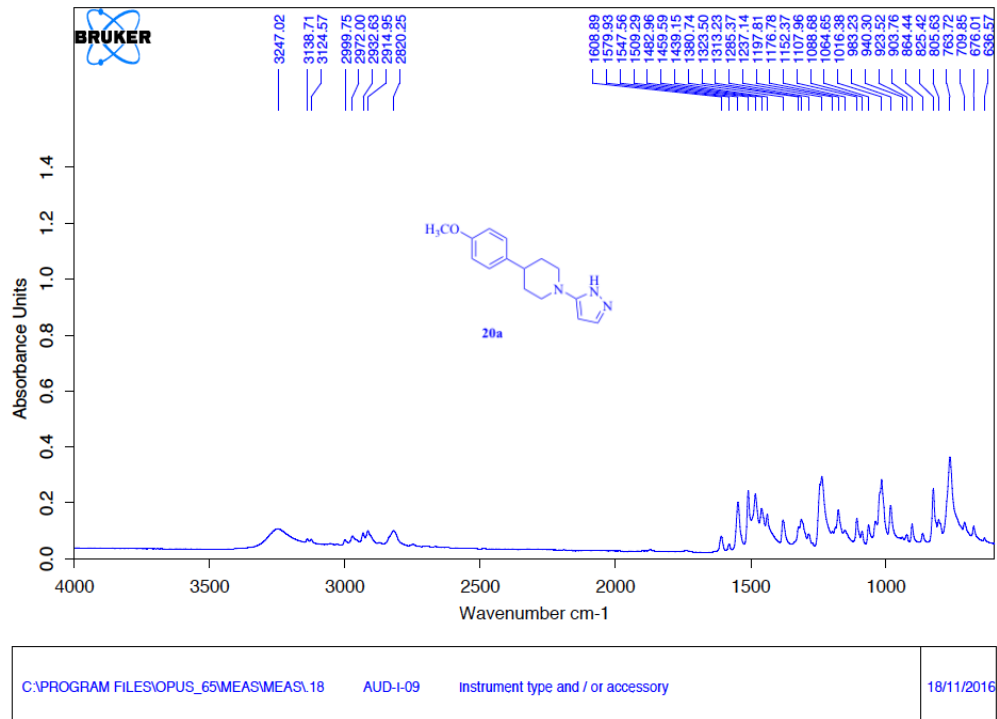
10-SUYS - undec-10-yn-1-yl sulfate

## **APPENDIX B**

### **EXPERIMENTAL SPECTRA**



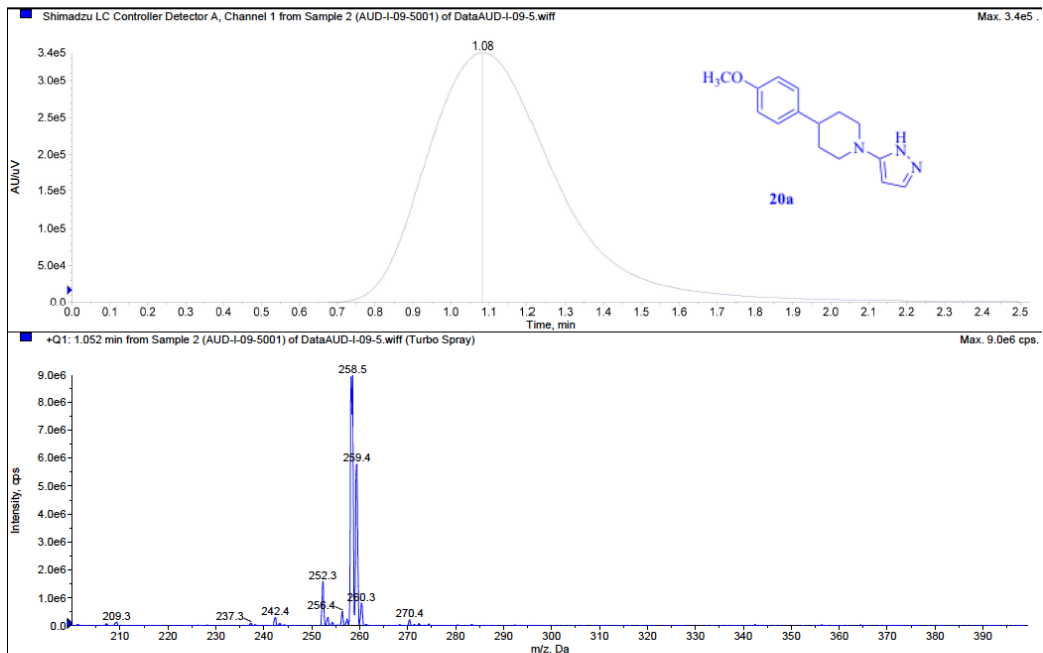




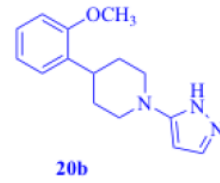
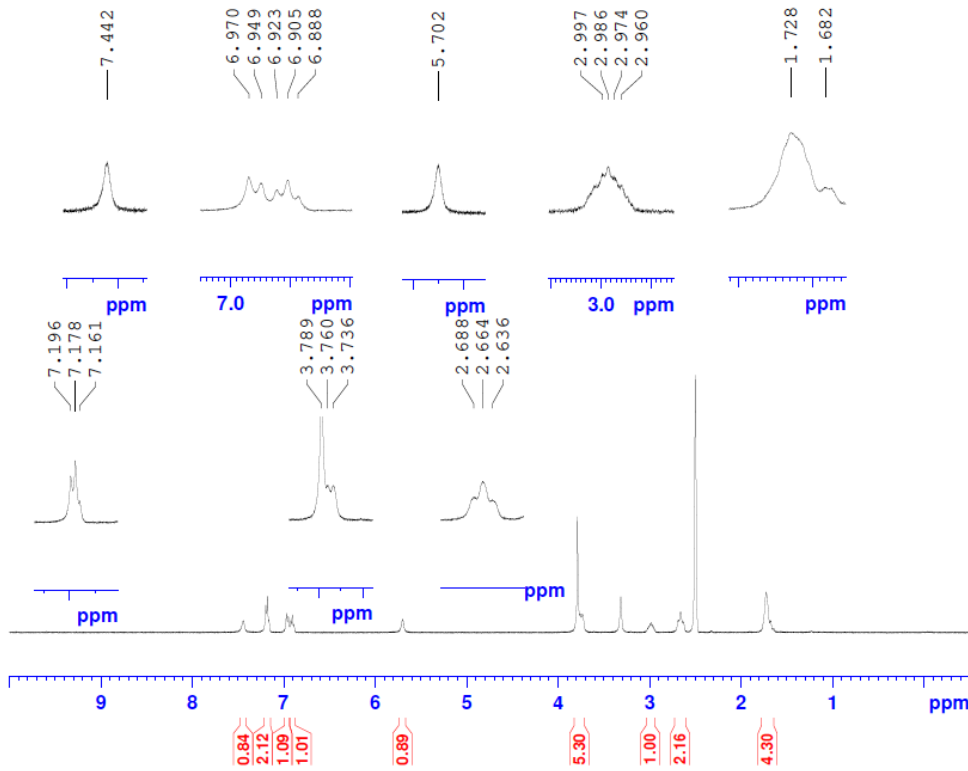
Instrument Settings  
\*Post PM

\*University of Pittsburgh, API2000 SM: B19200702  
\*Ryan Kuntz, Staff Engineer, SCIEX

Printing Time: 2:30:20 PM  
Printing Date: Friday, May 04, 2018



AUD-I-25-2

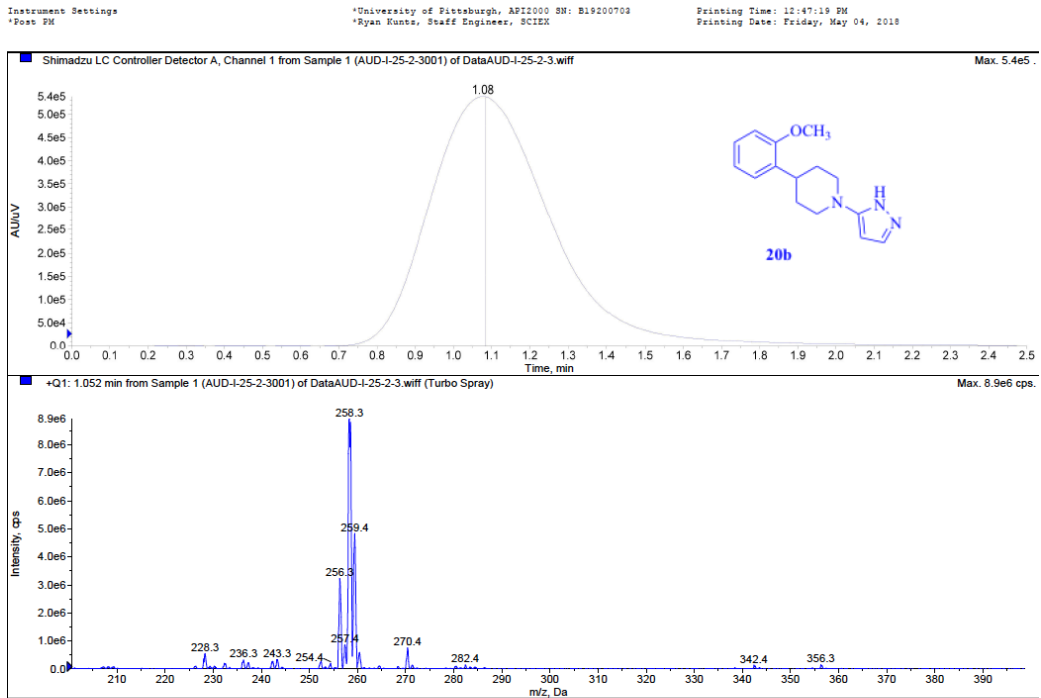
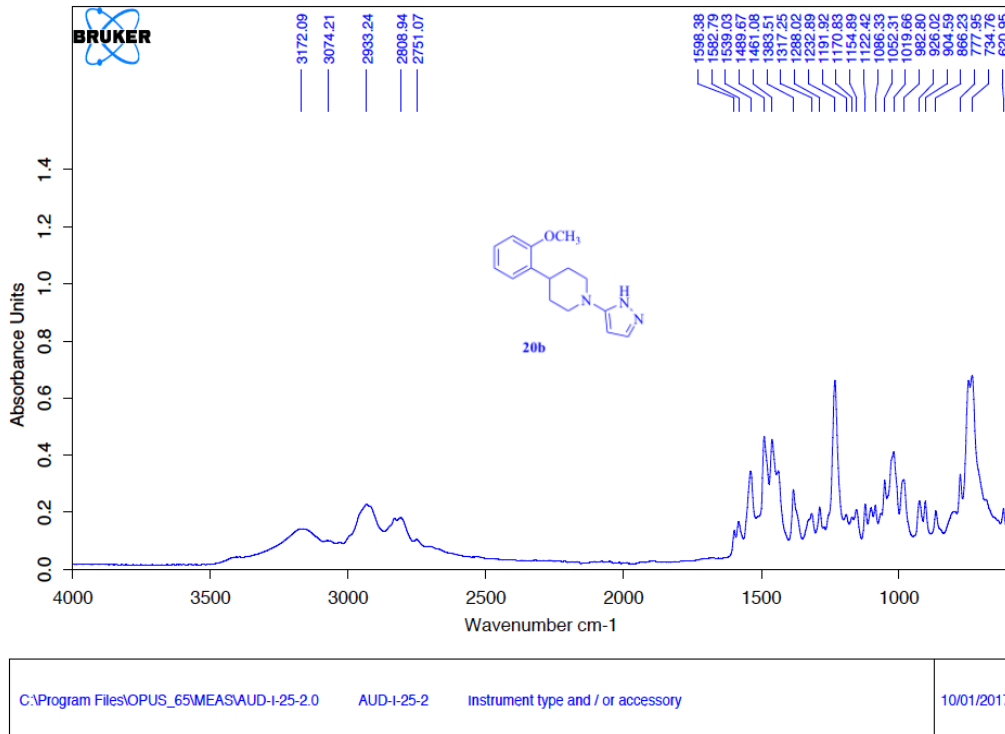


Current Data Parameters  
NAME AUD-I-25-2  
EXPNO 1  
PROCNO 1

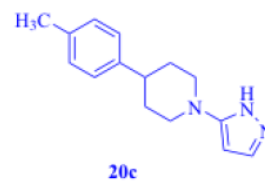
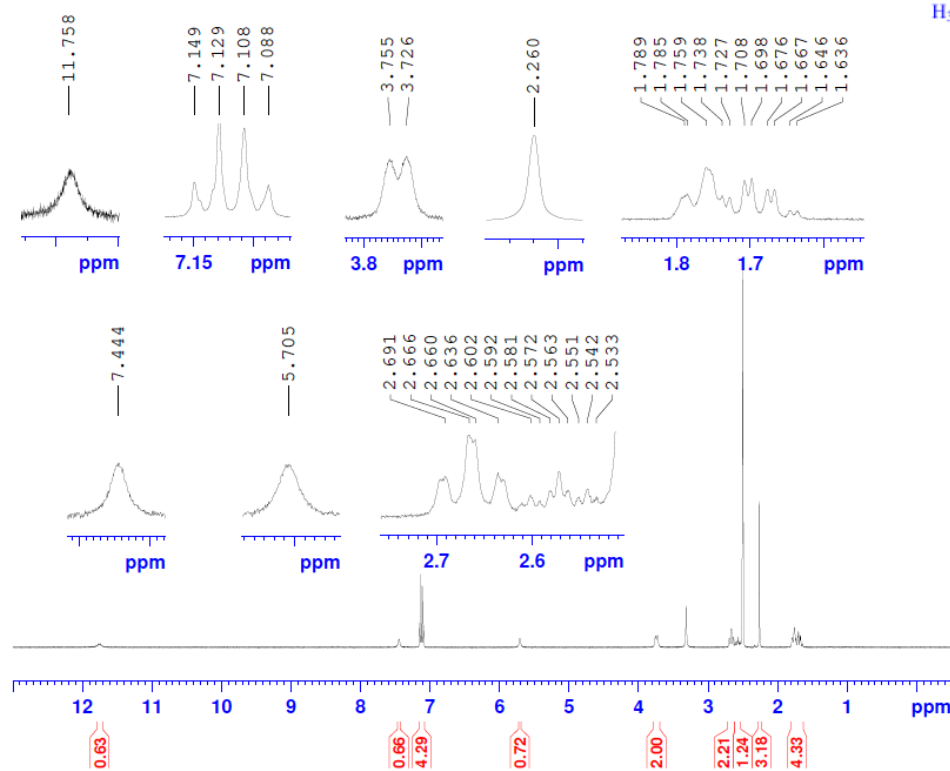
F2 - Acquisition Parameters  
Date\_ 20170110  
Time 18.16  
INSTRUM spect  
PROBHD 5 mm PABBO BB-  
PULPROG zg30  
TD 65536  
SOLVENT DMSO  
NS 16  
DS 2  
SWH 8223.685 Hz  
FIDRES 0.125483 Hz  
AQ 3.9846387 sec  
RG 228  
DW 60.800 usec  
DE 6.50 usec  
TE 298.1 K  
D1 1.00000000 sec

===== CHANNEL f1 =====  
NUC1 1H  
P1 12.19 usec  
PLW1 11.98999977 W  
SFO1 400.1324710 MHz

F2 - Processing parameters  
SI 65536  
SF 400.1300042 MHz  
WDW no  
SSB 0  
LB 0 Hz  
GB 0  
PC 1.00



AUD-I-40

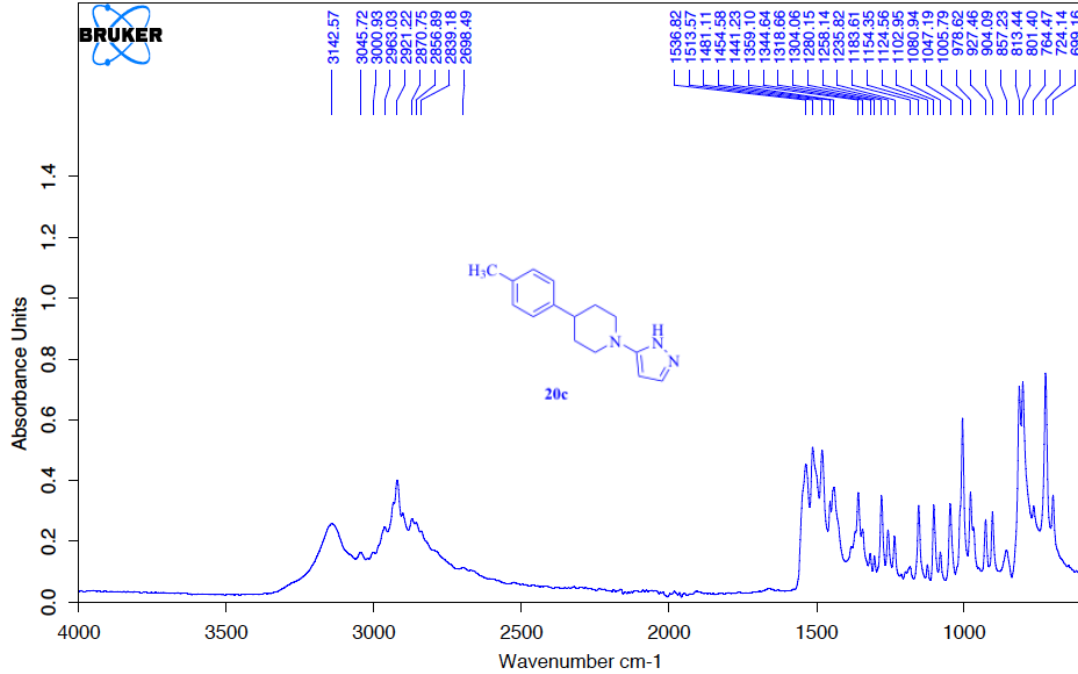


Current Data Parameters  
NAME AUD-I-40  
EXPNO 2  
PROCNO 1

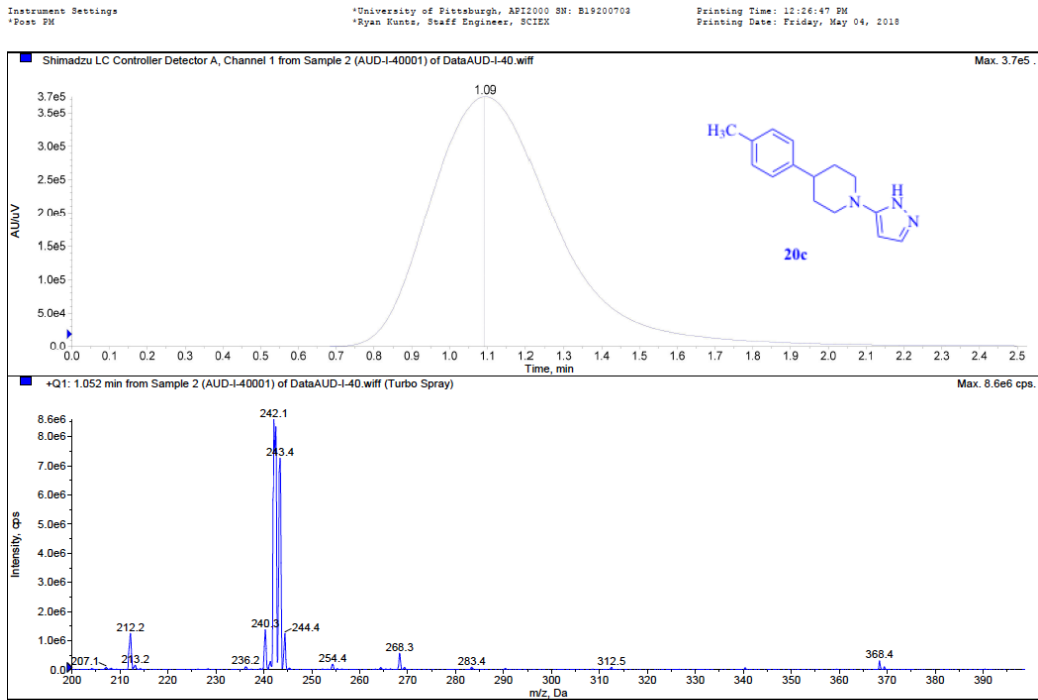
F2 - Acquisition Parameters  
Date\_ 20170314  
Time 14.26  
INSTRUM spect  
PROBHD 5 mm PABBO BB-  
PULPROG zg30  
TD 65536  
SOLVENT DMSO  
NS 17  
DS 0  
SWH 8223.685 Hz  
FIDRES 0.125483 Hz  
AQ 3.9846387 sec  
RG 228  
DW 60.800 usec  
DE 6.50 usec  
TE 298.5 K  
D1 2.0000000 sec

CHANNEL f1  
NUC1 1H  
P1 12.19 usec  
PLW1 11.9899977 W  
SFO1 400.1324710 MHz

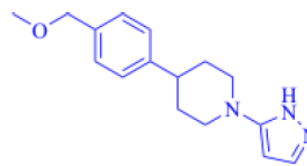
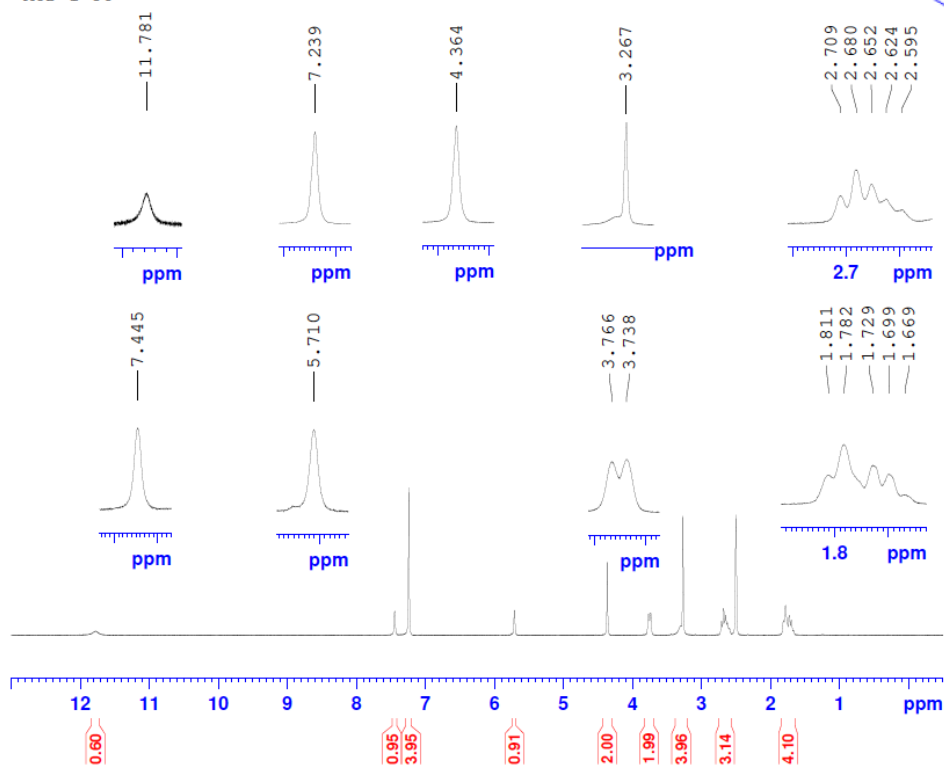
F2 - Processing parameters  
SI 32768  
SF 400.1300023 MHz  
WDW no  
SSB 0  
LB 0 Hz  
GB 0  
PC 1.00



C:\PROGRAM FILES\OPUS\_65\MEAS\MEAS\AUD-I-40.0    AUD-I-40    Instrument type and / or accessory    15/01/2018



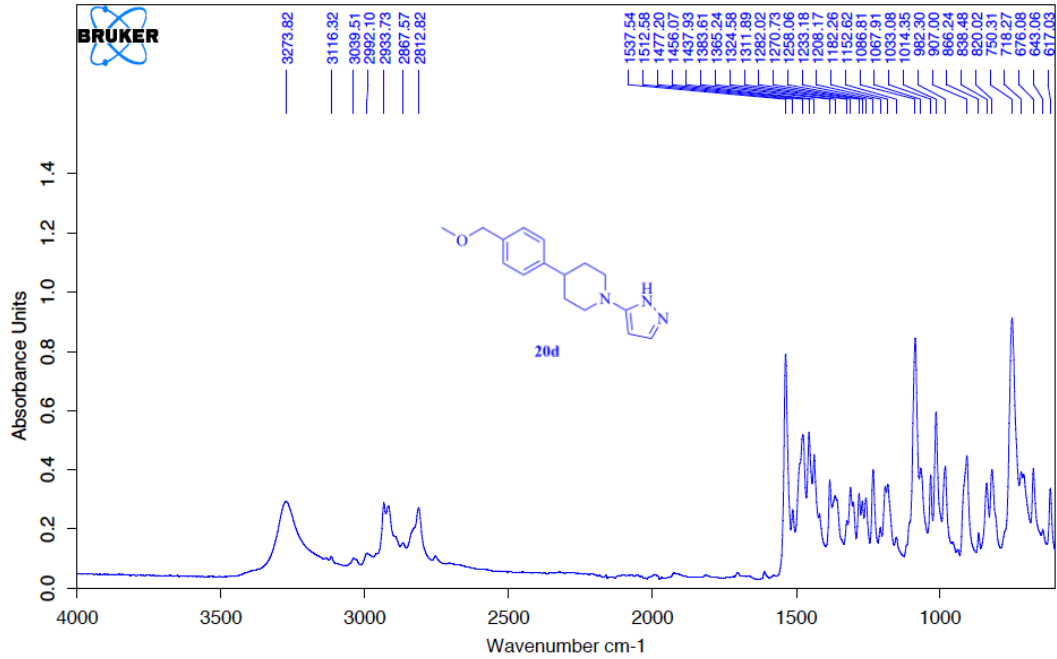
AUD-I-58



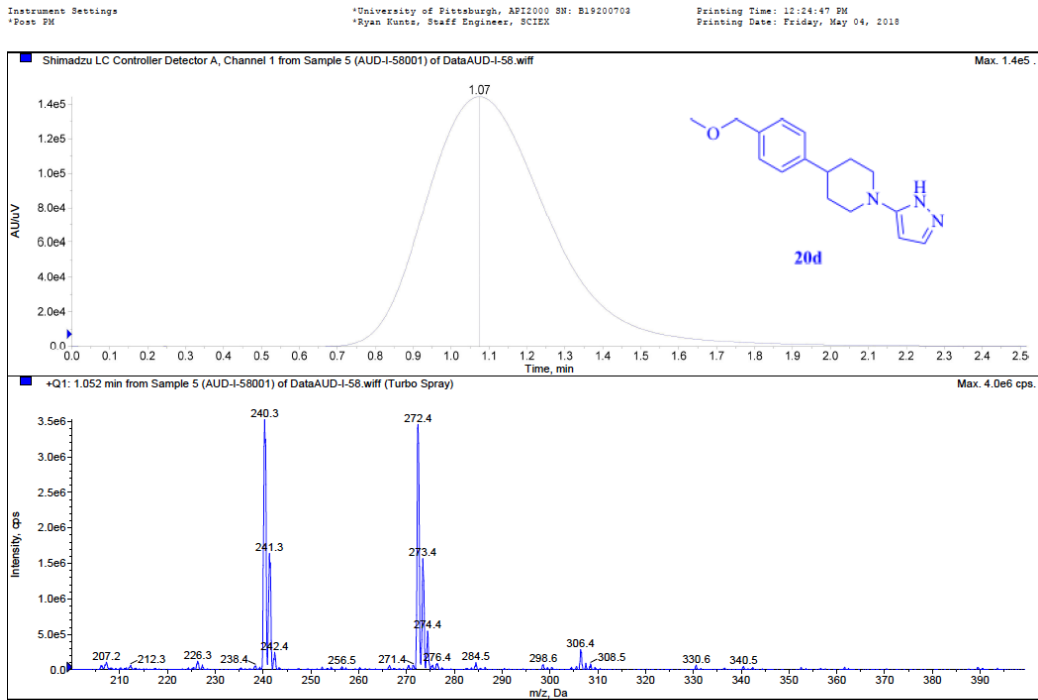
Current Data Parameters  
NAME AUD-I-58  
EXPNO 3  
PROCNO 1

F2 - Acquisition Parameters  
Date\_ 20170512  
Time 13.16  
INSTRUM spect  
PROBHD 5 mm PABBO BB-  
PULPROG zg30  
TD 65536  
SOLVENT DMSO  
NS 16  
DS 2  
SWH 8223.685 Hz  
FIDRES 0.125483 Hz  
AQ 3.9846387 sec  
RG 101  
DW 60.800 usec  
DE 6.50 usec  
TE 300.7 K  
D1 1.00000000 sec

===== CHANNEL f1 =====  
NUC1 1H  
P1 12.19 usec  
PLW1 11.98999977 W  
SFO1 400.1324710 MHz  
F2 - Processing parameters  
SI 65536  
SF 400.1300066 MHz  
WDW no  
SSB 0  
LB 0 Hz  
GB 0  
PC 1.00

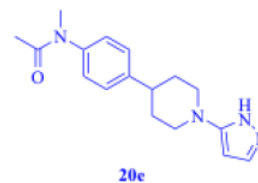
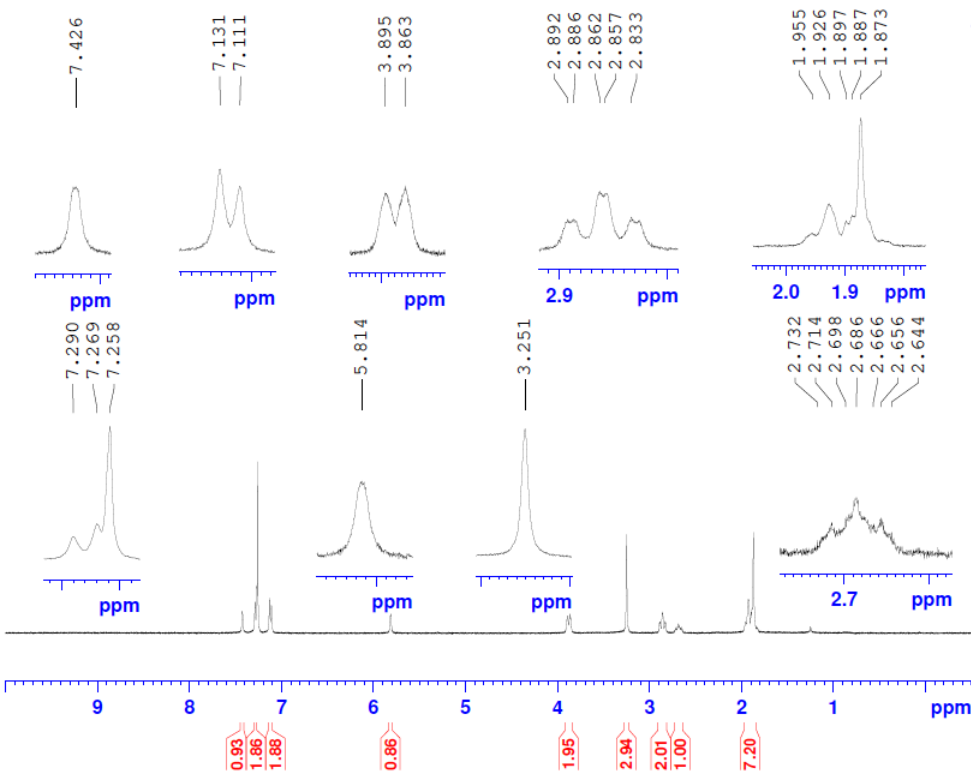


C:\Program Files\OPUS\_65\MEAS\AUD-I-58.0    AUD-I-58    Instrument type and / or accessory    12/05/2017





AUD-II-128-4

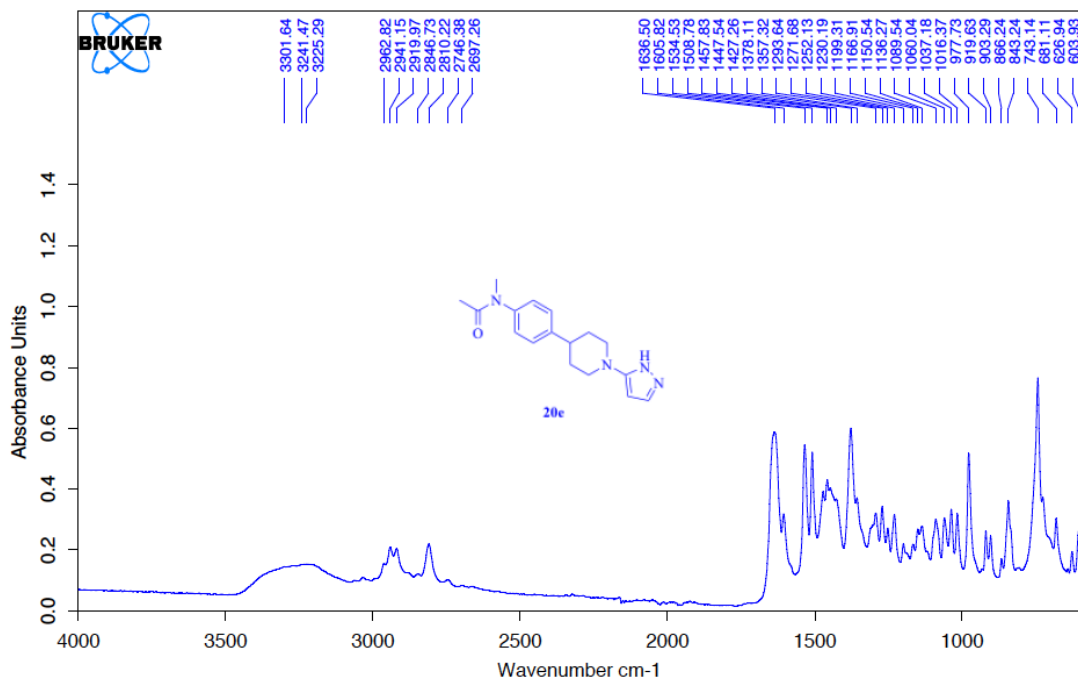


Current Data Parameters  
NAME AUD-II-128-4  
EXPNO 1  
PROCNO 1

F2 - Acquisition Parameters  
Date\_ 20171121  
Time 15.58  
INSTRUM spect  
PROBHD 5 mm PABBO BB-  
PULPROG zg30  
TD 65536  
SOLVENT CDC13  
NS 16  
DS 2  
SWH 8223.685 Hz  
FIDRES 0.125483 Hz  
AQ 3.9846387 sec  
RG 256  
DW 60.800 usec  
DE 6.50 usec  
TE 297.6 K  
D1 1.0000000 sec

===== CHANNEL f1 =====  
NUC1 1H  
P1 12.19 usec  
PLW1 11.98999977 W  
SFO1 400.1324710 MHz

F2 - Processing parameters  
SI 65536  
SF 400.1300114 MHz  
WDW no  
SSB 0  
LB 0 Hz  
GB 0  
PC 1.00



C:\Program Files\OPUS\_65\MEAS\MEAS\38

AUD-II-128-4

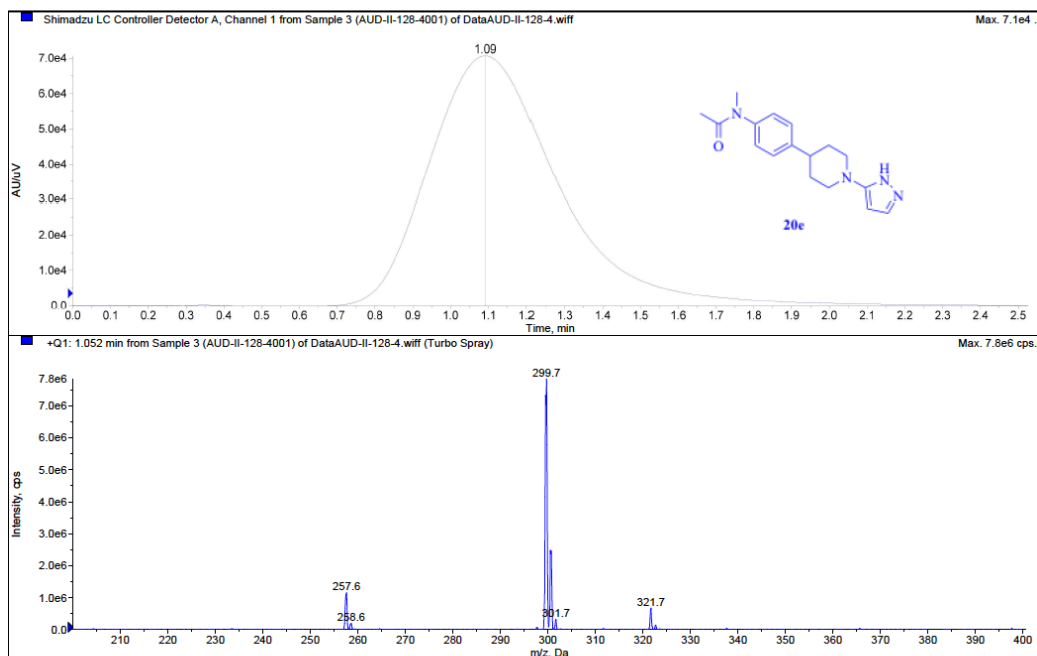
Instrument type and / or accessory

21/11/2017

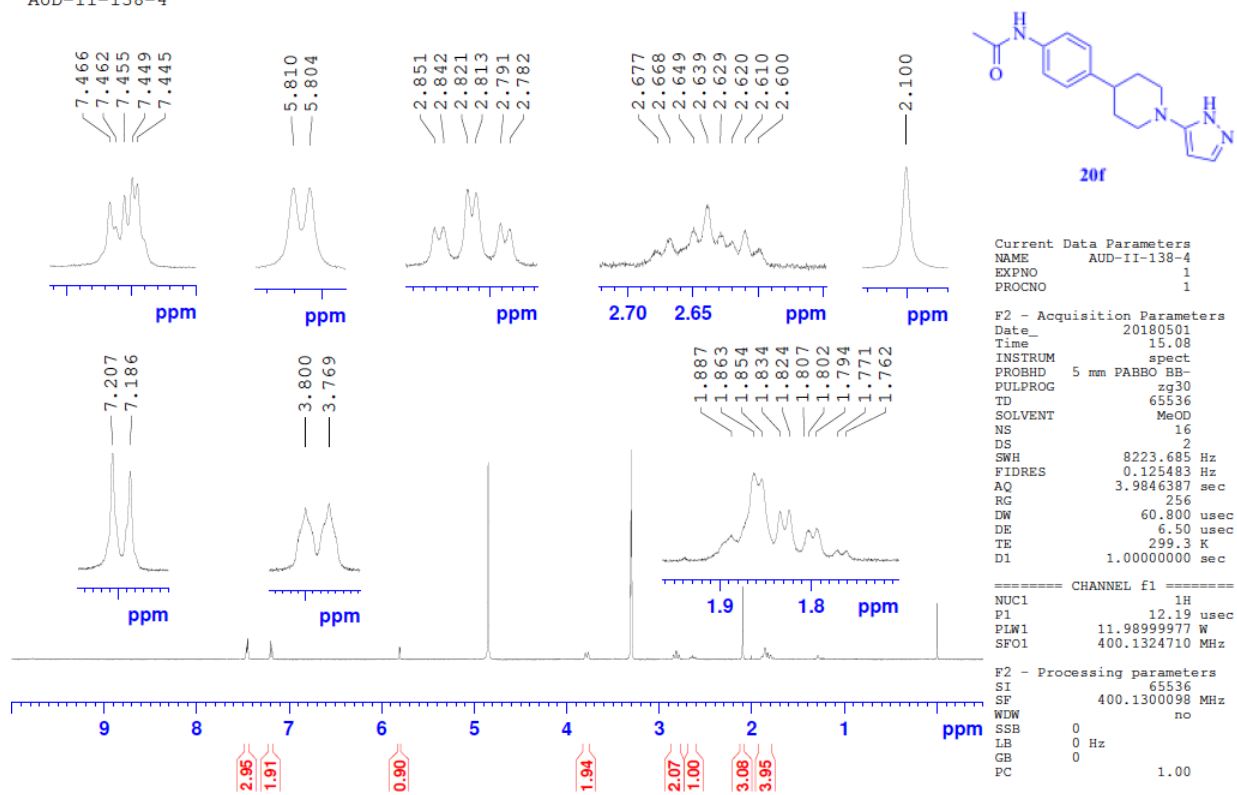
Instrument Settings  
\*Post PM

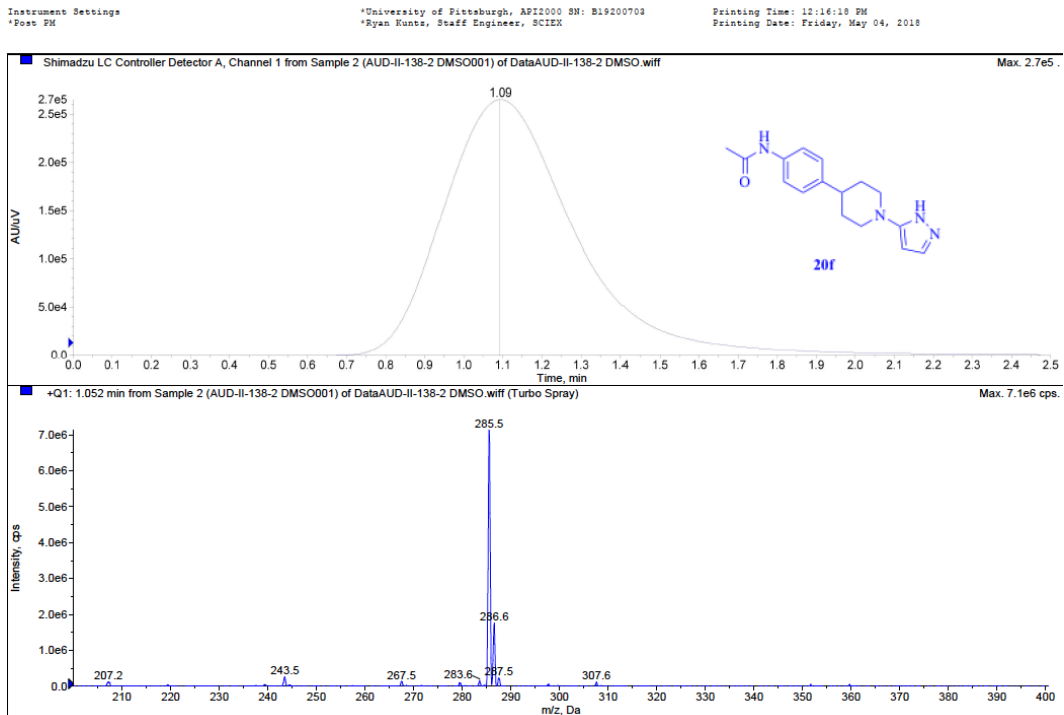
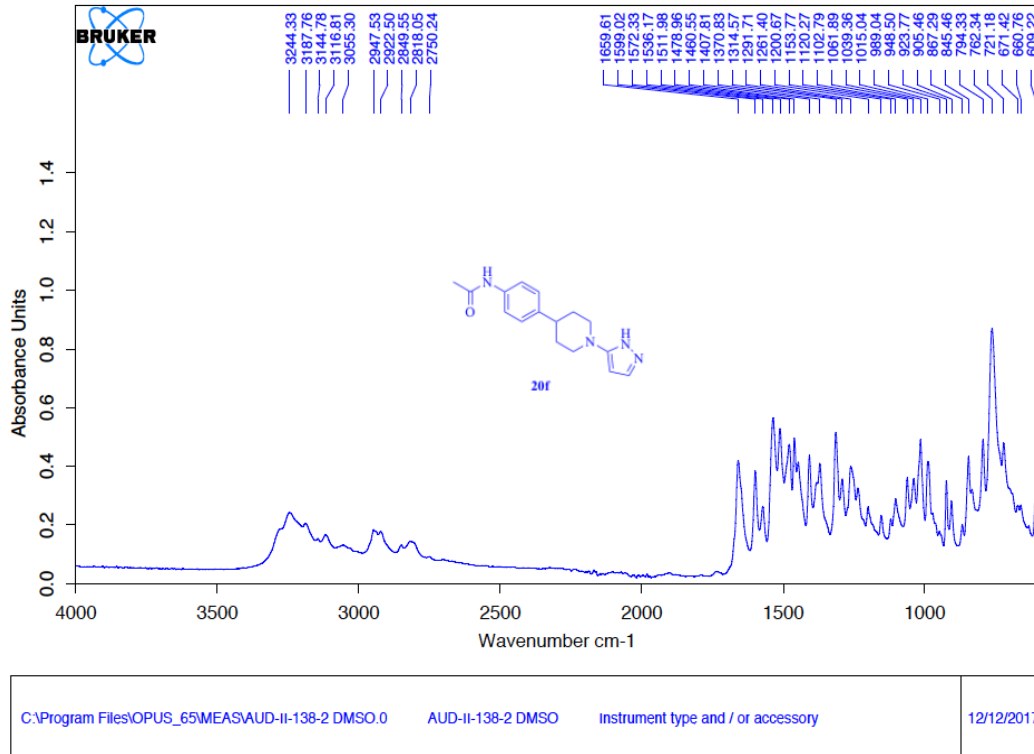
\*University of Pittsburgh, AP12000 SN: B19200703  
\*Ryan Kuntz, Staff Engineer, SCIX

Printing Time: 12:17:16 PM  
Printing Date: Friday, May 04, 2018

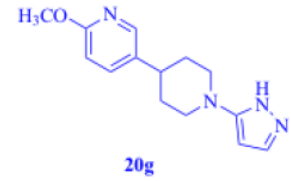
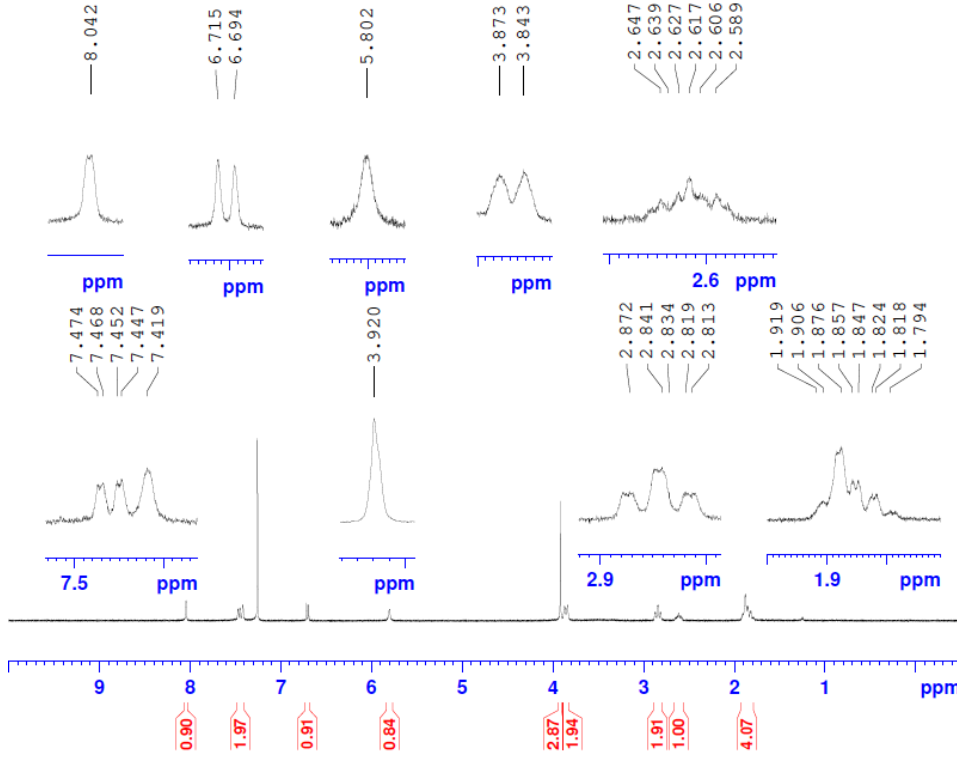


AUD-II-138-4





AUD-II-147-2



Current Data Parameters  
NAME AUD-II-147-2  
EXPNO 1  
PROCNO 1

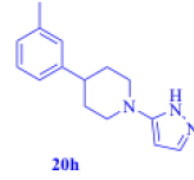
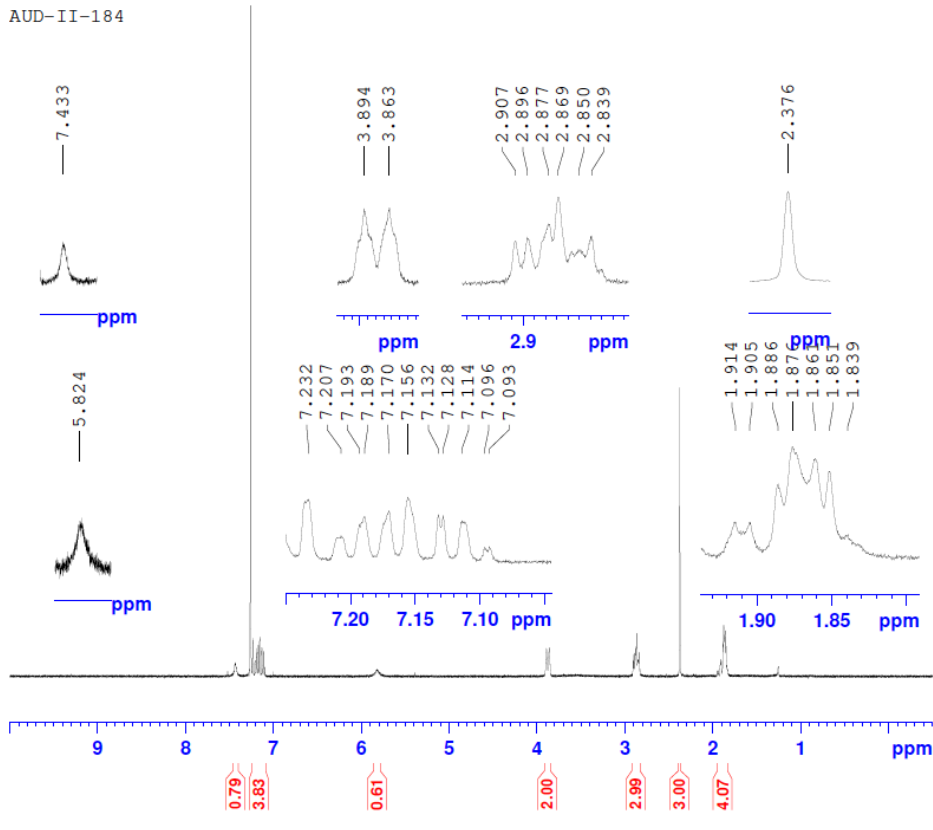
F2 - Acquisition Parameters  
Date\_ 20180101  
Time 16.09  
INSTRUM spect  
PROBHD 5 mm PABBO BB-  
PULPROG zg30  
TD 65536  
SOLVENT CDCl3  
NS 16  
DS 2  
SWH 8223.685 Hz  
FIDRES 0.125483 Hz  
AQ 3.9846387 sec  
RG 287  
DW 60.800 usec  
DE 6.50 usec  
TE 299.0 K  
D1 1.00000000 sec

===== CHANNEL f1 =====  
NUC1 1H  
P1 12.19 usec  
PLW1 11.98999977 W  
SFO1 400.1324710 MHz

F2 - Processing parameters  
SI 65536  
SF 400.1300123 MHz  
WDW no  
SSB 0  
LB 0 Hz  
GB 0  
PC 1.00



AUD-II-184

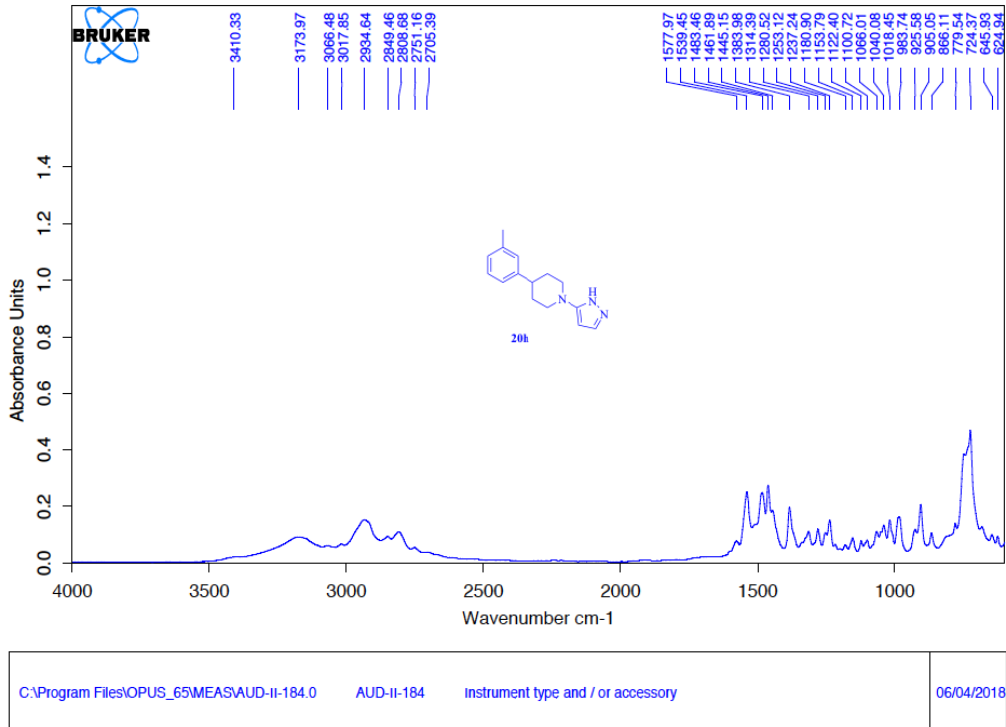


Current Data Parameters  
NAME AUD-II-184  
EXPNO 2  
PROCNO 1

F2 - Acquisition Parameters  
Date\_ 20180405  
Time 14.07  
INSTRUM spect  
PROBHD 5 mm PABBO BB-  
PULPROG zg30  
TD 65536  
SOLVENT CDCl3  
NS 16  
DS 2  
SWH 8223.685 Hz  
FIDRES 0.125483 Hz  
AQ 3.9846387 sec  
RG 287  
DW 60.800 usec  
DE 6.50 usec  
TE 298.1 K  
D1 1.00000000 sec

==== CHANNEL f1 =====  
NUC1 1H  
P1 12.19 usec  
PLW1 11.98999977 W  
SF01 400.1324710 MHz

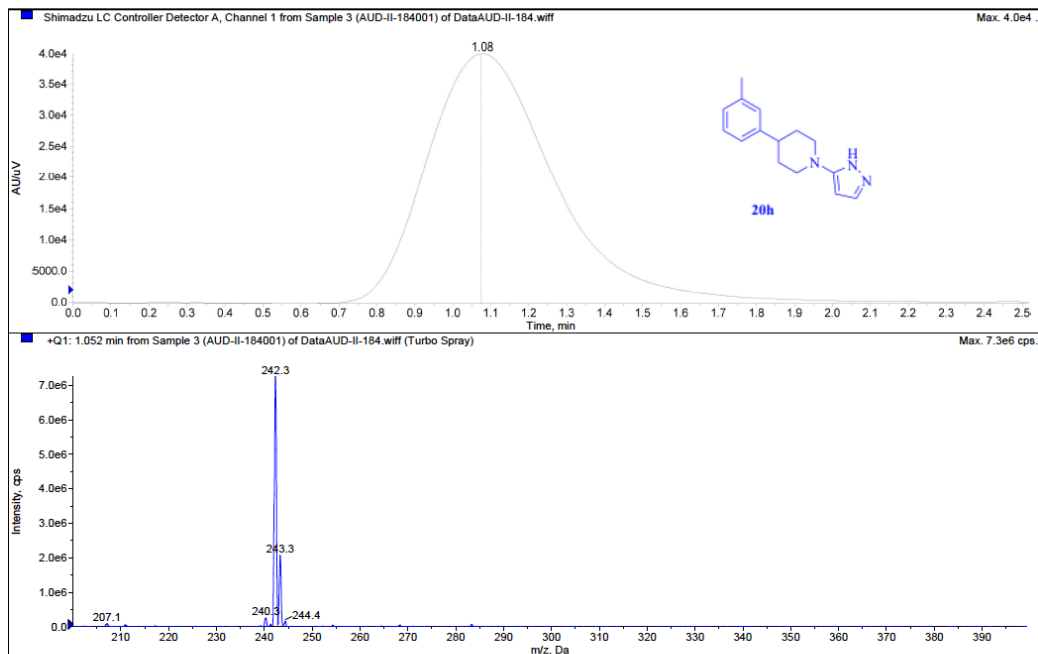
F2 - Processing parameters  
SI 65536  
SF 400.1300099 MHz  
WDW no  
SSB 0  
LB 0 Hz  
GB 0  
PC 1.00



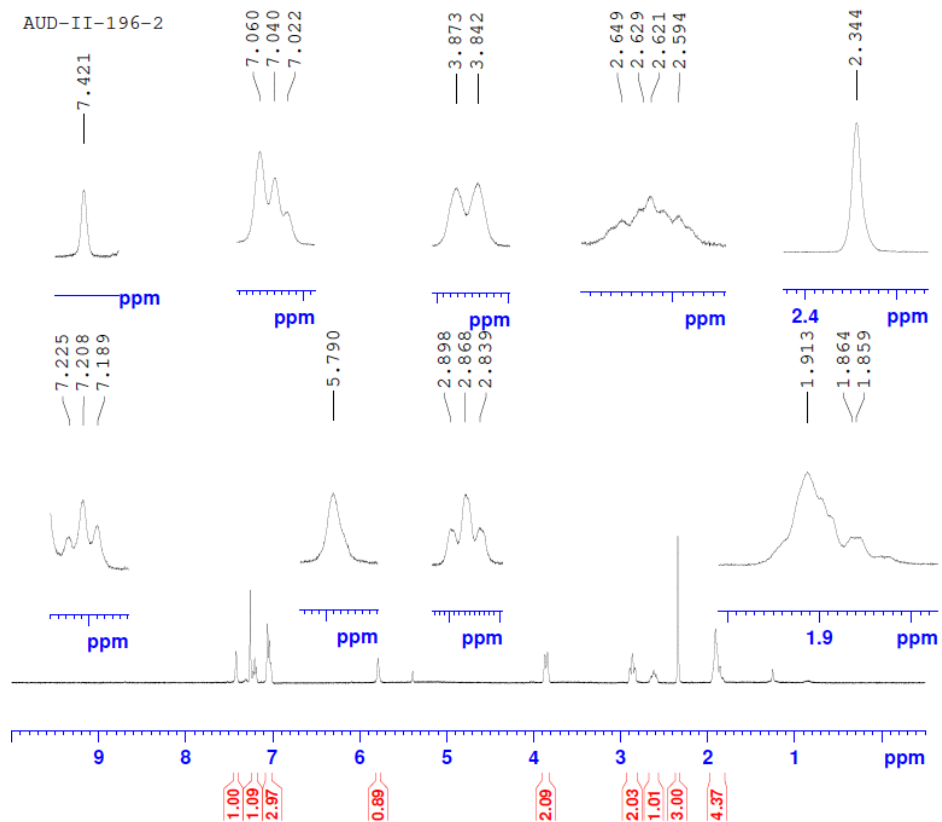
Instrument Settings  
\*Post SW

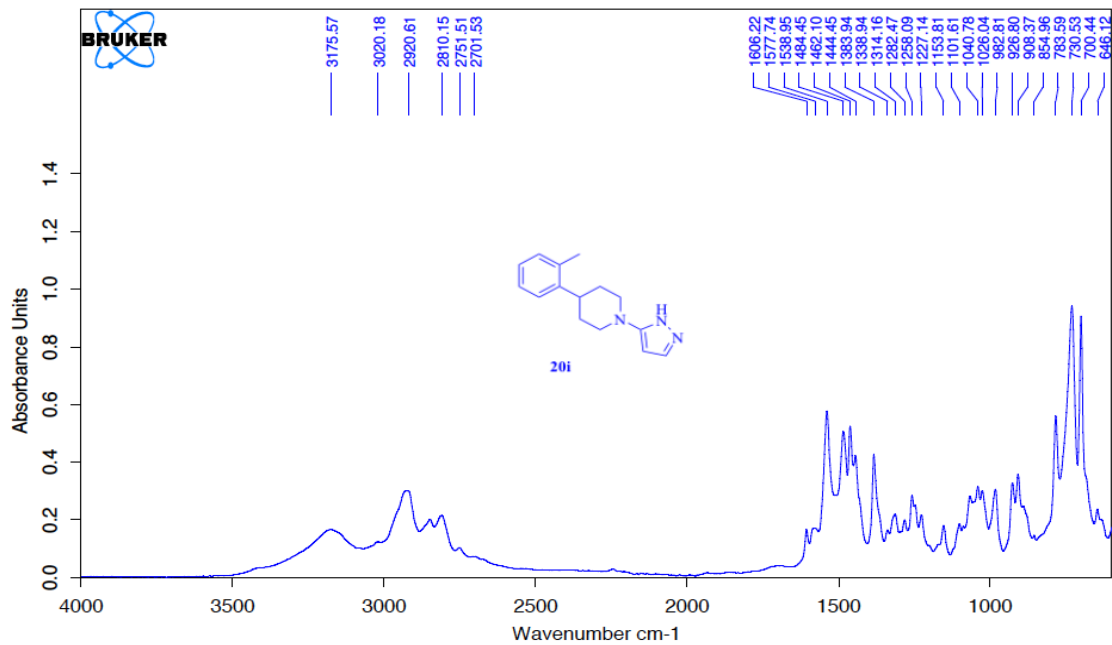
\*University of Pittsburgh, AP12000 SW: B19200703  
\*Ryan Kuntz, Staff Engineer, SCIEX

Printing Time: 11:09:07 PM  
Printing Date: Friday, May 04, 2018

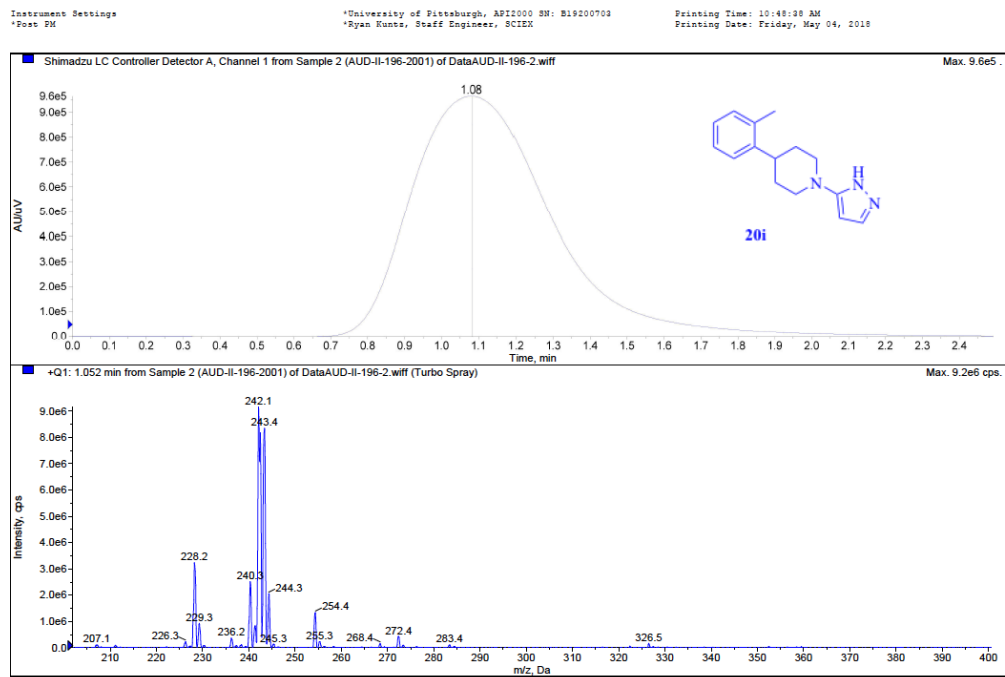




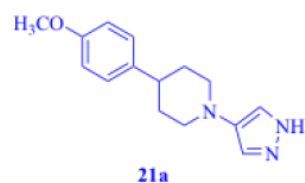
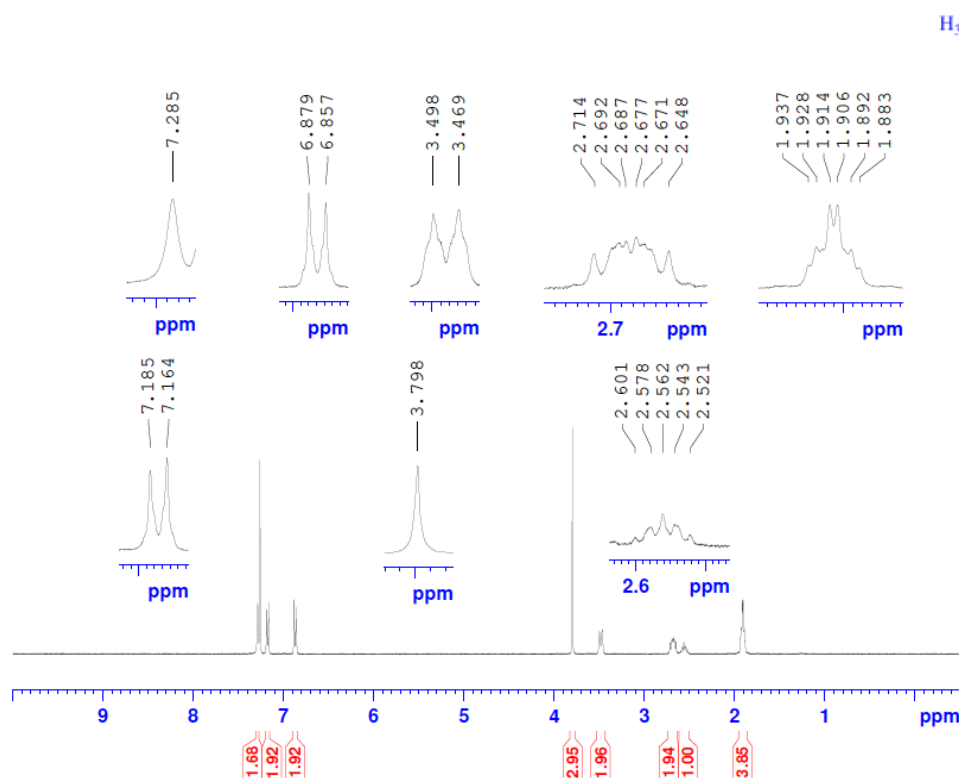




C:\Program Files\OPUS\_65\MEAS\193    AUD-II-196-2    Instrument type and / or accessory    01/05/2018



AUD-I-15-6

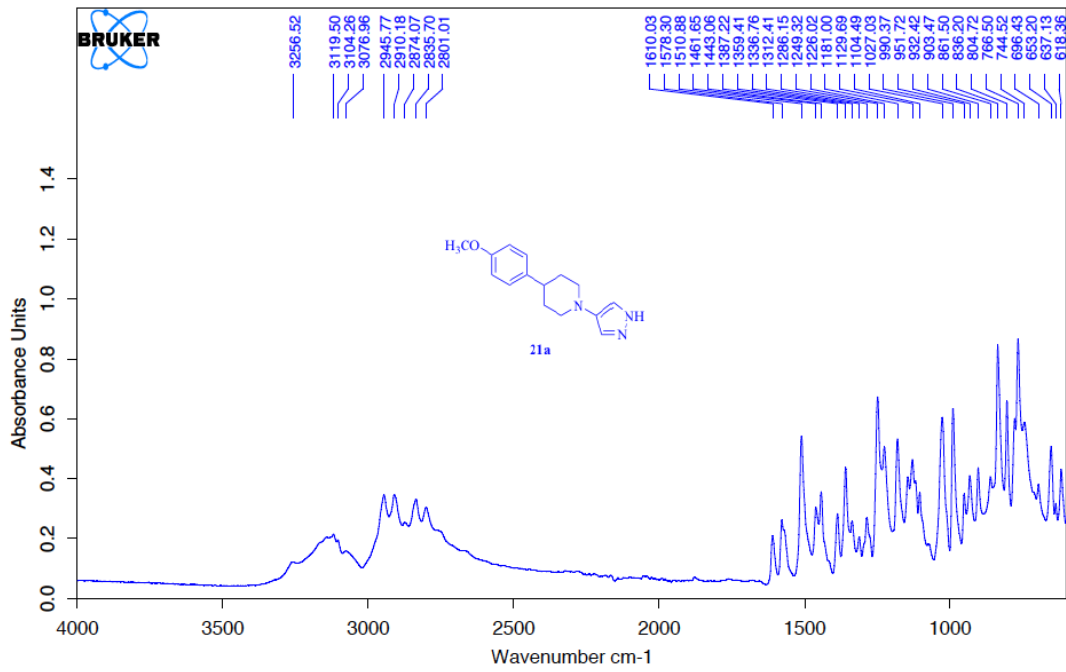


Current Data Parameters  
NAME AUD-I-15-6  
EXPNO 1  
PROCNO 1

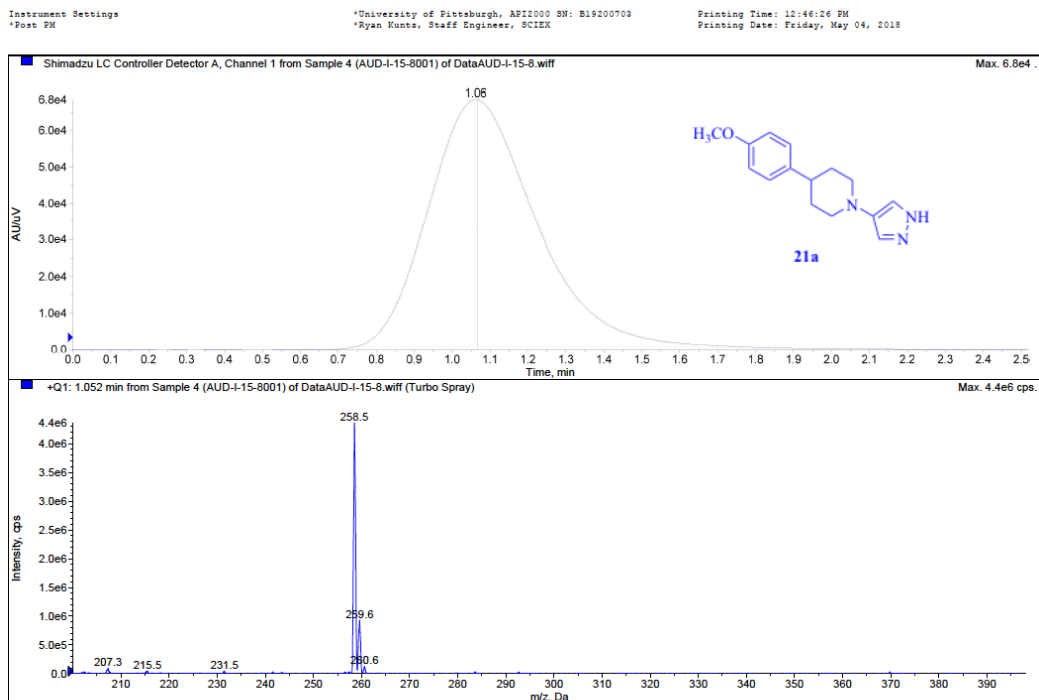
F2 - Acquisition Parameters  
Date\_ 20161202  
Time 12.57  
INSTRUM spect  
PROBHD 5 mm PABBO BB-  
PULPROG zg30  
TD 65536  
SOLVENT CDC13  
NS 16  
DS 2  
SWH 8223.685 Hz  
FIDRES 0.125483 Hz  
AQ 3.9846397 sec  
RG 287  
DW 60.800 usec  
DE 6.50 usec  
TE 297.9 K  
D1 1.00000000 sec

==== CHANNEL f1 =====  
NUC1 1H  
P1 12.19 usec  
PLW1 11.98999977 W  
SFO1 400.1324710 MHz

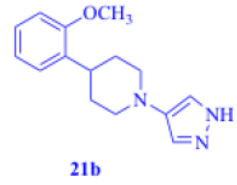
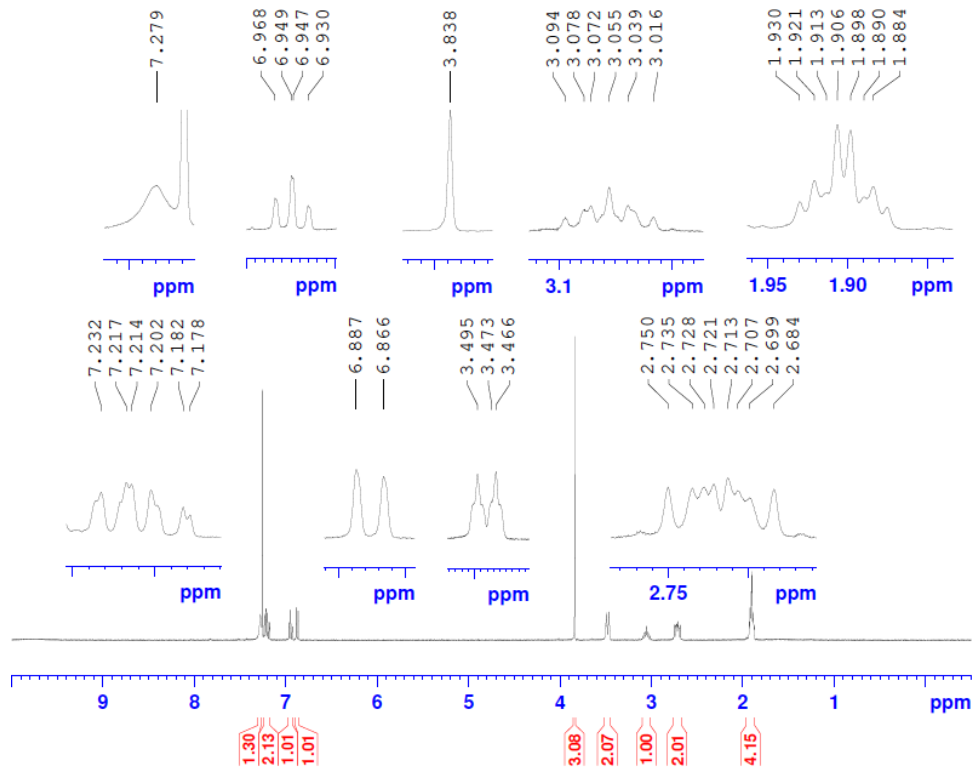
F2 - Processing parameters  
SI 65536  
SF 400.1300107 MHz  
WDW no  
SSB 0  
LB 0 Hz  
GB 0  
PC 1.00



C:\Program Files\OPUS\_65\MEAS\AUD-I-15-6.0    AUD-I-15-6    Instrument type and / or accessory    02/12/2016



AUD-I-28-2 CDCL3

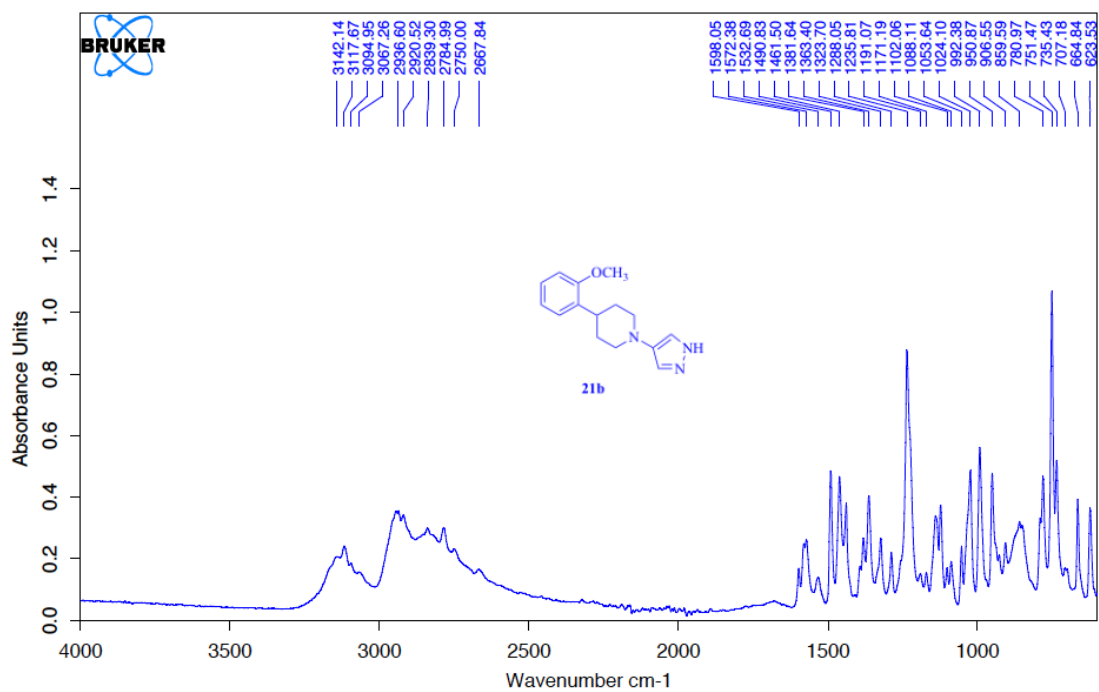


Current Data Parameters  
NAME AUD-I-28-2 CDCL3  
EXPNO 1  
PROCNO 1

F2 - Acquisition Parameters  
Date\_ 20180327  
Time 17.10  
INSTRUM spect  
PROBHD 5 mm PABBO BB-  
PULPROG zg30  
TD 65536  
SOLVENT CDCL3  
NS 16  
DS 2  
SWH 8223.685 Hz  
FIDRES 0.125483 Hz  
AQ 3.9846387 sec  
RG 256  
DW 60.800 usec  
DE 6.50 usec  
TE 297.4 K  
D1 1.00000000 sec

==== CHANNEL f1 =====  
NUC1 1H  
P1 12.19 usec  
PLW1 11.9899977 W  
SFO1 400.1324710 MHz

F2 - Processing parameters  
SI 65536  
SF 400.1300102 MHz  
WDW no  
SSB 0  
LB 0 Hz  
GB 0  
PC 1.00

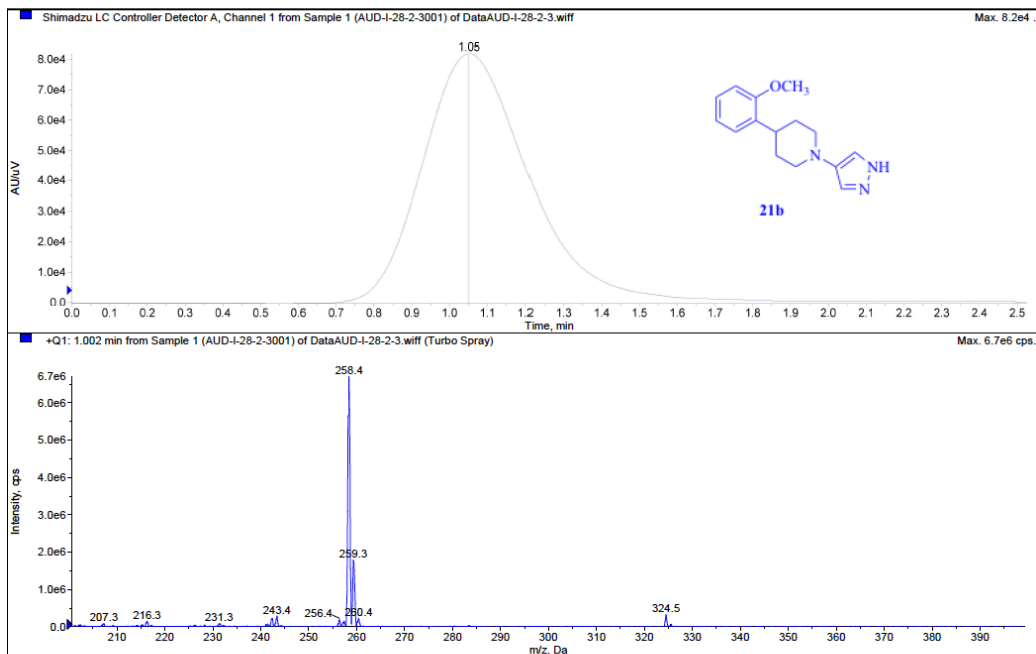


C:\Program Files\OPUS\_65\MEAS\AUD-I-28-2.0    AUD-I-28-2    Instrument type and / or accessory    16/01/2017

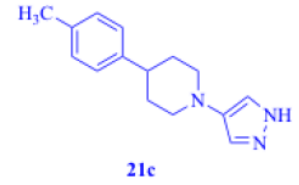
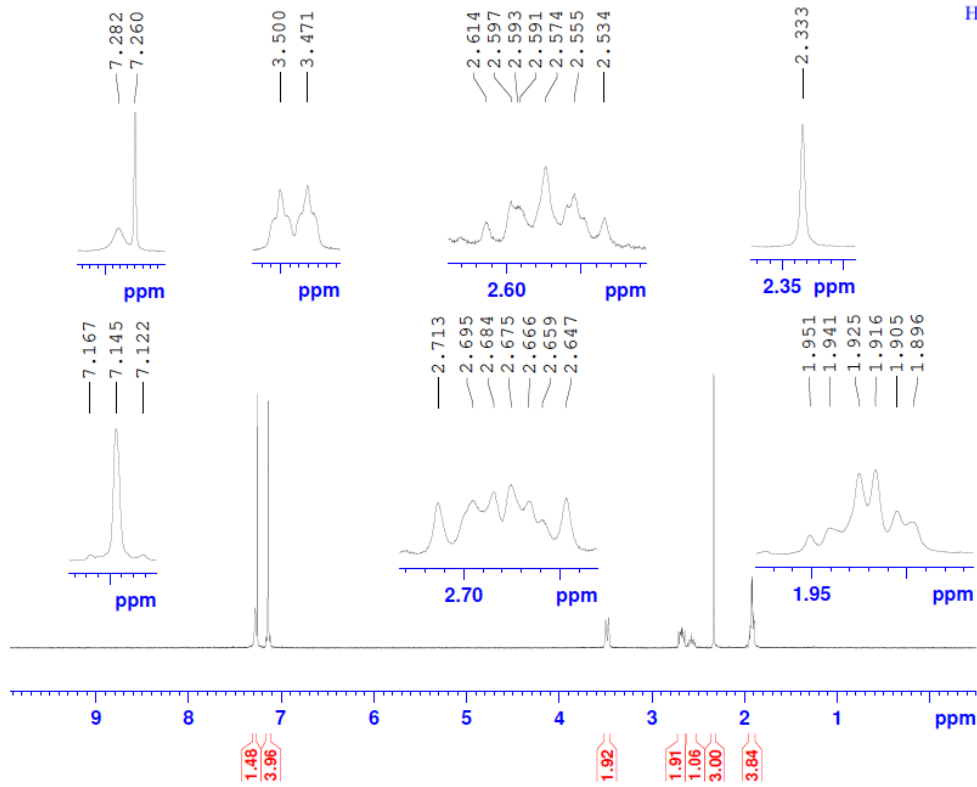
Instrument Settings  
\*Post PM

\*University of Pittsburgh, AP12000 SN: B19200708  
\*Ryan Kuntz, Staff Engineer, SCIEX

Printing Time: 12:48:10 PM  
Printing Date: Friday, May 04, 2018



AUD-I-45-3

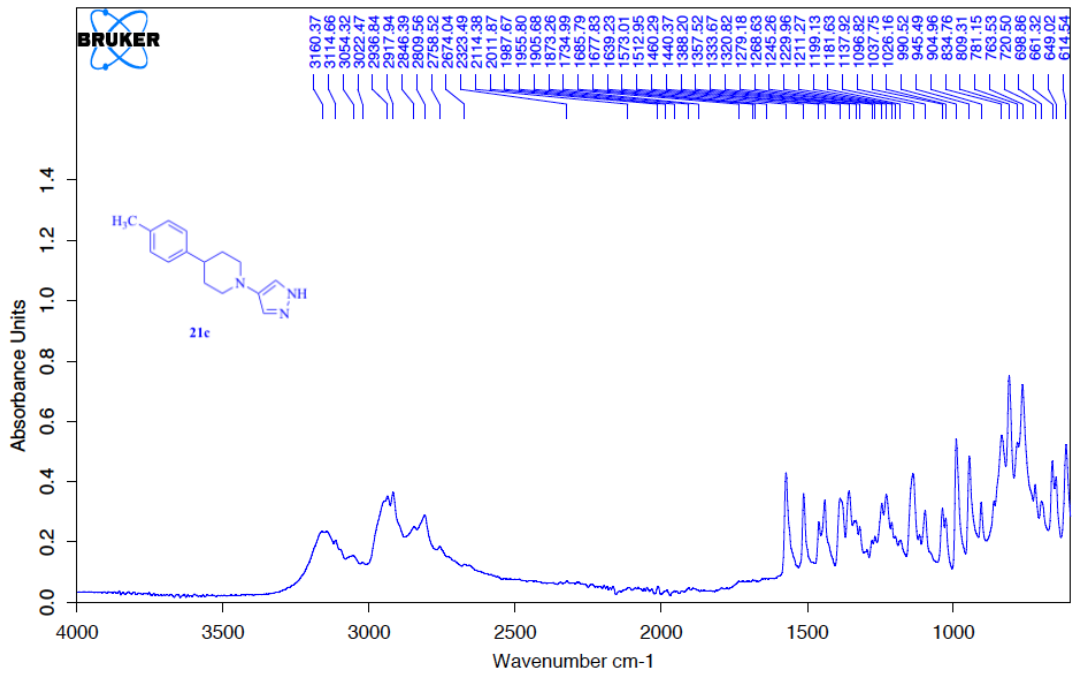


Current Data Parameters  
NAME AUD-I-45-4  
EXPNO 1  
PROCNO 1

F2 - Acquisition Parameters  
Date\_ 20180328  
Time 14.32  
INSTRUM spect  
PROBHD 5 mm PABBO BB-  
PULPROG zg30  
TD 65536  
SOLVENT CDCl3  
NS 16  
DS 2  
SWH 8223.685 Hz  
FIDRES 0.125483 Hz  
AQ 3.9846387 sec  
RG 256  
DW 60.800 usec  
DE 6.50 usec  
TE 297.9 K  
D1 1.00000000 sec

===== CHANNEL f1 =====  
NUC1 1H  
P1 12.19 usec  
PLW1 11.98999977 W  
SFO1 400.1324710 MHz

F2 - Processing parameters  
SI 65536  
SF 400.1300102 MHz  
WDW no  
SSB 0  
LB 0 Hz  
GB 0  
PC 1.00

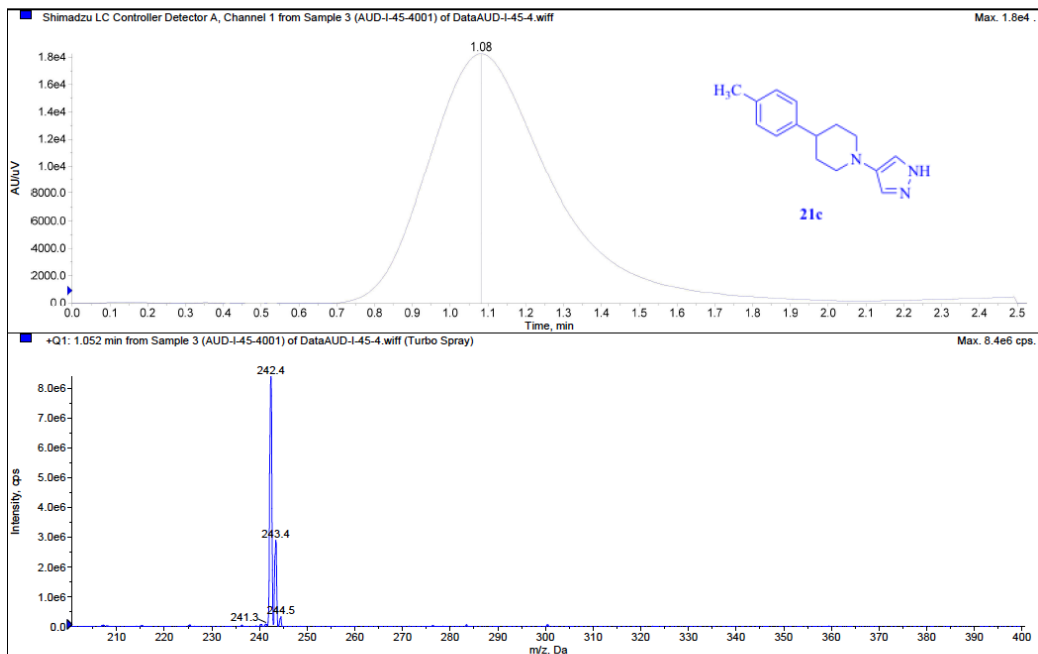


C:\Documents and Settings\Wanli Pu.UNIVERSI-CC6494\Desktop\IR DATA\Gordon IRMEAS\AUD-I-45-3.0    AUD-I-45-3    Instrument type 29/03/2017

Instrument Settings  
\*Post PM

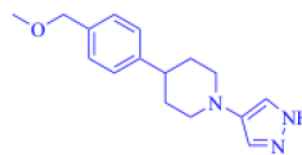
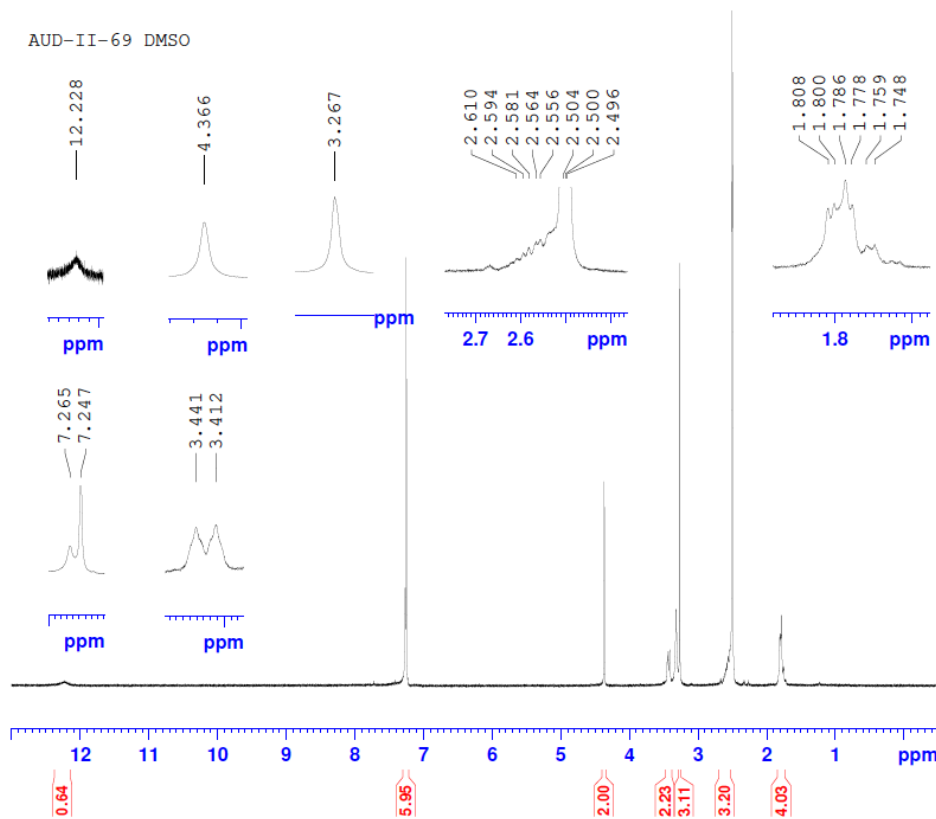
\*University of Pittsburgh, AP2000 SN: B19200703  
\*Ryan Kuntz, Staff Engineer, SCIEX

Printing Time: 12:16:03 PM  
Printing Date: Friday, May 04, 2018





AUD-II-69 DMSO

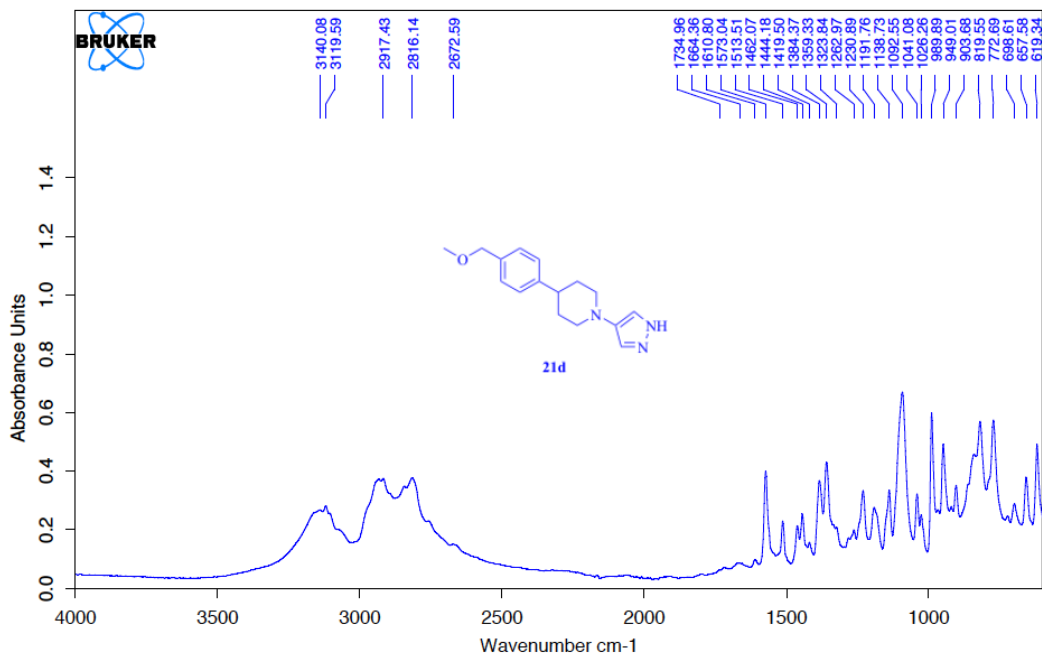


Current Data Parameters  
NAME AUD-II-69 DMSO  
EXPNO 1  
PROCNO 1

F2 - Acquisition Parameters  
Date\_ 20170609  
Time 13.29  
INSTRUM spect  
PROBHD 5 mm PABBO BB-  
PULPROG zg30  
TD 65536  
SOLVENT DMSO  
NS 16  
DS 2  
SWH 8223.685 Hz  
FIDRES 0.125483 Hz  
AQ 3.9846387 sec  
RG 256  
DW 60.800 usec  
DE 6.50 usec  
TE 298.0 K  
D1 1.00000000 sec

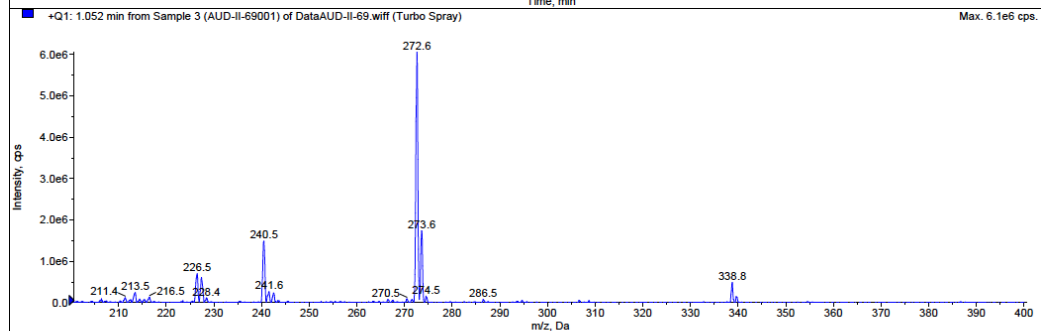
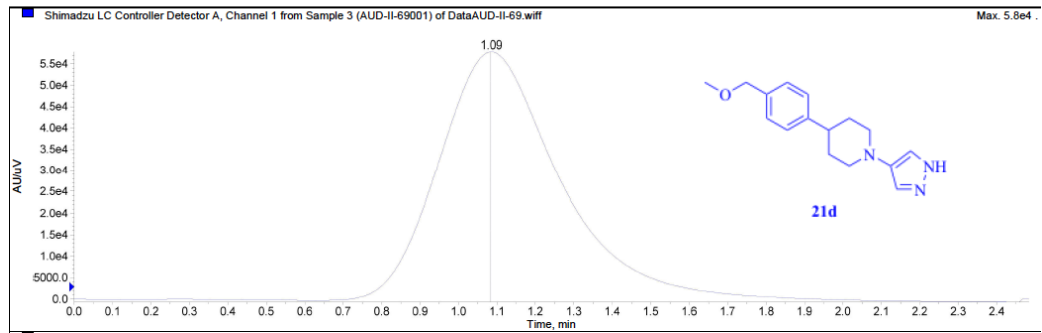
===== CHANNEL f1 =====  
NUC1 1H  
P1 12.19 usec  
PLW1 11.98999977 W  
SFO1 400.1324710 MHz

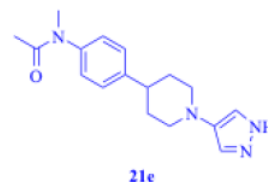
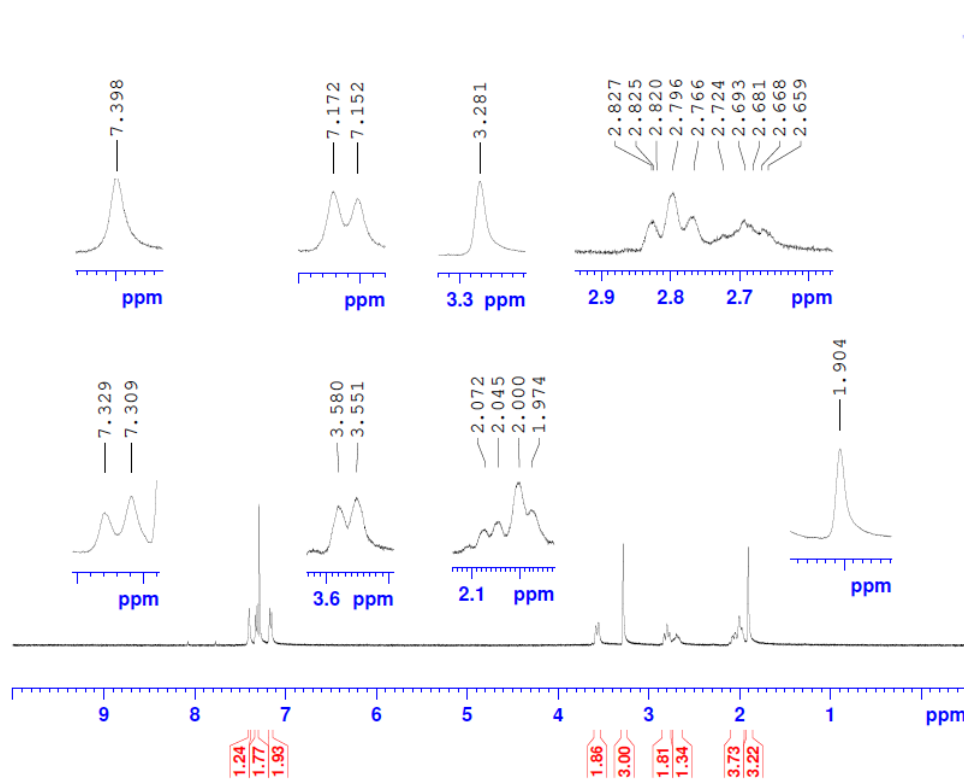
F2 - Processing parameters  
SI 65536  
SF 400.1300047 MHz  
WDW no  
SSB 0  
LB 0 Hz  
GB 0  
PC 1.00



C:\MEAS\AUD-II-69.0    AUD-II-69    Instrument type and / or accessory    09/06/2017

Instrument Settings    \*University of Pittsburgh, API2000 SN: B19200703    Printing Time: 12:23:53 PM  
 \*Post PM    \*Ryan Kuntz, Staff Engineer, SCIEX    Printing Date: Friday, May 04, 2018



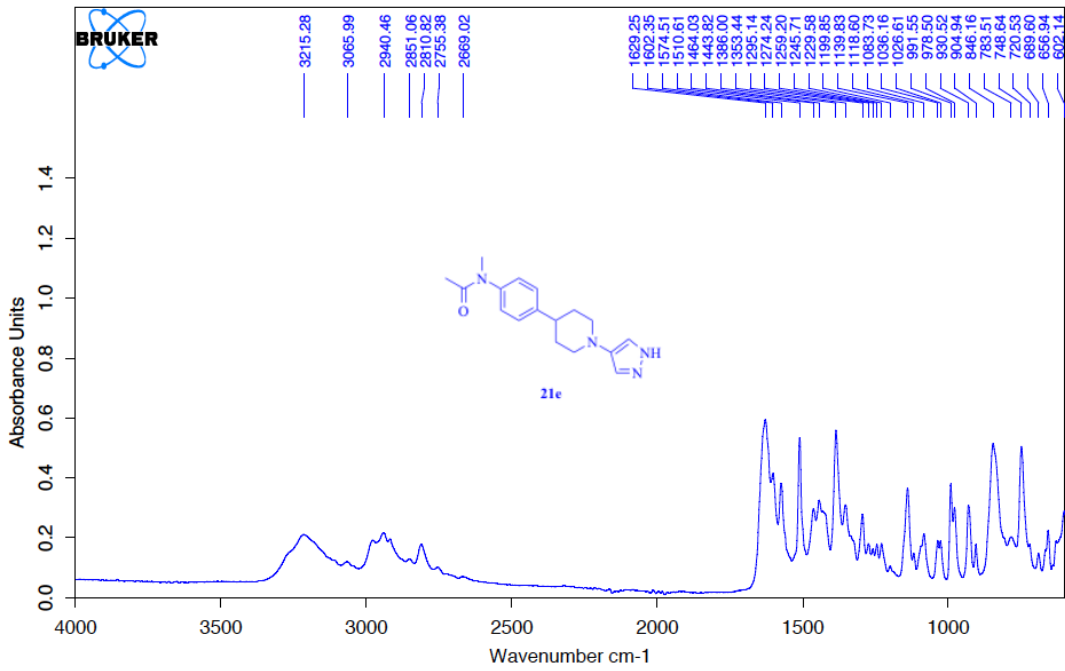


Current Data Parameters  
 NAME AUD-II-125 CDCL3  
 EXPNO 1  
 PROCNO 1

F2 - Acquisition Parameters  
 Date\_ 20171023  
 Time 13.18  
 INSTRUM spect  
 PROBHD 5 mm PABBO BB-  
 PULPROG zg30  
 TD 65536  
 SOLVENT CDCL3  
 NS 16  
 DS 2  
 SWH 8223.685 Hz  
 FIDRES 0.125483 Hz  
 AQ 3.9846387 sec  
 RG 322  
 DW 60.800 usec  
 DE 6.50 usec  
 TE 299.0 K  
 D1 1.00000000 sec

===== CHANNEL f1 =====  
 NUC1 1H  
 P1 12.19 usec  
 PLW1 11.98999977 W  
 SFO1 400.1324710 MHz

F2 - Processing parameters  
 SI 65536  
 SF 400.1300000 MHz  
 WDW no  
 SSB 0 Hz  
 LB 0  
 GB 0  
 PC 1.00

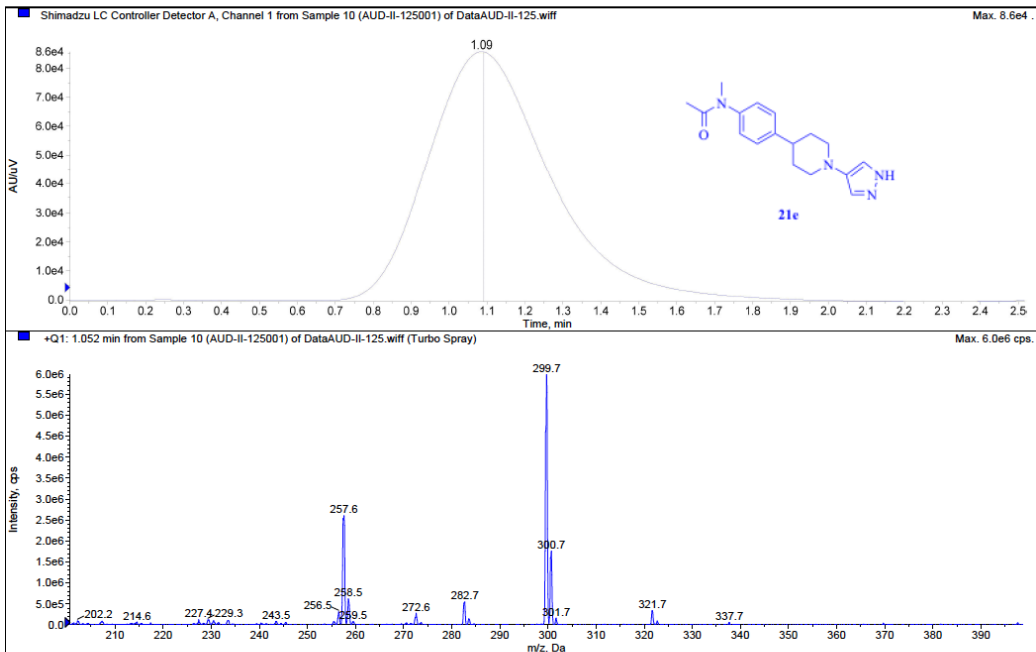


C:\Program Files\OPUS\_65\MEAS\119    AUD-II-125    Instrument type and / or accessory    23/10/2017

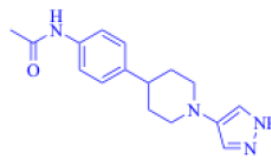
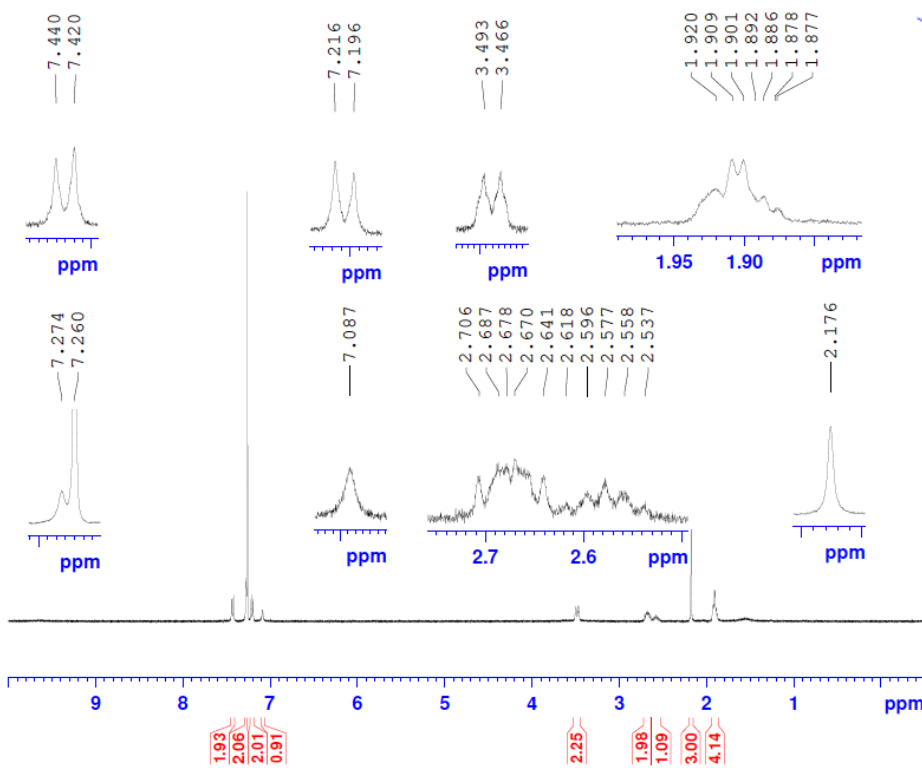
Instrument Settings  
\*Post PM

\*University of Pittsburgh, AP12000 SN: B19200708  
\*Ryan Kuntz, Staff Engineer, SCIEX

Printing Time: 12:18:09 PM  
Printing Date: Friday, May 04, 2018



AUD-II-163 CDCL3

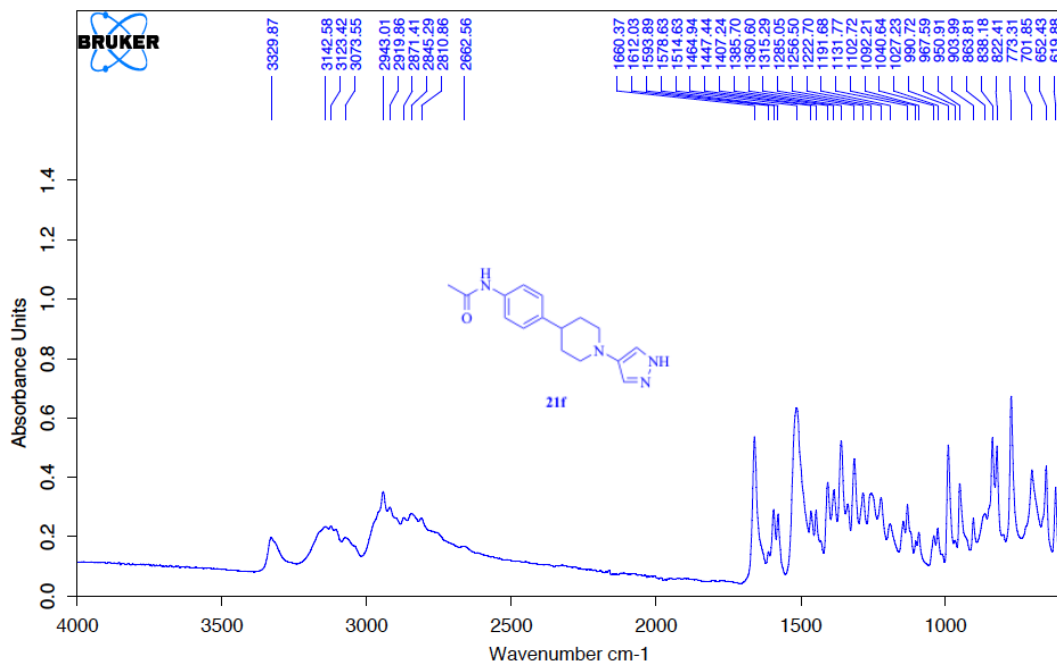


Current Data Parameters  
NAME AUD-II-163 CDCL3  
EXPNO 1  
PROCNO 1

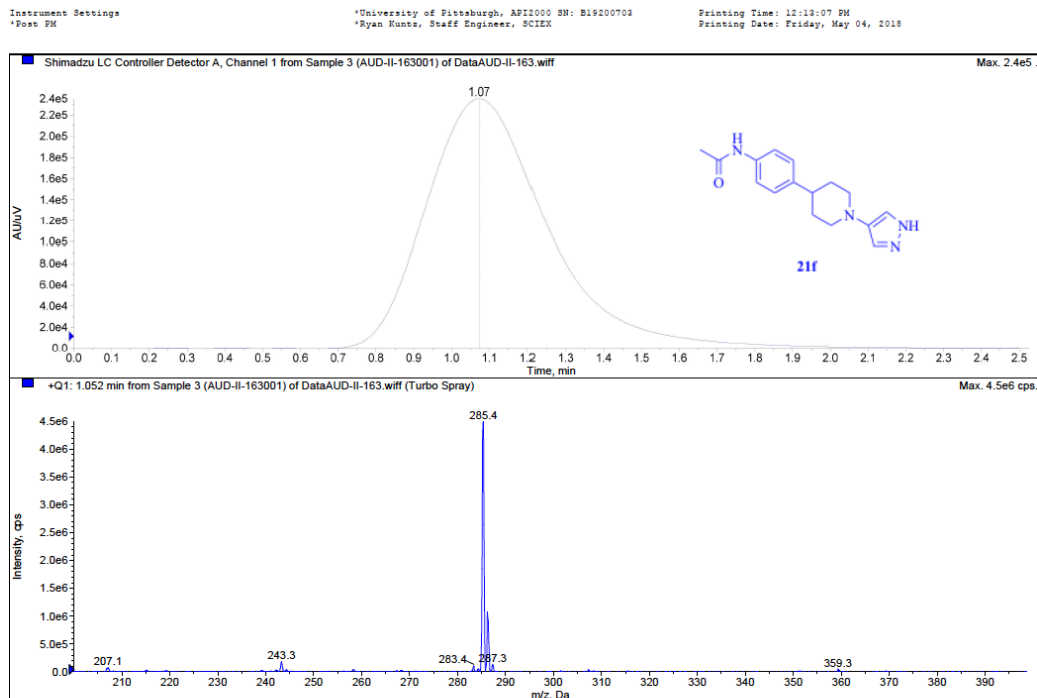
F2 - Acquisition Parameters  
Date\_ 20180201  
Time 14.49  
INSTRUM spect  
PROBHD 5 mm PABBO BB-  
PULPROG zg30  
TD 65536  
SOLVENT CDCL3  
NS 16  
DS 2  
SWH 8223.685 Hz  
FIDRES 0.125483 Hz  
AQ 3.9846387 sec  
RG 287  
DW 60.800 usec  
DE 6.50 usec  
TE 297.0 K  
D1 1.00000000 sec

===== CHANNEL f1 =====  
NUC1 1H  
P1 12.19 usec  
PIW1 11.9899977 W  
SFO1 400.1324710 MHz

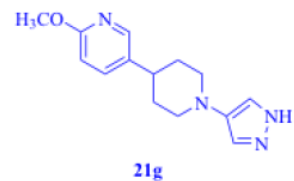
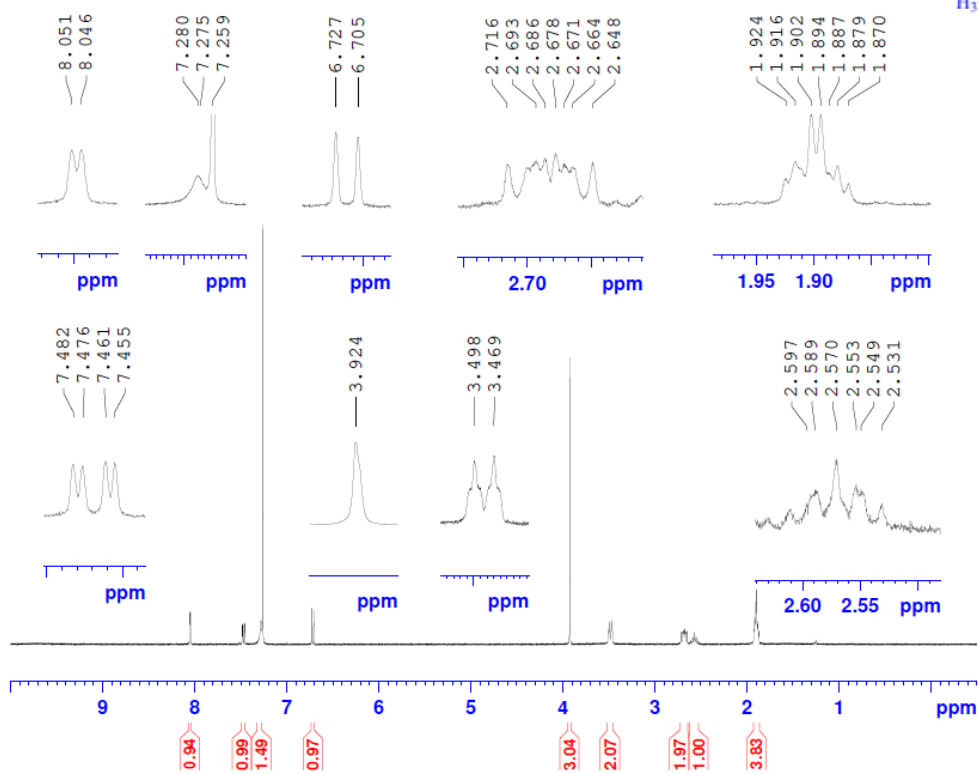
F2 - Processing parameters  
SI 65536  
SF 400.1300098 MHz  
WDW no  
SSB 0  
LB 0 Hz  
GB 0  
PC 1.00



C:\PROGRAM FILES\OPUS_65MEAS\MEAS\AUD-II-163.0	AUD-II-163	Instrument type and / or accessory	01/02/2018
--	------------	------------------------------------	------------



AUD-II-151-2

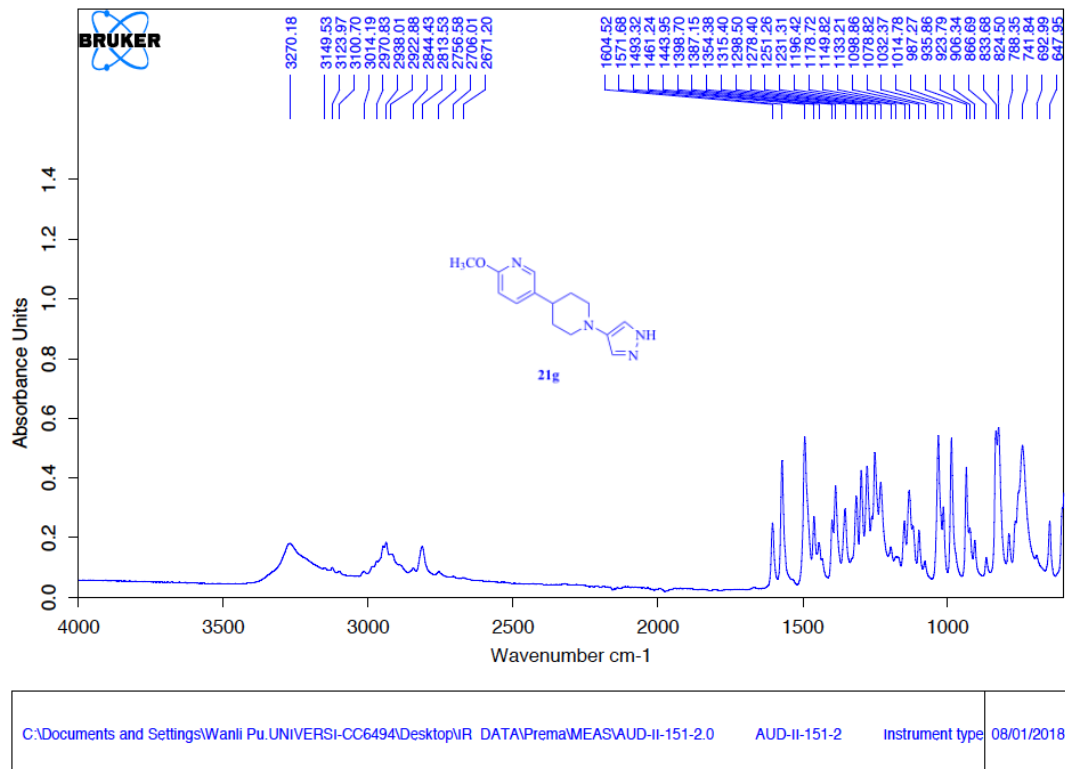


Current Data Parameters  
NAME AUD-II-151-2  
EXPNO 1  
PROCNO 1

F2 - Acquisition Parameters  
Date\_ 20180108  
Time 15.02  
INSTRUM spect  
PROBHD 5 mm PABBO BB-  
PULPROG zg30  
TD 65536  
SOLVENT CDCl3  
NS 16  
DS 2  
SWH 8223.685 Hz  
FIDRES 0.125483 Hz  
AQ 3.9846387 sec  
RG 287  
DW 60.800 usec  
DE 6.50 usec  
TE 297.6 K  
D1 1.0000000 sec

===== CHANNEL f1 =====  
NUC1 1H  
P1 12.19 usec  
PLW1 11.98999977 W  
SFO1 400.1324710 MHz

F2 - Processing parameters  
SI 65536  
SF 400.1300112 MHz  
WDW no  
SSB 0  
LB 0 Hz  
GB 0  
PC 1.00

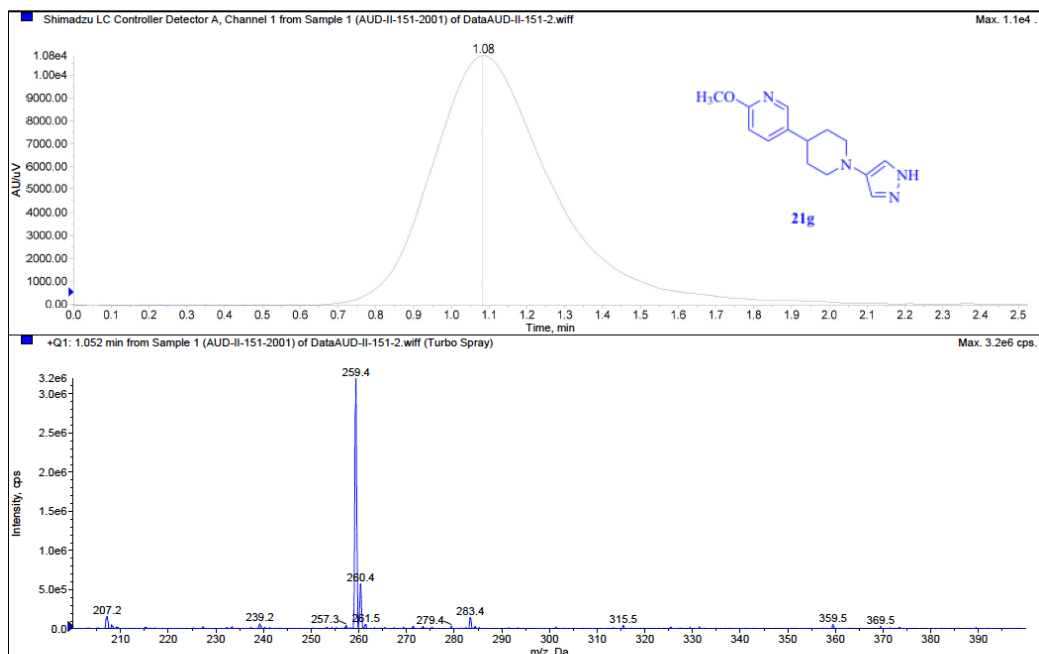


Page 4/4

Instrument Settings  
\*Post PM

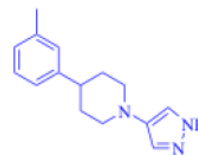
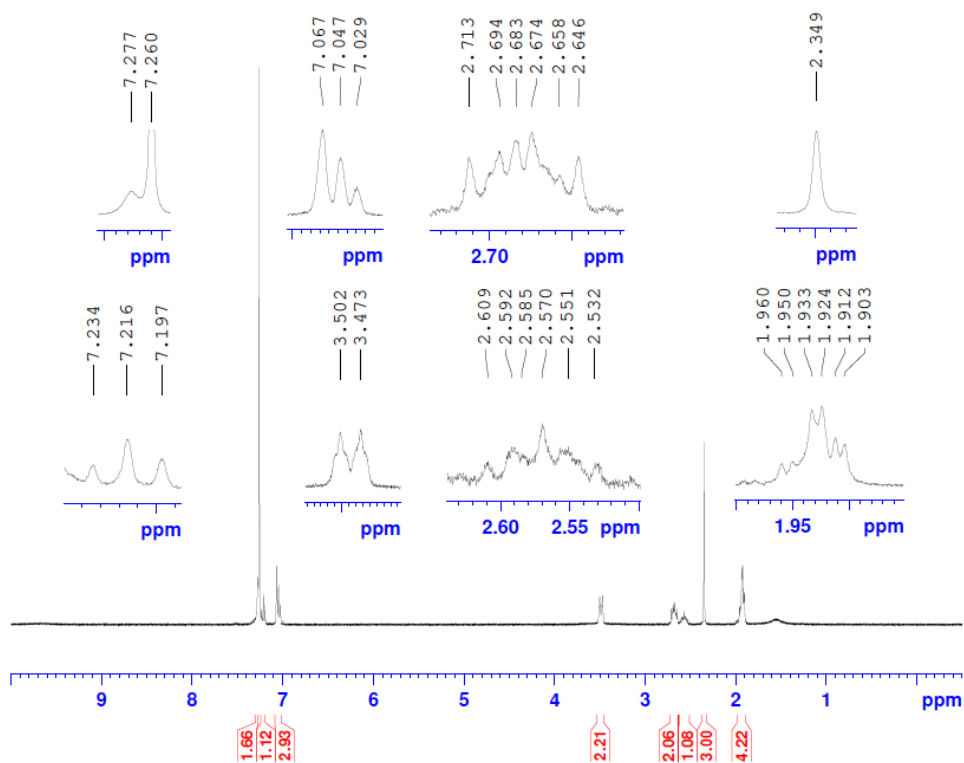
\*University of Pittsburgh, API2000 SN: B19200703  
\*Ryan Kuntz, Staff Engineer, SCIEX

Printing Time: 12:14:07 PM  
Printing Date: Friday, May 04, 2018





AUD-II-169-2

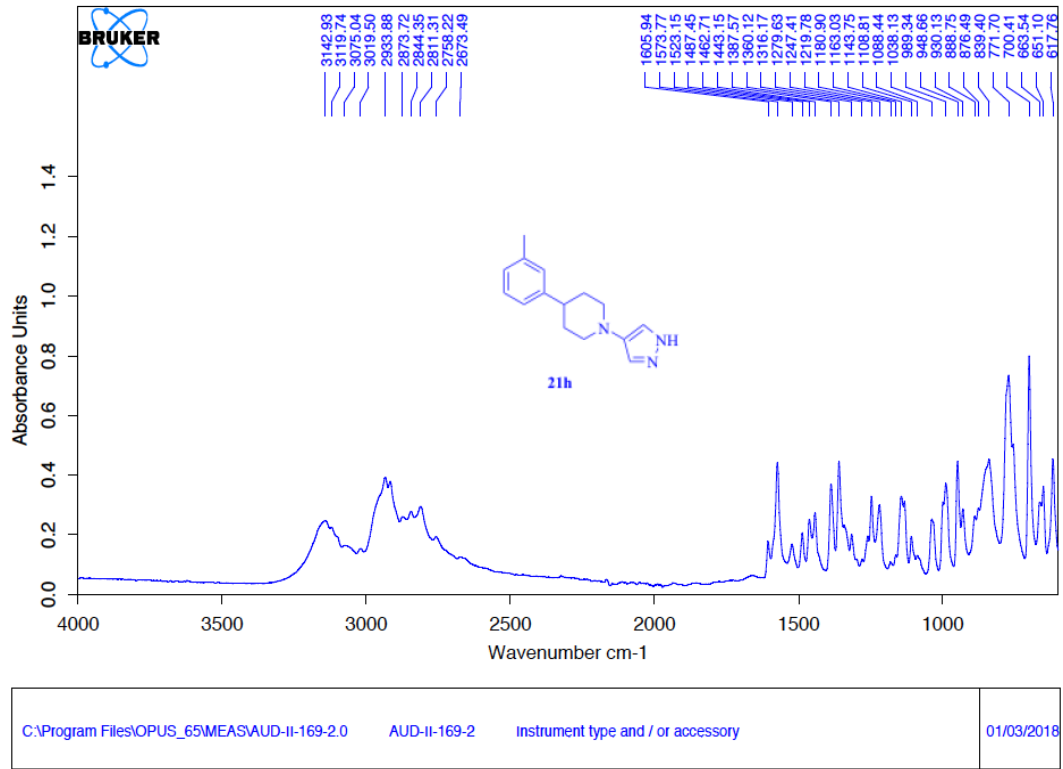


Current Data Parameters  
NAME AUD-II-169-2  
EXPNO 1  
PROCNO 1

F2 - Acquisition Parameters  
Date\_ 20180301  
Time 13.05  
INSTRUM spect  
PROBHD 5 mm PABBO BB-  
PULPROG zg30  
TD 65536  
SOLVENT CDC13  
NS 16  
DS 2  
SWH 8223.685 Hz  
FIDRES 0.125483 Hz  
AQ 3.9846387 sec  
RG 287  
DW 60.800 usec  
DE 6.50 usec  
TE 298.0 K  
D1 1.00000000 sec

CHANNEL f1  
NUC1 1H  
P1 12.19 usec  
PLW1 11.9899977 W  
SFO1 400.1324710 MHz

F2 - Processing parameters  
SI 65536  
SF 400.1300103 MHz  
WDW no  
SSB 0  
LB 0 Hz  
GB 0  
PC 1.00

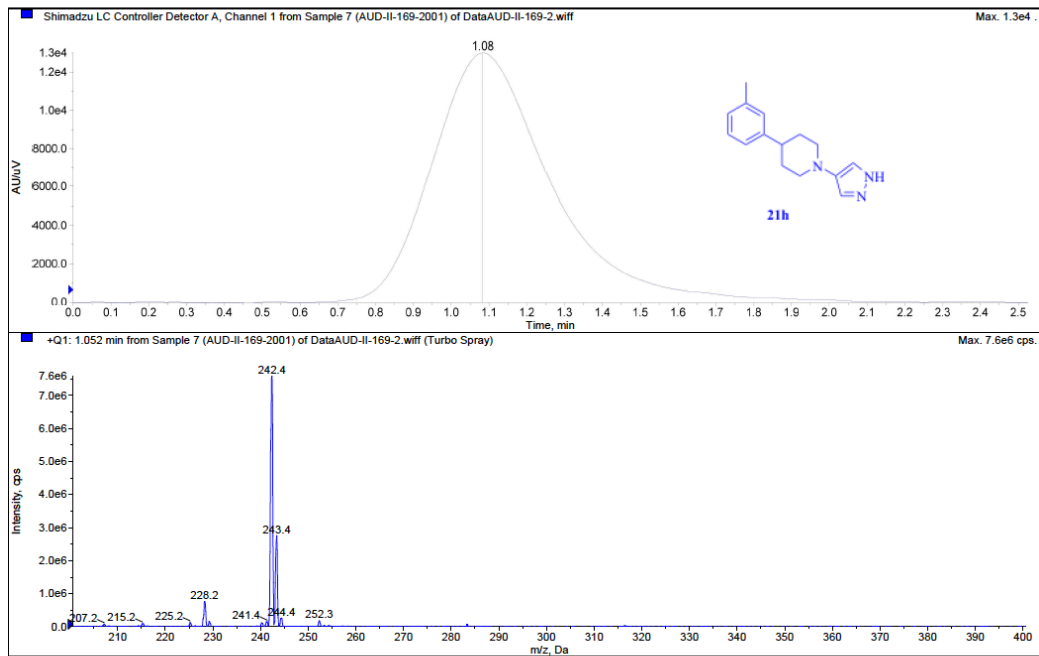


Page 44

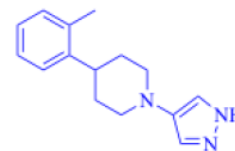
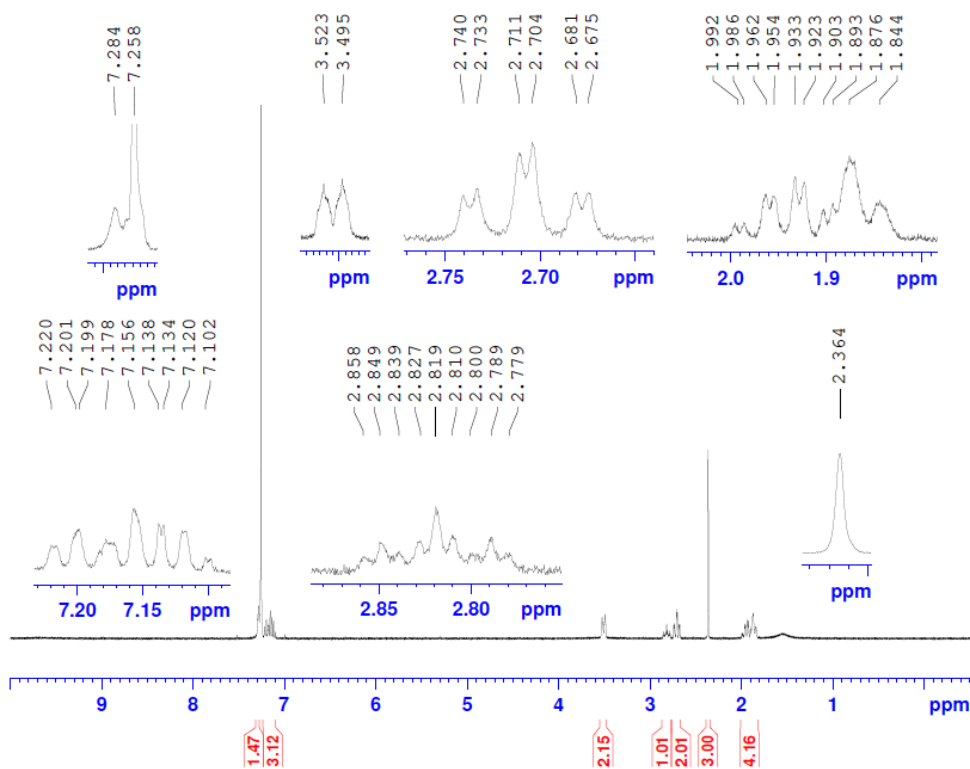
Instrument Settings  
\*Post PM

\*University of Pittsburgh, API2000 SN: B19200703  
\*Ryan Kuntz, Staff Engineer, SCIEX

Printing Time: 2:02:58 PM  
Printing Date: Friday, May 04, 2018



AUD-II-181



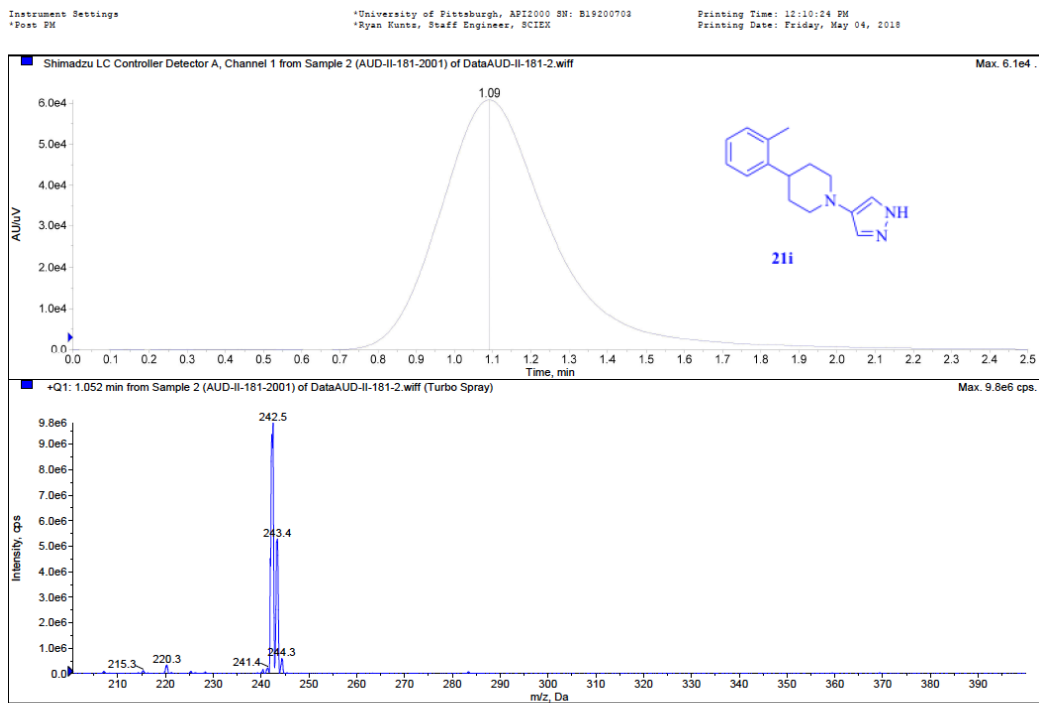
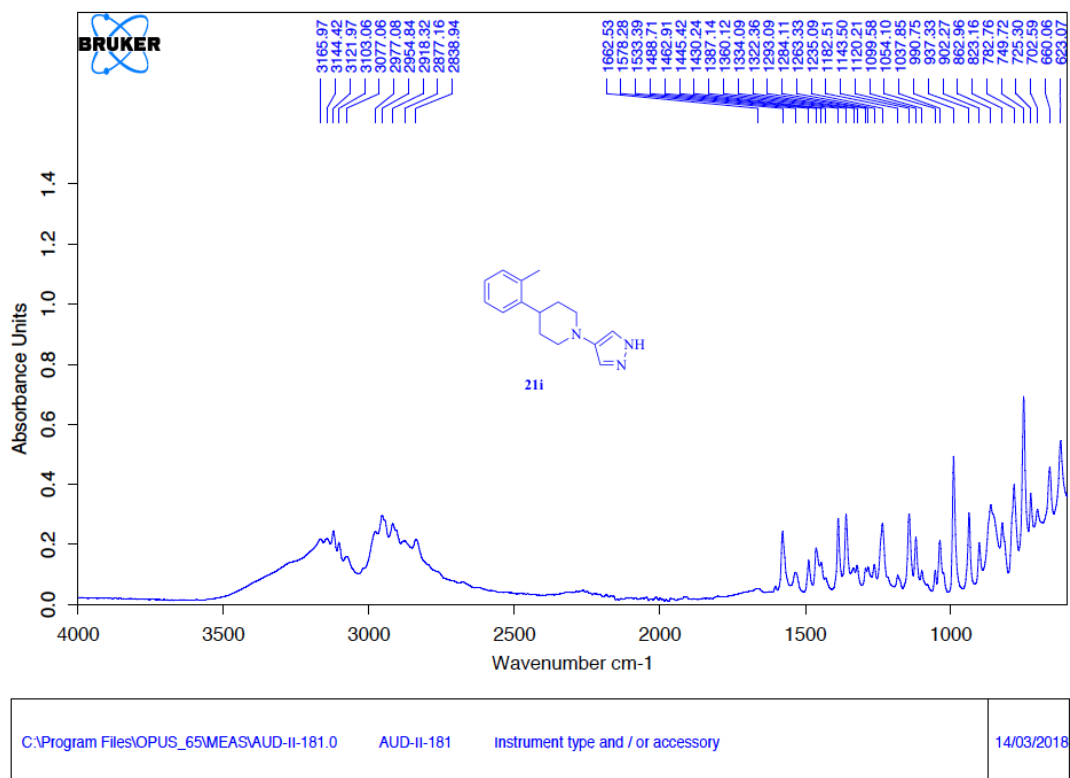
21i

Current Data Parameters  
 NAME AUD-II-181  
 EXPNO 1  
 PROCNO 1

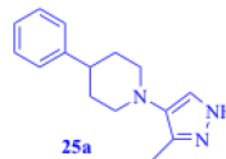
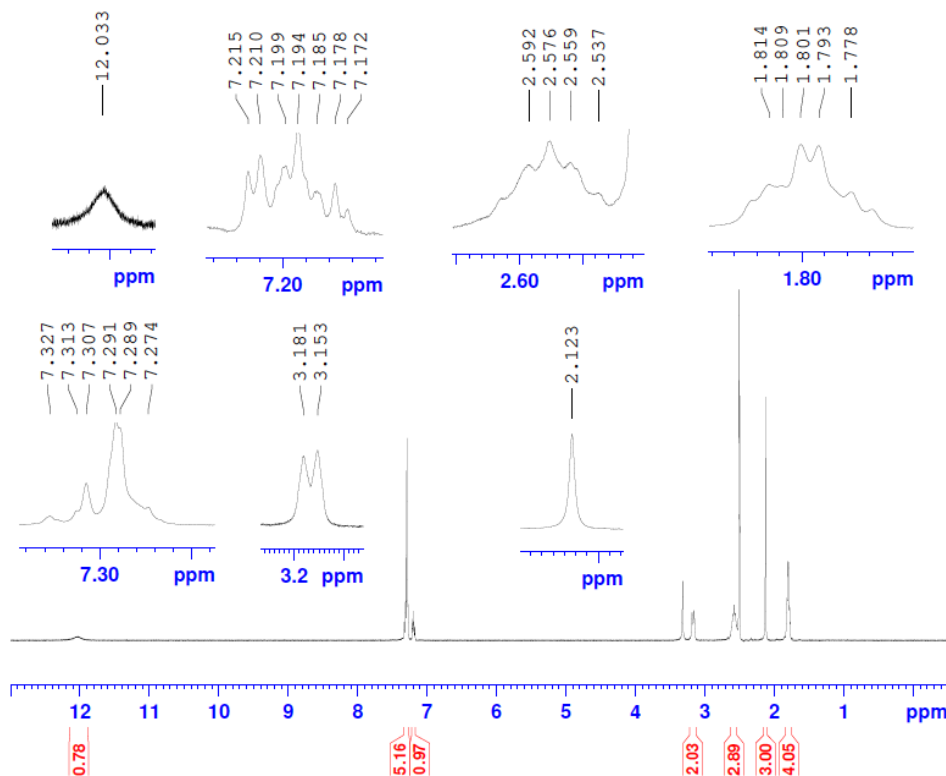
F2 - Acquisition Parameters  
 Date\_ 20180314  
 Time 12.33  
 INSTRUM spect  
 PROBHD 5 mm PABBO BB-  
 PULPROG zg30  
 TD 65536  
 SOLVENT CDC13  
 NS 16  
 DS 2  
 SWH 8223.685 Hz  
 FIDRES 0.125483 Hz  
 AQ 3.9846387 sec  
 RG 287  
 DW 60.800 usec  
 DE 6.50 usec  
 TE 297.5 K  
 D1 1.0000000 sec

===== CHANNEL f1 =====  
 NUC1 1H  
 P1 12.19 usec  
 PLW1 11.9899977 W  
 SFO1 400.1324710 MHz

F2 - Processing parameters  
 SI 65536  
 SF 400.1300109 MHz  
 WDW no  
 SSB 0  
 LB 0 Hz  
 GB 0  
 PC 1.00



AUD-II-71

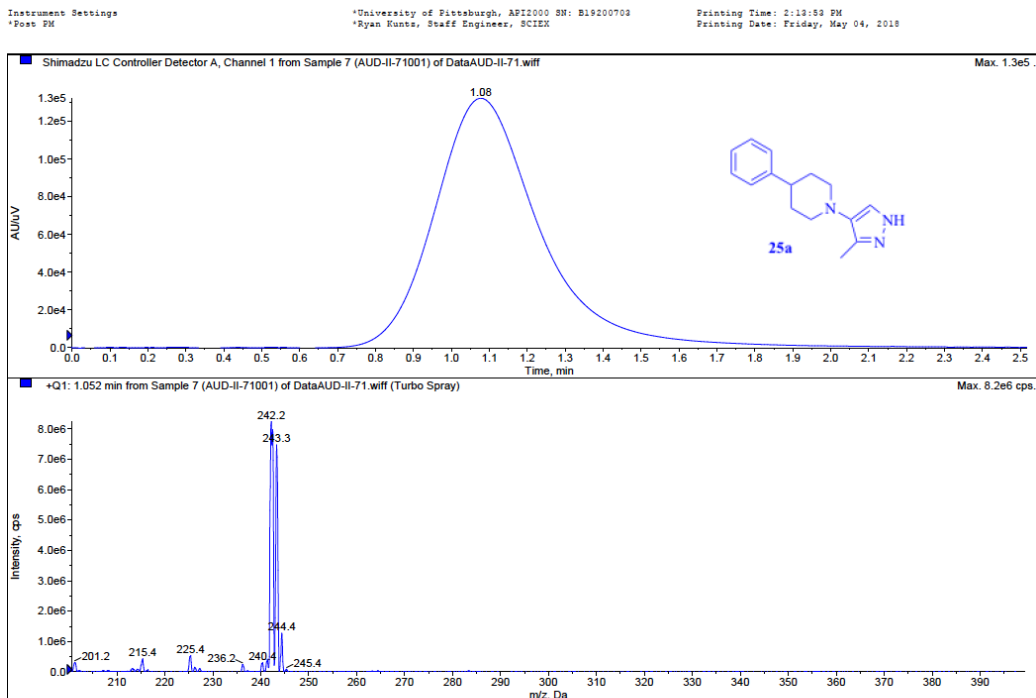
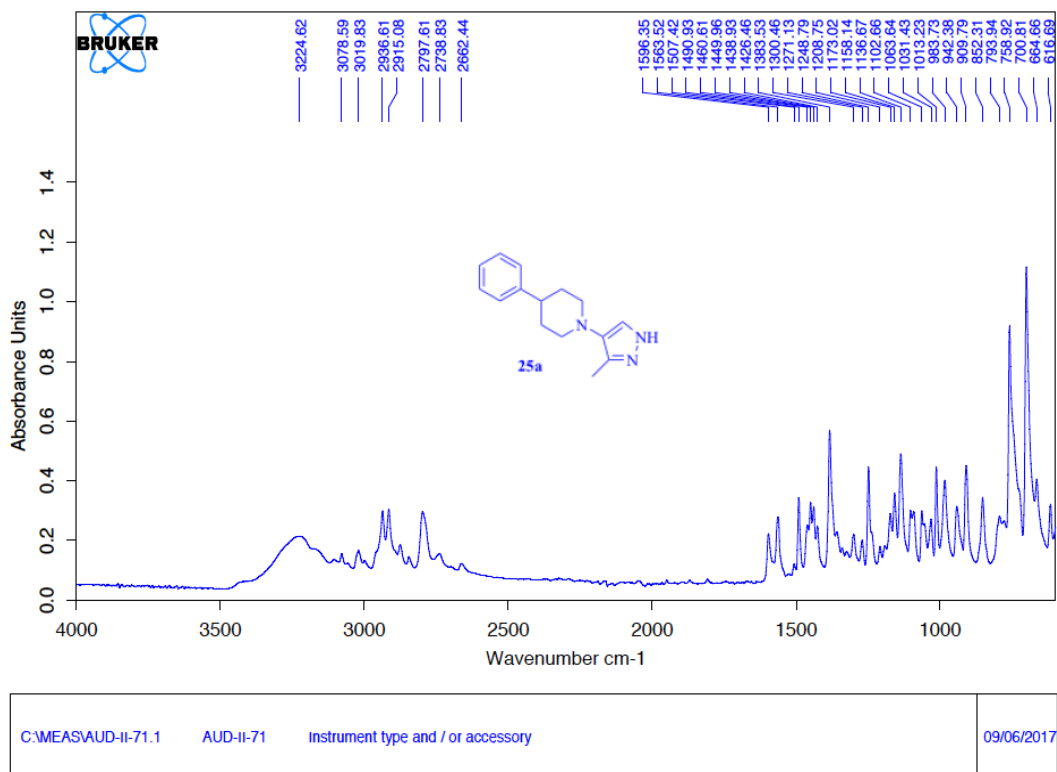


Current Data Parameters  
NAME AUD-II-71 DMSO  
EXPNO 1  
PROCNO 1

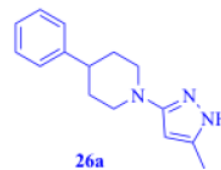
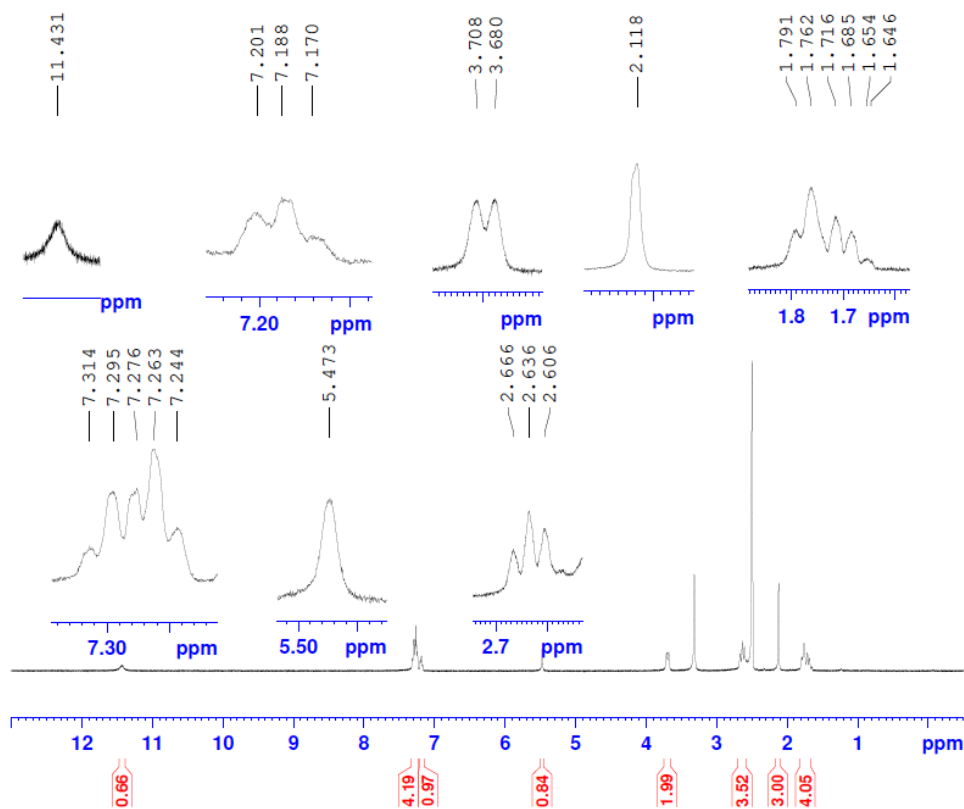
F2 - Acquisition Parameters  
Date\_ 20170609  
Time 13.01  
INSTRUM spect  
PROBHD 5 mm PABBO BB-  
PULPROG zg30  
TD 65536  
SOLVENT DMSO  
NS 16  
DS 2  
SWH 8223.685 Hz  
FIDRES 0.125483 Hz  
AQ 3.9846387 sec  
RG 228  
DW 60.800 usec  
DE 6.50 usec  
TE 298.0 K  
D1 1.00000000 sec

===== CHANNEL f1 =====  
NUC1 1H  
P1 12.19 usec  
PLW1 11.9899977 W  
SFO1 400.1324710 MHz

F2 - Processing parameters  
SI 65536  
SF 400.130033 MHz  
WDW no  
SSB 0  
LB 0 Hz  
GB 0  
PC 1.00



AUD-II-76

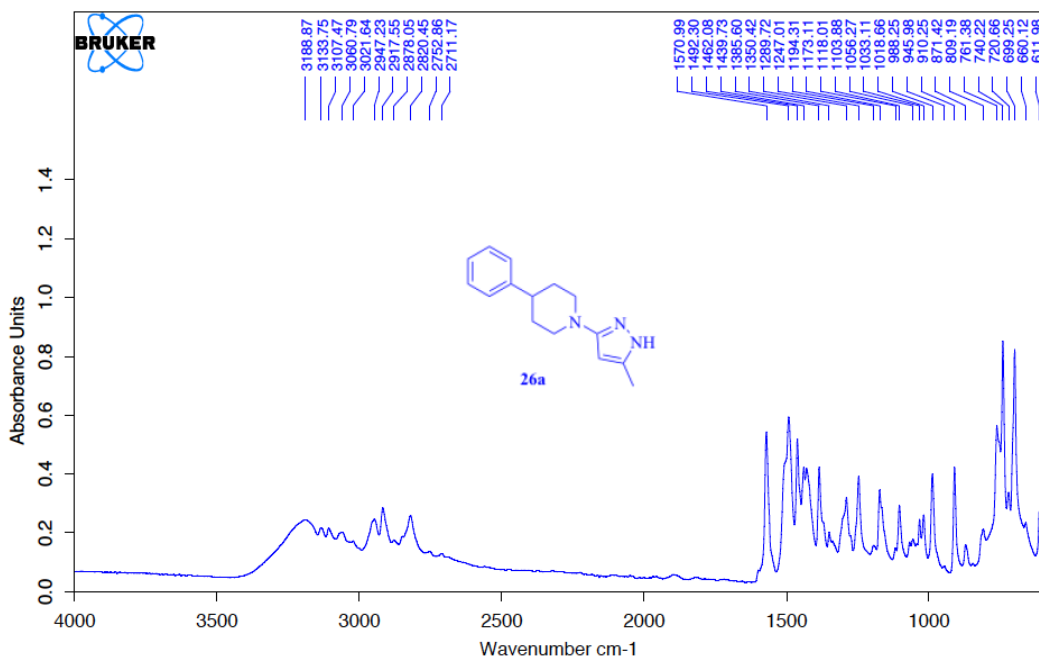


Current Data Parameters  
 NAME AUD-II-76  
 EXPNO 3  
 PROCNO 1

F2 - Acquisition Parameters  
 Date\_ 20170614  
 Time 11.34  
 INSTRUM spect  
 PROBHD 5 mm PABBO BB-  
 PULPROG zg30  
 TD 65536  
 SOLVENT DMSO  
 NS 16  
 DS 2  
 SWH 8223.685 Hz  
 FIDRES 0.125483 Hz  
 AQ 3.9846387 sec  
 RG 256  
 DW 60.800 usec  
 DE 6.50 usec  
 TE 298.0 K  
 D1 1.00000000 sec

===== CHANNEL f1 =====  
 NUC1 1H  
 P1 12.19 usec  
 PLW1 11.98999977 W  
 SFO1 400.1324710 MHz

F2 - Processing parameters  
 SI 65536  
 SF 400.1300063 MHz  
 WDW no  
 SSB 0  
 LB 0 Hz  
 GB 0  
 PC 1.00

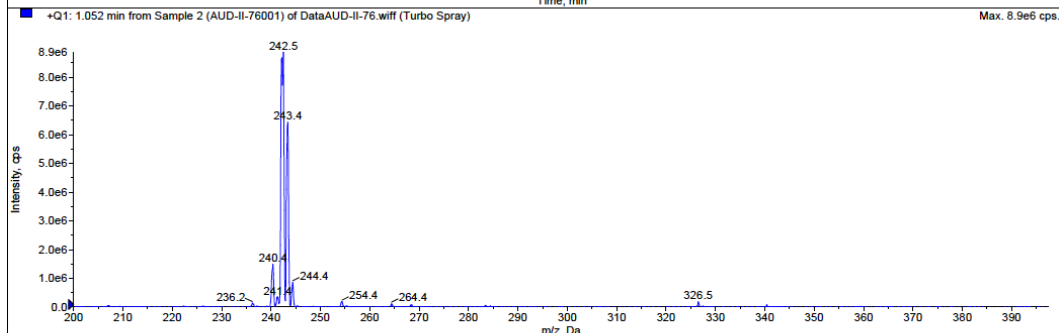
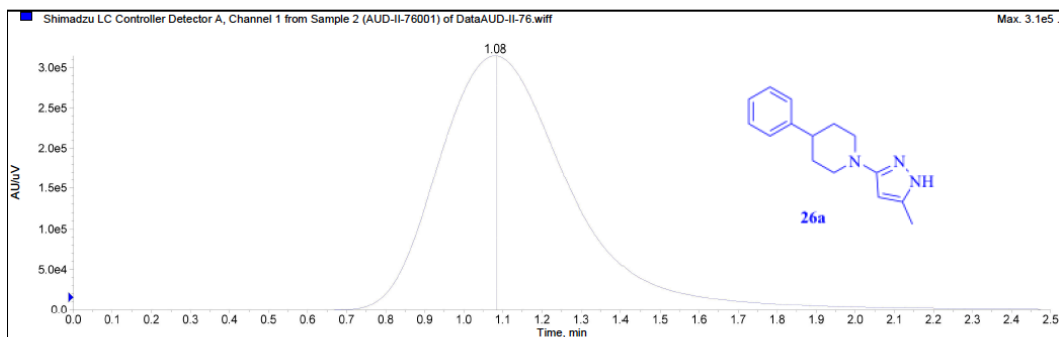


C:\MEASAUD-II-76.0	AUD-II-76	instrument type and / or accessory	14/06/2017
--------------------	-----------	------------------------------------	------------

Instrument Settings  
\*Post PM

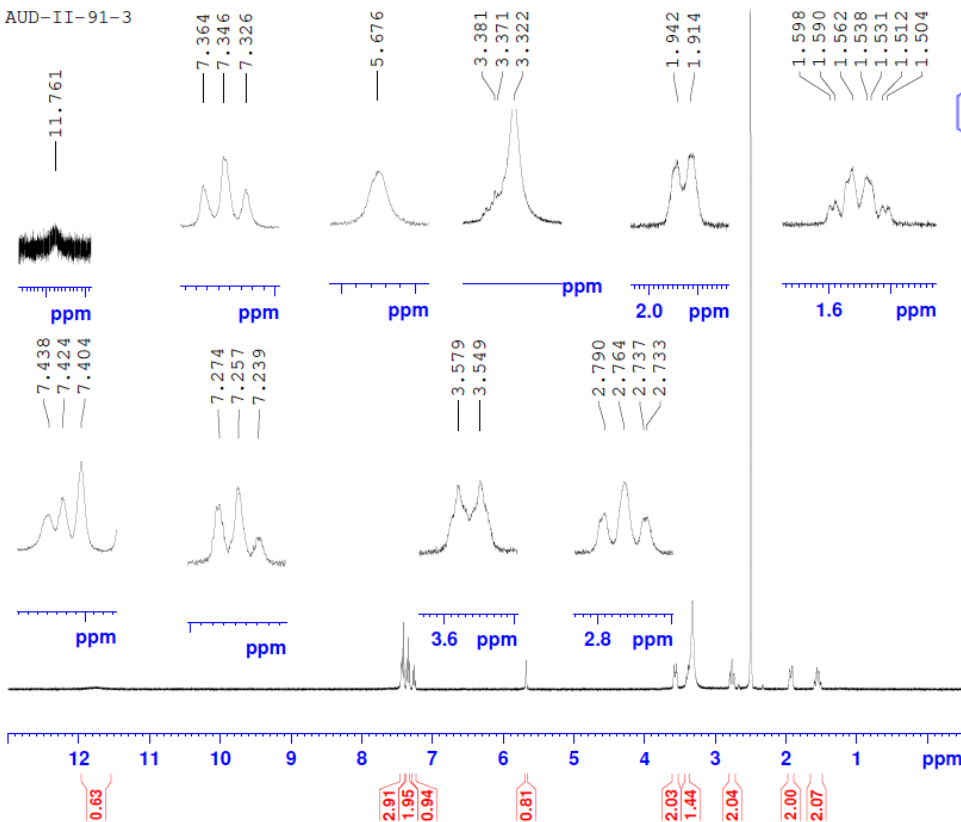
\*University of Pittsburgh, API2000 SN: B19200703  
\*Ryan Kuntz, Staff Engineer, SCIEX

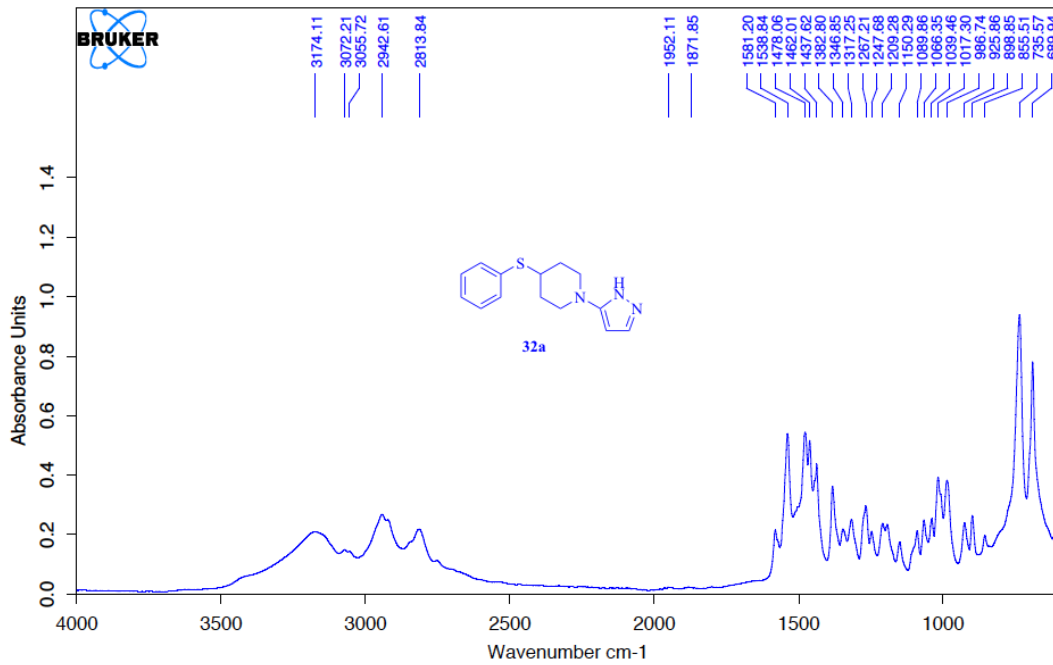
Printing Time: 2:19:20 PM  
Printing Date: Friday, May 04, 2018



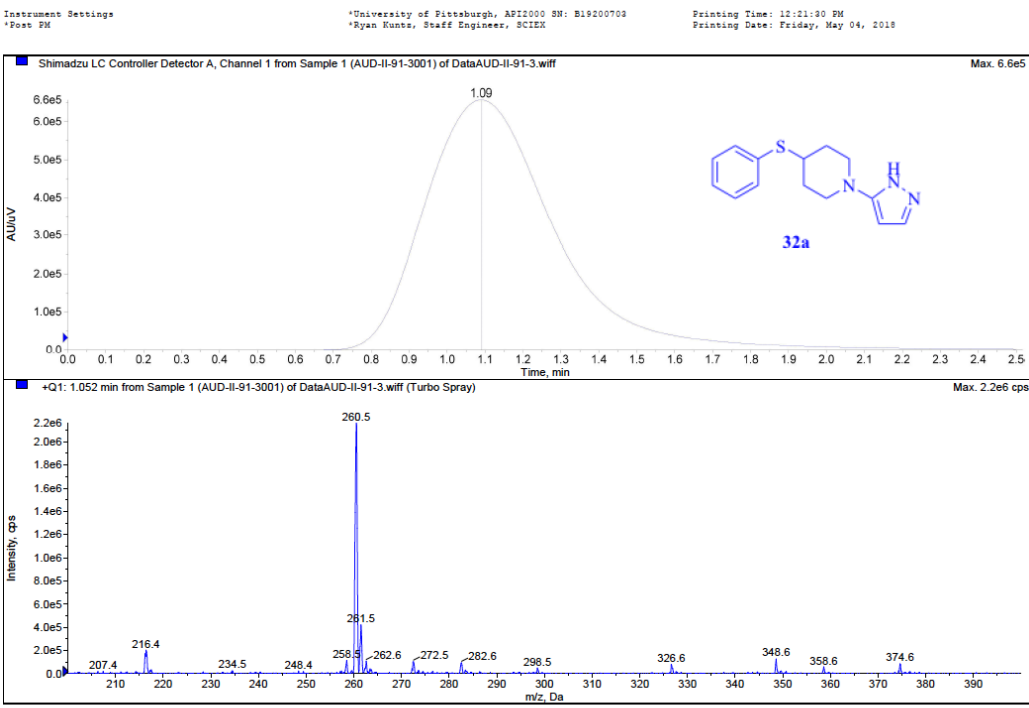


AUD-II-91-3

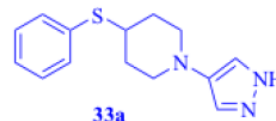
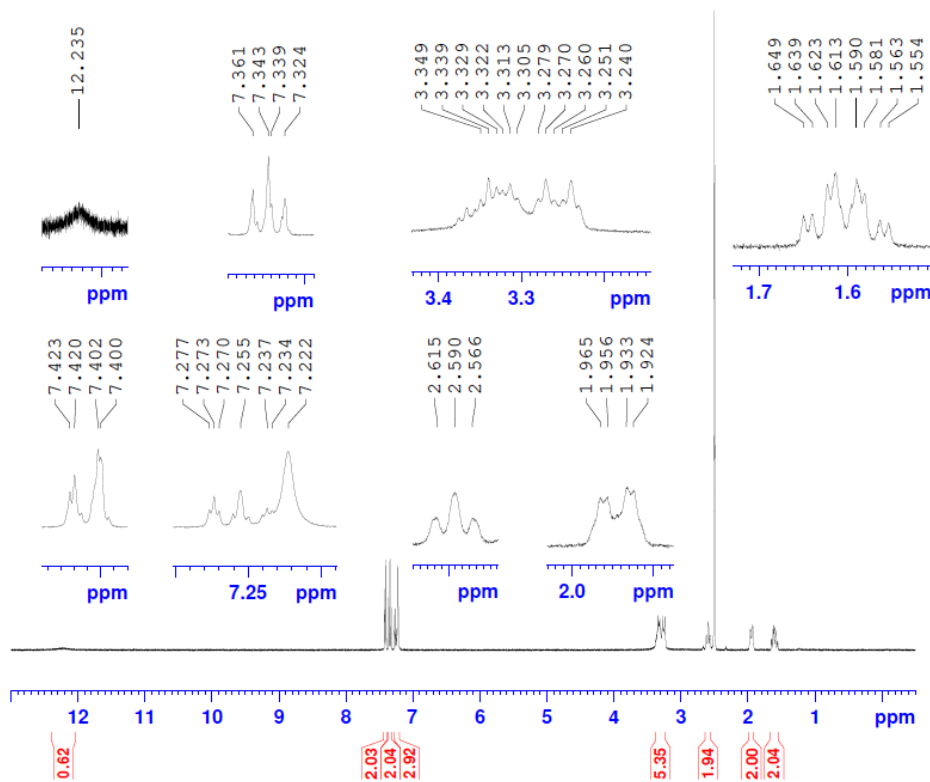




C:\MEAS\AUD-II-91-3.0	AUD-II-91-3	Instrument type and / or accessory	19/07/2017
-----------------------	-------------	------------------------------------	------------



AUD-II-94

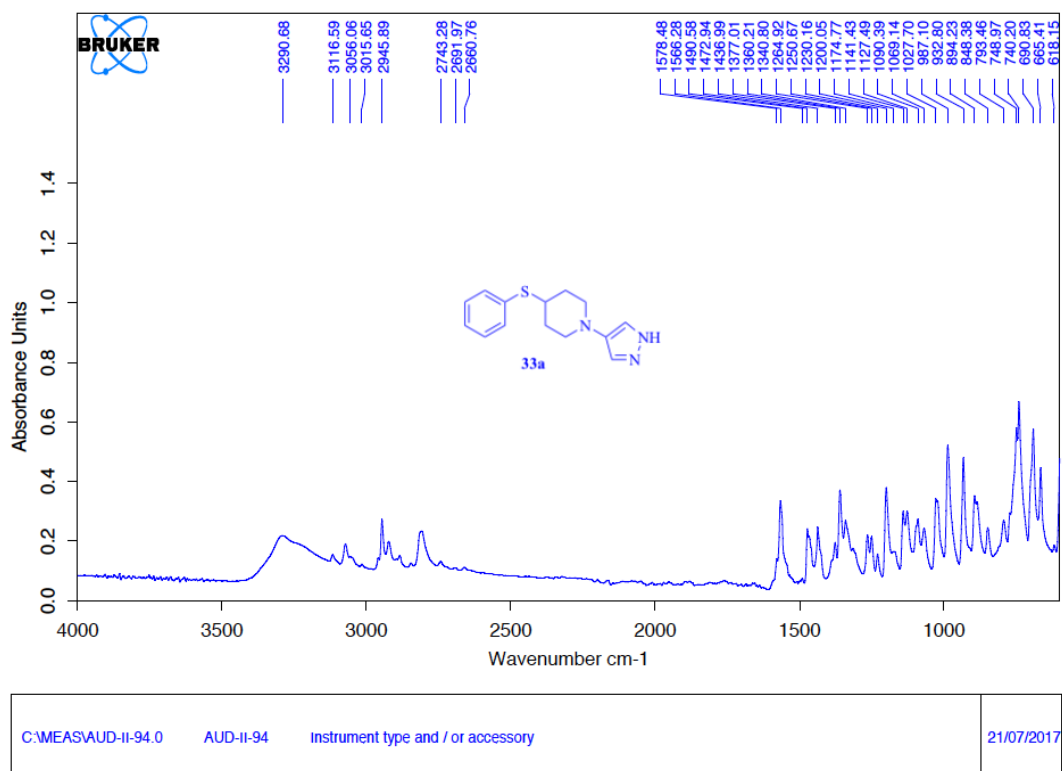


Current Data Parameters  
 NAME AUD-II-94  
 EXPNO 1  
 PROCNO 1

F2 - Acquisition Parameters  
 Date\_ 20170721  
 Time 11.05  
 INSTRUM spect  
 PROBHD 5 mm PABBO BB-  
 PULPROG zg30  
 TD 65536  
 SOLVENT DMSO  
 NS 16  
 DS 2  
 SWH 8223.685 Hz  
 FIDRES 0.125483 Hz  
 AQ 3.9846387 sec  
 RG 287  
 DW 60.800 usec  
 DE 6.50 usec  
 TE 298.0 K  
 D1 1.0000000 sec

===== CHANNEL f1 =====  
 NUC1 1H  
 P1 12.19 usec  
 PLW1 11.98999977 W  
 SFO1 400.1324710 MHz

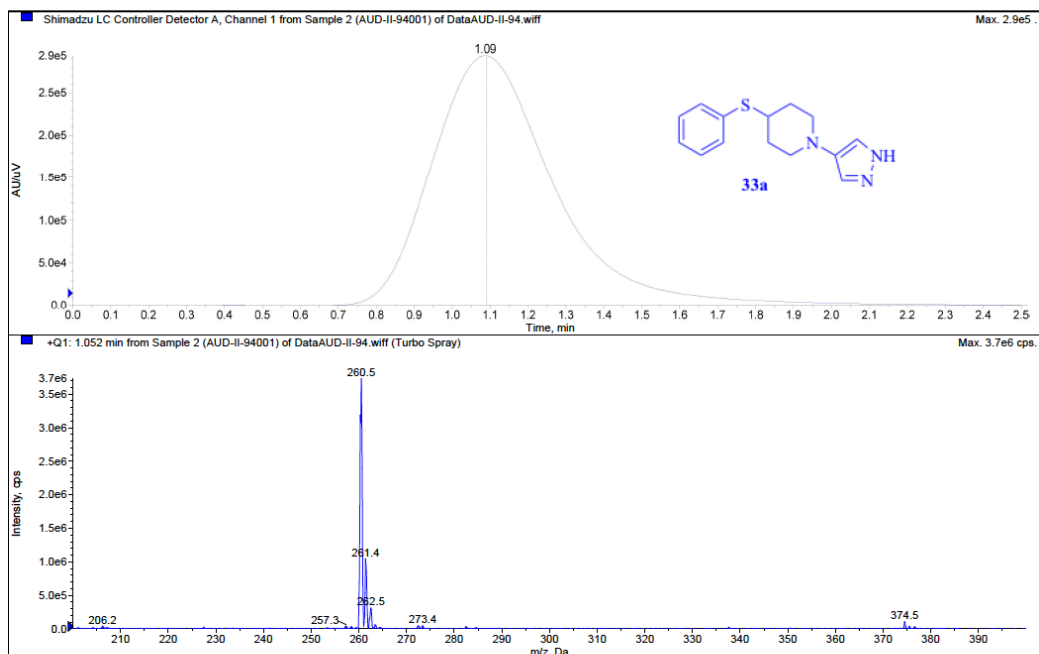
F2 - Processing parameters  
 SI 65536  
 SF 400.1300049 MHz  
 WDW no  
 SSB no  
 LB 0 Hz  
 GB 0  
 PC 1.00



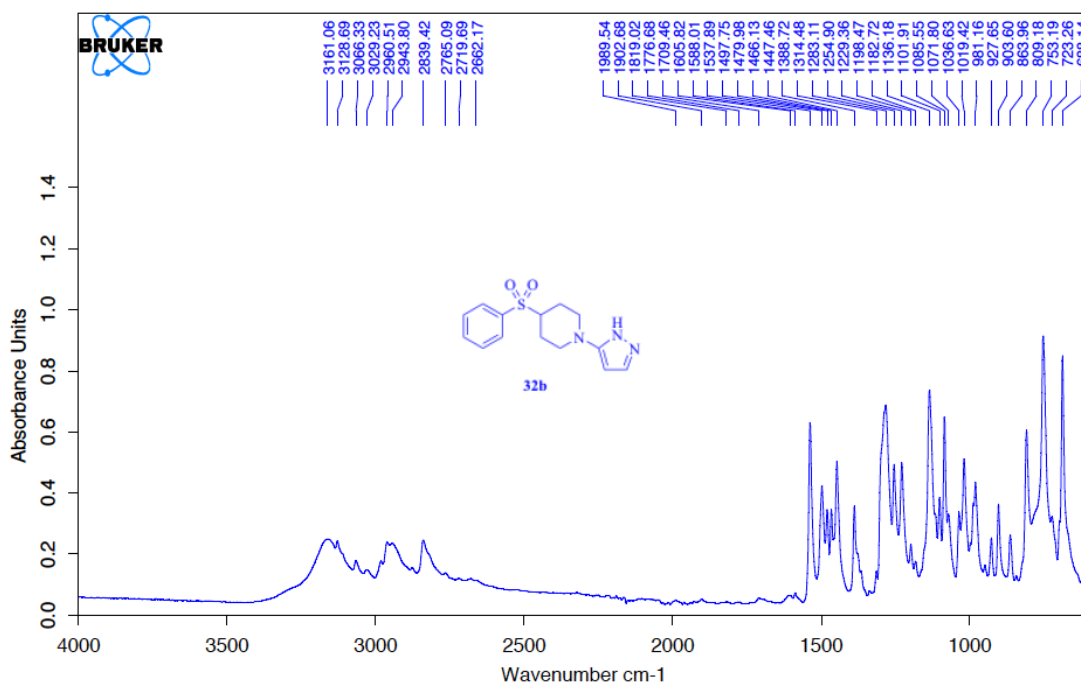
Instrument Settings  
\*Post PM

\*University of Pittsburgh, API2000 SN: B19200703  
\*Ryan Kuntz, Staff Engineer, SCIEX

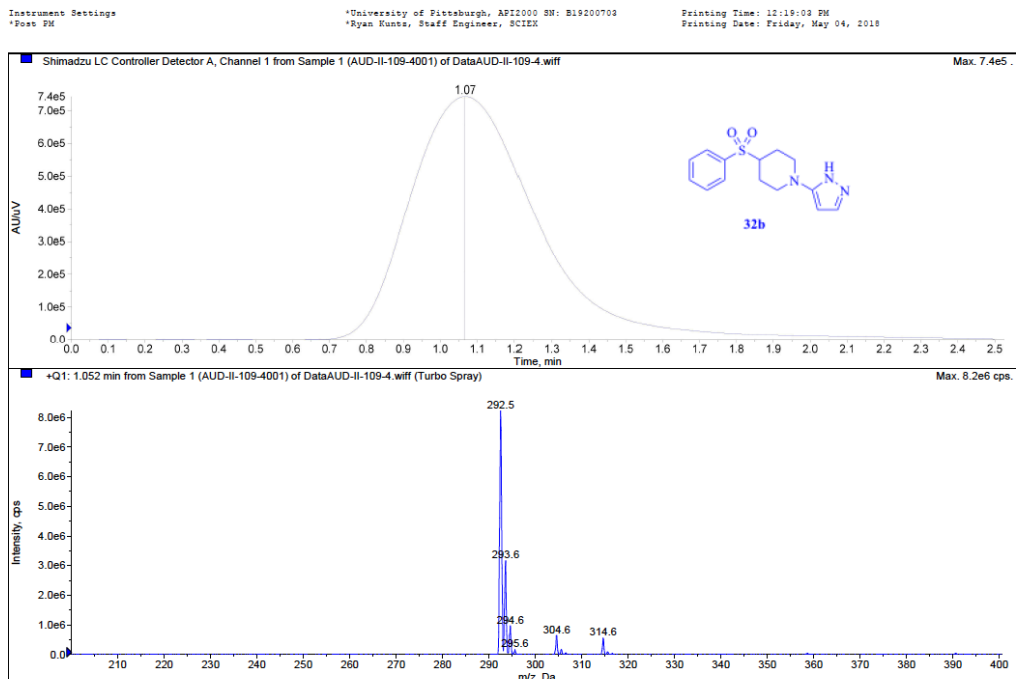
Printing Time: 12:20:43 PM  
Printing Date: Friday, May 04, 2018



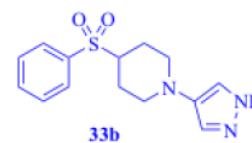
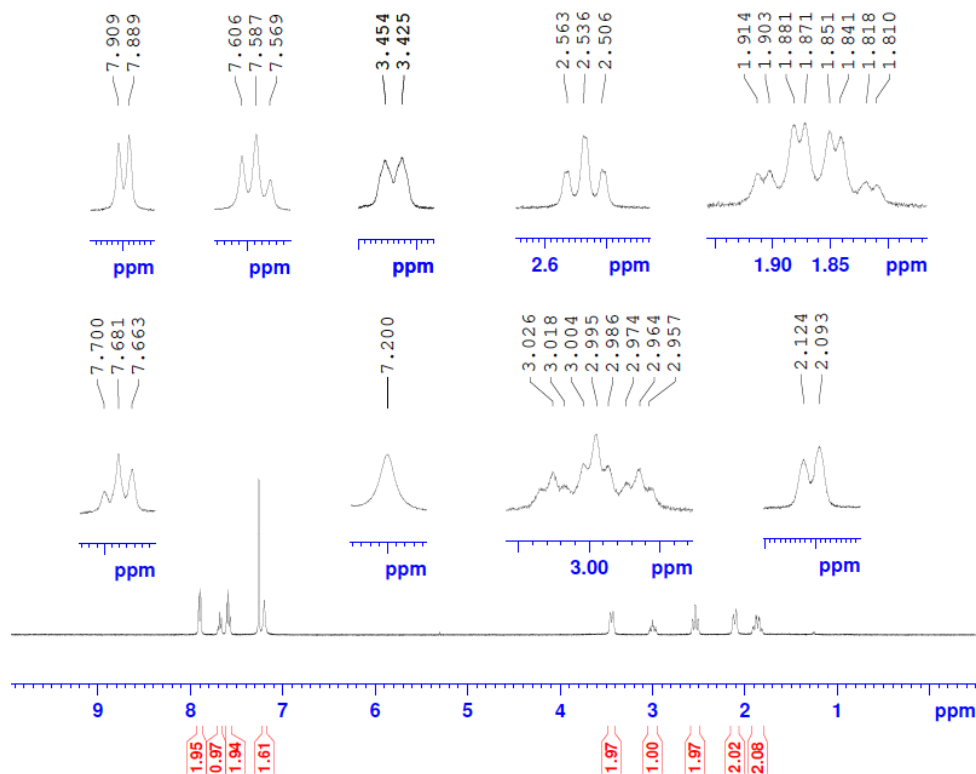




C:\Program Files\OPUS_65\MEAS\108	AUD-II-109-4	Instrument type and / or accessory	02/10/2017
-----------------------------------	--------------	------------------------------------	------------



AUD-II-101

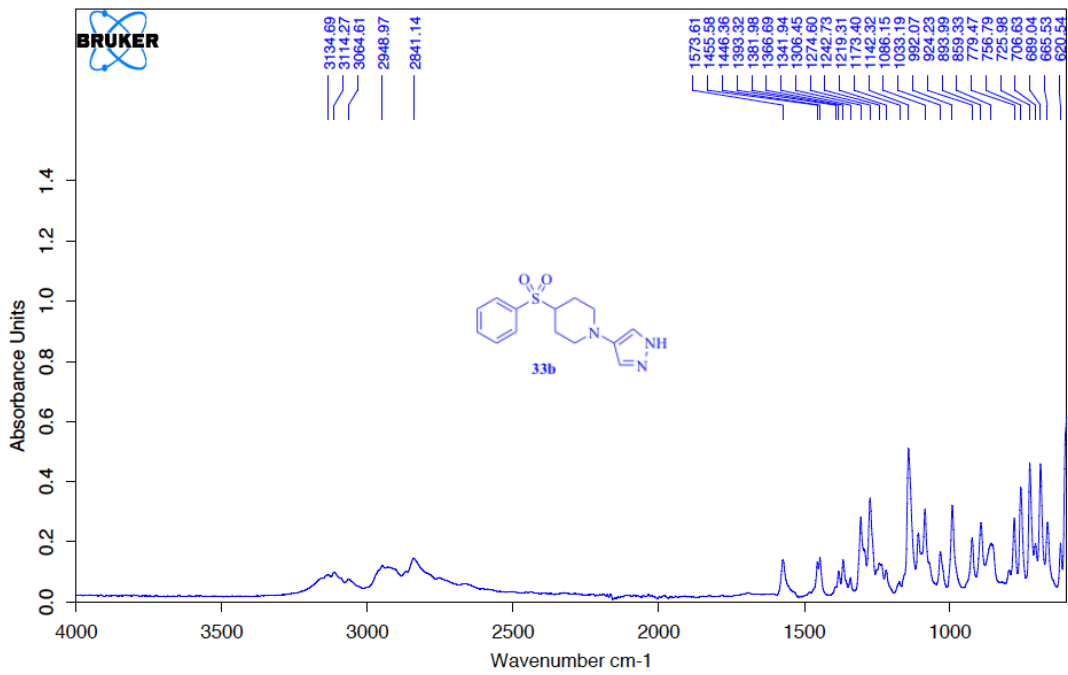


Current Data Parameters  
NAME AUD-II-101-2  
EXPNO 1  
PROCNO 1

F2 - Acquisition Parameters  
Date\_ 20180228  
Time 14.14  
INSTRUM spect  
PROBHD 5 mm PABBO BB-  
PULPROG zg30  
TD 65536  
SOLVENT CDCl3  
NS 16  
DS 2  
SWH 8223.685 Hz  
FIDRES 0.125483 Hz  
AQ 3.9846387 sec  
RG 256  
DW 60.800 usec  
DE 6.50 usec  
TE 298.0 K  
D1 1.00000000 sec

==== CHANNEL f1 =====  
NUC1 1H  
P1 12.19 usec  
PLW1 11.98999977 W  
SF01 400.1324710 MHz

F2 - Processing parameters  
SI 65536  
SF 400.1300102 MHz  
WDW no  
SSB 0  
LB 0 Hz  
GB 0  
PC 1.00



C:\Program Files\OPUS\_65\MEAS\AUD-II-101.0

AUD-II-101

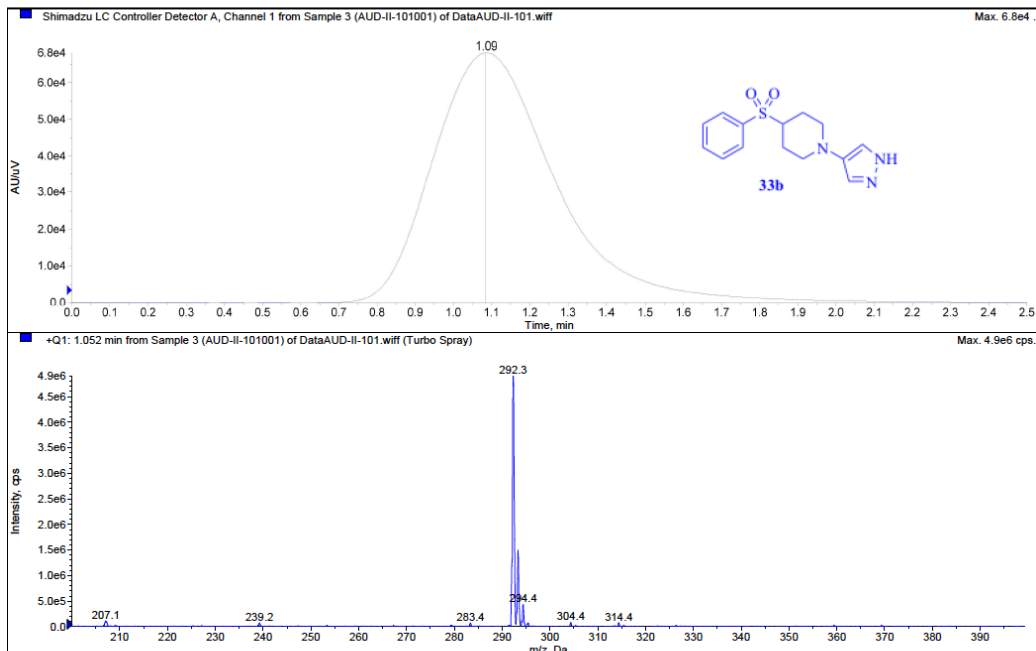
Instrument type and / or accessory

16/08/2017

Instrument Settings  
\*Post PM

\*University of Pittsburgh, API2000 SN: B19200703  
\*Ryan Kuntz, Staff Engineer, SCIEX

Printing Time: 12:19:51 PM  
Printing Date: Friday, May 04, 2018





## BIBLIOGRAPHY

1. Isseroff RR1, Z. V., Chapkin RS, Martinez DT, Conversion of linoleic acid into arachidonic acid by cultured murine and human keratinocytes. *J Lipid Res.* **1987**, 28 (11), 1342-9.
2. Zeldin, D. C., Epoxygenase pathways of arachidonic acid metabolism. *The Journal of biological chemistry* **2001**, 276 (39), 36059-62.
3. Roman, R. J., P-450 Metabolites of Arachidonic Acid in the Control of Cardiovascular Function. *Physiol Rev* 82 (1), 131-185.
4. Dr. H. A. O. Hill, D. A. R. d., and Dr. R.J.P. Williams, The Chemical Nature and Reactivity of Cytochrome P-450. *Struct Bond* **1970**, 8, 123-51.
5. Nishimura M1, Y. H., Yoshitsugu H, Naito S, Satoh T., Tissue distribution of mRNA expression of human cytochrome P450 isoforms assessed by high-sensitivity real-time reverse transcription PCR. *Yakugaku Zasshi.* **2003**, 123 (5), 369-75.
6. Manikandan, P.; Nagini, S., Cytochrome P450 Structure, Function and Clinical Significance: A Review. *Current drug targets* **2018**, 19 (1), 38-54.
7. Jorge H. Capdevila<sup>1</sup>, John R. Falck<sup>§</sup> and Raymond C. Harris\*, Cytochrome P450 and arachidonic acid bioactivation: molecular and functional properties of the arachidonate monooxygenase. *The Journal of Lipid Research* **2000** 41, 163-181.
8. H.Oliw, E., bis-Allylic hydroxylation of linoleic acid and arachidonic acid by human hepatic monooxygenases. *Biochimica et Biophysica Acta (BBA) - Lipids and Lipid Metabolism* **1993**, 1166 (2-3), 258-263.
9. El-Sherbeni, A. A.; El-Kadi, A. O., Repurposing Resveratrol and Fluconazole To Modulate Human Cytochrome P450-Mediated Arachidonic Acid Metabolism. *Molecular pharmaceutics* **2016**, 13 (4), 1278-88.
10. Roman, R. J., P-450 Metabolites of Arachidonic acid in Control of Cardiovascular Funtion. *Physiol Rev* **2002**, 82 (1), 131-85.

11. Jerome M. Lasker‡, W. B. C., Imre Wolf, Barbara P. Bloswick§, Patricia D. Wilson§, and Pnina K. Powell, Formation of 20-Hydroxyeicosatetraenoic Acid, a Vasoactive and Natriuretic Eicosanoid, in Human Kidney. *J Biol Chem.* **2000**, 275 (6), 4118-26.
12. Fer, M.; Corcos, L.; Dreano, Y.; Plee-Gautier, E.; Salaun, J. P.; Berthou, F.; Amet, Y., Cytochromes P450 from family 4 are the main omega hydroxylating enzymes in humans: CYP4F3B is the prominent player in PUFA metabolism. *Journal of lipid research* **2008**, 49 (11), 2379-89.
13. Kroetz, D. L.; Xu, F., Regulation and inhibition of arachidonic acid omega-hydroxylases and 20-HETE formation. *Annual review of pharmacology and toxicology* **2005**, 45, 413-38.
14. Roman, R. J.; Renic, M.; Dunn, K. M.; Takeuchi, K.; Hacein-Bey, L., Evidence that 20-HETE contributes to the development of acute and delayed cerebral vasospasm. *Neurological research* **2006**, 28 (7), 738-49.
15. D. Gebremedhin, Y. H. M., J. R. Falck, R. J. Roman, M. VanRollins, and D. R. Harder, Mechanism of action of cerebral epoxyeicosatrienoic acids on cerebral arterial smooth muscle. *Am J Physiol* **1992**, 263 (2), H519.
16. Garcia, V.; Cheng, J.; Weidenhammer, A.; Ding, Y.; Wu, C. C.; Zhang, F.; Gotlinger, K.; Falck, J. R.; Schwartzman, M. L., Androgen-induced hypertension in angiotensinogen deficient mice: role of 20-HETE and EETS. *Prostaglandins & other lipid mediators* **2015**, 116-117, 124-30.
17. Imig, J. D., Epoxyeicosatrienoic Acids and 20-Hydroxyeicosatetraenoic Acid on Endothelial and Vascular Function. *Advances in pharmacology* **2016**, 77, 105-41.
18. Spector, A. A., Arachidonic acid cytochrome P450 epoxygenase pathway. *Journal of lipid research* **2009**, 50 Suppl, S52-6.
19. Cazade, M.; Bidaud, I.; Hansen, P. B.; Lory, P.; Chemin, J., 5,6-EET potently inhibits T-type calcium channels: implication in the regulation of the vascular tone. *Pflugers Archiv : European journal of physiology* **2014**, 466 (9), 1759-68.
20. Tyndale, S. L. M. a. R. F., Drug-metabolizing cytochrome P450s in the brain. *J Psychiatry Neurosci.* **2002**, 27 (6), 406-415.
21. Qu, W.; Bradbury, J. A.; Tsao, C. C.; Maronpot, R.; Harry, G. J.; Parker, C. E.; Davis, L. S.; Breyer, M. D.; Waalkes, M. P.; Falck, J. R.; Chen, J.; Rosenberg, R. L.; Zeldin, D. C., Cytochrome P450 CYP2J9, a new mouse arachidonic acid omega-1 hydroxylase predominantly expressed in brain. *The Journal of biological chemistry* **2001**, 276 (27), 25467-79.
22. Debebe Gebremedhin, A. R. L., Timothy F. Lowry, M. Reza Taheri, Eric K. Birks, Antal G. Hudetz, Jayashree Narayanan, John R. Falck, Hirotsugu Okamoto, Richard J. Roman,

- Kasem Nithipatikom, William B. Campbell, David R. Harder, Production of 20-HETE and Its Role in Autoregulation of Cerebral Blood Flow. *INTEGRATIVE PHYSIOLOGY* **2000**, 87 (1), 60-5.
23. Shivachar C. Amruthesh, J. R. F., and Earl F. Ellis, Brain Synthesis and Cerebrovascular Action of Epoxygenase Metabolites of Arachidonic Acid. *Journal of Neurochemistry* **1992**, 58, 503-510.
  24. Miller, T. M.; Donnelly, M. K.; Crago, E. A.; Roman, D. M.; Sherwood, P. R.; Horowitz, M. B.; Poloyac, S. M., Rapid, simultaneous quantitation of mono and dioxygenated metabolites of arachidonic acid in human CSF and rat brain. *Journal of chromatography. B, Analytical technologies in the biomedical and life sciences* **2009**, 877 (31), 3991-4000.
  25. Huang, H.; Al-Shabrawey, M.; Wang, M. H., Cyclooxygenase- and cytochrome P450-derived eicosanoids in stroke. *Prostaglandins & other lipid mediators* **2016**, 122, 45-53.
  26. Benjamin, E. J.; Blaha, M. J.; Chiuve, S. E.; Cushman, M.; Das, S. R.; Deo, R.; de Ferranti, S. D.; Floyd, J.; Fornage, M.; Gillespie, C.; Isasi, C. R.; Jimenez, M. C.; Jordan, L. C.; Judd, S. E.; Lackland, D.; Lichtman, J. H.; Lisabeth, L.; Liu, S.; Longenecker, C. T.; Mackey, R. H.; Matsushita, K.; Mozaffarian, D.; Mussolino, M. E.; Nasir, K.; Neumar, R. W.; Palaniappan, L.; Pandey, D. K.; Thiagarajan, R. R.; Reeves, M. J.; Ritchey, M.; Rodriguez, C. J.; Roth, G. A.; Rosamond, W. D.; Sasson, C.; Towfighi, A.; Tsao, C. W.; Turner, M. B.; Virani, S. S.; Voeks, J. H.; Willey, J. Z.; Wilkins, J. T.; Wu, J. H.; Alger, H. M.; Wong, S. S.; Muntner, P.; American Heart Association Statistics, C.; Stroke Statistics, S., Heart Disease and Stroke Statistics-2017 Update: A Report From the American Heart Association. *Circulation* **2017**, 135 (10), e146-e603.
  27. Durrant, J. C.; Hinson, H. E., Rescue therapy for refractory vasospasm after subarachnoid hemorrhage. *Current neurology and neuroscience reports* **2015**, 15 (2), 521.
  28. Kusaka, G.; Ishikawa, M.; Nanda, A.; Granger, D. N.; Zhang, J. H., Signaling pathways for early brain injury after subarachnoid hemorrhage. *Journal of cerebral blood flow and metabolism : official journal of the International Society of Cerebral Blood Flow and Metabolism* **2004**, 24 (8), 916-25.
  29. Cahill, J.; Calvert, J. W.; Zhang, J. H., Mechanisms of early brain injury after subarachnoid hemorrhage. *Journal of cerebral blood flow and metabolism : official journal of the International Society of Cerebral Blood Flow and Metabolism* **2006**, 26 (11), 1341-53.
  30. Toru FUKUHARA, C. M. D., J. Paul ELIOTT, David W. NEWELL, and H. Richard WINN, Relationship between Intracranial Pressure and the Development of Vasospasm after Aneurysmal Subarachnoid Hemorrhage. *Neurol Med Chir* **1998**, 38, 710-717.
  31. Dhar, R.; Scalfani, M. T.; Blackburn, S.; Zazulia, A. R.; Videen, T.; Diring, M., Relationship between angiographic vasospasm and regional hypoperfusion in aneurysmal subarachnoid hemorrhage. *Stroke* **2012**, 43 (7), 1788-94.

32. Vergouwen, M. D.; Vermeulen, M.; van Gijn, J.; Rinkel, G. J.; Wijdicks, E. F.; Muizelaar, J. P.; Mendelow, A. D.; Juvela, S.; Yonas, H.; Terbrugge, K. G.; Macdonald, R. L.; Diring, M. N.; Broderick, J. P.; Dreier, J. P.; Roos, Y. B., Definition of delayed cerebral ischemia after aneurysmal subarachnoid hemorrhage as an outcome event in clinical trials and observational studies: proposal of a multidisciplinary research group. *Stroke* **2010**, *41* (10), 2391-5.
33. Macdonald, R. L.; Kassell, N. F.; Mayer, S.; Ruefenacht, D.; Schmiedek, P.; Weidauer, S.; Frey, A.; Roux, S.; Pasqualin, A.; Investigators, C.-. Clazosentan to overcome neurological ischemia and infarction occurring after subarachnoid hemorrhage (CONSCIOUS-1): randomized, double-blind, placebo-controlled phase 2 dose-finding trial. *Stroke* **2008**, *39* (11), 3015-21.
34. Poloyac, S. M.; Reynolds, R. B.; Yonas, H.; Kerr, M. E., Identification and quantification of the hydroxyeicosatetraenoic acids, 20-HETE and 12-HETE, in the cerebrospinal fluid after subarachnoid hemorrhage. *Journal of neuroscience methods* **2005**, *144* (2), 257-63.
35. Crago, E. A.; Thampatty, B. P.; Sherwood, P. R.; Kuo, C. W.; Bender, C.; Balzer, J.; Horowitz, M.; Poloyac, S. M., Cerebrospinal fluid 20-HETE is associated with delayed cerebral ischemia and poor outcomes after aneurysmal subarachnoid hemorrhage. *Stroke* **2011**, *42* (7), 1872-7.
36. Kehl F1, C.-S. L., Maier KG, Miyata N, Kametani S, Okamoto H, Hudetz AG, Schulte ML, Zagorac D, Harder DR, Roman RJ., 20-HETE contributes to the acute fall in cerebral blood flow after subarachnoid hemorrhage in the rat. *Am J Physiol Heart Circ Physiol.* **2002**, (282(4)), H1556-65.
37. Miyata, N.; Seki, T.; Tanaka, Y.; Omura, T.; Taniguchi, K.; Doi, M.; Bandou, K.; Kametani, S.; Sato, M.; Okuyama, S.; Cambj-Sapunar, L.; Harder, D. R.; Roman, R. J., Beneficial effects of a new 20-hydroxyeicosatetraenoic acid synthesis inhibitor, TS-011 [N-(3-chloro-4-morpholin-4-yl) phenyl-N'-hydroxyimido formamide], on hemorrhagic and ischemic stroke. *The Journal of pharmacology and experimental therapeutics* **2005**, *314* (1), 77-85.
38. Iordanova, B.; Li, L.; Clark, R. S. B.; Manole, M. D., Alterations in Cerebral Blood Flow after Resuscitation from Cardiac Arrest. *Frontiers in pediatrics* **2017**, *5*, 174.
39. Sabri, M.; Lass, E.; Macdonald, R. L., Early brain injury: a common mechanism in subarachnoid hemorrhage and global cerebral ischemia. *Stroke research and treatment* **2013**, *2013*, 394036.
40. Svetlana Pundik, K. X., Sophia Sundararajan, Reperfusion brain injury, Focus on cellular bioenergetics. *Neurology* **2012**, *79* (13), S44-S51.
41. Chan, P. H., Reactive Oxygen Radicals in Signaling and Damage in the Ischemic Brain. *Journal of Cerebral Blood Flow & Metabolism* **2001**, *21* (1), 2-14.

42. Manole, M. D.; Kochanek, P. M.; Fink, E. L.; Clark, R. S., Postcardiac arrest syndrome: focus on the brain. *Current opinion in pediatrics* **2009**, *21* (6), 745-50.
43. Nolan, J. P.; Neumar, R. W.; Adrie, C.; Aibiki, M.; Berg, R. A.; Bottiger, B. W.; Callaway, C.; Clark, R. S.; Geocadin, R. G.; Jauch, E. C.; Kern, K. B.; Laurent, I.; Longstreth, W. T.; Merchant, R. M.; Morley, P.; Morrison, L. J.; Nadkarni, V.; Peberdy, M. A.; Rivers, E. P.; Rodriguez-Nunez, A.; Sellke, F. W.; Spaulding, C.; Sunde, K.; Hoek, T. V., Post-cardiac arrest syndrome: epidemiology, pathophysiology, treatment, and prognostication. A Scientific Statement from the International Liaison Committee on Resuscitation; the American Heart Association Emergency Cardiovascular Care Committee; the Council on Cardiovascular Surgery and Anesthesia; the Council on Cardiopulmonary, Perioperative, and Critical Care; the Council on Clinical Cardiology; the Council on Stroke. *Resuscitation* **2008**, *79* (3), 350-79.
44. Shaik, J. S.; Poloyac, S. M.; Kochanek, P. M.; Alexander, H.; Tudorascu, D. L.; Clark, R. S.; Manole, M. D., 20-Hydroxyeicosatetraenoic Acid Inhibition by HET0016 Offers Neuroprotection, Decreases Edema, and Increases Cortical Cerebral Blood Flow in a Pediatric Asphyxial Cardiac Arrest Model in Rats. *Journal of cerebral blood flow and metabolism : official journal of the International Society of Cerebral Blood Flow and Metabolism* **2015**, *35* (11), 1757-63.
45. Yang, Z. J.; Carter, E. L.; Kibler, K. K.; Kwansa, H.; Crafa, D. A.; Martin, L. J.; Roman, R. J.; Harder, D. R.; Koehler, R. C., Attenuation of neonatal ischemic brain damage using a 20-HETE synthesis inhibitor. *J Neurochem* **2012**, *121* (1), 168-79.
46. MATHEWS, P. R. O. D. M. a. J. M., Autocatalytic alkylation of the cytochrome P-450 prosthetic haem group by 1-aminobenzotriazole. *Biochem. J.* **1981**, (195), 761-764.
47. Su P1, K. K., Kroetz DL, Inhibition of renal arachidonic acid omega-hydroxylase activity with ABT reduces blood pressure in the SHR. *Am J Physiol* **1998**, (275(2 Pt 2)), R426-38.
48. A P Zou, Y. H. M., Z H Sui, P R Ortiz de Montellano, J E Clark, B S Masters and R J Roman, Effects of 17-octadecynoic acid, a suicide-substrate inhibitor of cytochrome P450 fatty acid omega-hydroxylase, on renal function in rats. *The Journal of pharmacology and experimental therapeutics* **1994**, *268* (1), 474-481.
49. Xu F1, S. W., Pak W, Su P, Maier KG, Yu M, Roman RJ, Ortiz De Montellano PR, Kroetz DL, Antihypertensive effect of mechanism-based inhibition of renal arachidonic acid omega-hydroxylase activity. *Am J Physiol Regul Integr Comp Physiol.* **2002**, *283* (3), R710-20.
50. Wang MH1, B.-S. E., Zand BA, Nguyen X, Falck JR, Balu N, Schwartzman ML, Cytochrome P450-derived arachidonic acid metabolism in the rat kidney: characterization of selective inhibitors. *J Pharmacol Exp Ther.* **1998**, *284* (3), 966-73.

51. Yu, M.; Cambj-Sapunar, L.; Kehl, F.; Maier, K. G.; Takeuchi, K.; Miyata, N.; Ishimoto, T.; Reddy, L. M.; Falck, J. R.; Gebremedhin, D.; Harder, D. R.; Roman, R. J., Effects of a 20-HETE antagonist and agonists on cerebral vascular tone. *European journal of pharmacology* **2004**, *486* (3), 297-306.
52. Sato M1, I. T., Kobayashi-Matsunaga Y, Amada H, Taniguchi K, Miyata N, Kameo K, Discovery of a N1-Hydroxyphenylformamidine Derivative HET0016y as a Potent and Selective 20-HETE Synthase Inhibitor. *Bioorg Med Chem Lett.* **2001**, *11* (23), 2993-5.
53. Miyata N1, T. K., Seki T, Ishimoto T, Sato-Watanabe M, Yasuda Y, Doi M, Kametani S, Tomishima Y, Ueki T, Sato M, Kameo K., HET0016, a potent and selective inhibitor of 20-HETE synthesizing enzyme. *British journal of pharmacology* **2001**, *133* (3), 325-9.
54. Poloyac, S. M.; Zhang, Y.; Bies, R. R.; Kochanek, P. M.; Graham, S. H., Protective effect of the 20-HETE inhibitor HET0016 on brain damage after temporary focal ischemia. *Journal of cerebral blood flow and metabolism : official journal of the International Society of Cerebral Blood Flow and Metabolism* **2006**, *26* (12), 1551-61.
55. Nakamura T1, S. M., Kakinuma H, Miyata N, Taniguchi K, Bando K, Koda A, Kameo K, Pyrazole and Isoxazole Derivatives as New, Potent, and Selective 20-Hydroxy-5,8,11,14-eicosatetraenoic Acid Synthase Inhibitors. *J Med Chem* **2003**, *46* (25), 5416-27.
56. Christopher A Lipinski, F. L., Beryl W Dominy, Paul J Feeney, Experimental and computational approaches to estimate solubility and permeability in drug discovery and development settings. *Advanced Drug Delivery Reviews* **2001**, *46* ( 1-3), 3-26.
57. Serlin, Y.; Shelef, I.; Knyazer, B.; Friedman, A., Anatomy and physiology of the blood-brain barrier. *Seminars in cell & developmental biology* **2015**, *38*, 2-6.
58. Lenz, H. P. a. G. R., Medicinal Chemical Properties of Successful Central Nervous System Drugs. *NeuroRx.* **2005**, *2* (4), 541-553.
59. TAKASHI HIROTA, K. S. A.; YAMAMOTO, H., Anomalous products formed from N-(5,6-dihydrobenzo[h]quinazolin-4-yl)amidines and hydroxylamine hydrochloride. *Acta Cryst.* **1994**, (C50), 807-810.
60. Sun, H.; Tawa, G.; Wallqvist, A., Classification of scaffold-hopping approaches. *Drug discovery today* **2012**, *17* (7-8), 310-24.
61. Zhang, H.; Cai, Q.; Ma, D., Amino Acid Promoted CuI-Catalyzed C-N Bond Formation between Aryl Halides and Amines or N-Containing Heterocycles. *The Journal of Organic Chemistry* **2005**, *70* (13), 5164-5173.
62. Shelley Allen, S. A., James F. Blake, Kevin R. Condroski, Julia Haas, Lily Huang, Yutong Jiang, Timothy Kercher, Gabrielle R. Kolakowski, Jeonbeob, Pyrrolidinyl Urea, pyrrolidiniyl thiourea and pyrrolidinyl guanidine compounds as TRKA Kinase inhibitors. US Patent 9,878,997 B2. **Jan. 30, 2018.**

63. Ernesto G. Occhiato\*, F. L. G., and Antonio Guarna, Preparation and Suzuki-Miyaura Coupling Reactions of Tetrahydropyridine-2-boronic Acid Pinacol Esters. *J. Org. Chem* **2005**, *70* (18), 7324-7330.
64. Imamura S1, I. T., Nishikawa Y, Kanzaki N, Takashima K, Niwa S, Iizawa Y, Baba M, Sugihara Y, Discovery of a Piperidine-4-carboxamide CCR5 Antagonist (TAK-220) with Highly Potent Anti-HIV-1 Activity. *J Med Chem.* **2006**, *49* (9), 2784-93.
65. Fletcher, S. R.; Burkamp, F.; Blurton, P.; Cheng, S. K. F.; Clarkson, R.; O'Connor, D.; Spinks, D.; Tudge, M.; van Niel, M. B.; Patel, S.; Chapman, K.; Marwood, R.; Shephard, S.; Bentley, G.; Cook, G. P.; Bristow, L. J.; Castro, J. L.; Hutson, P. H.; MacLeod, A. M., 4-(Phenylsulfonyl)piperidines: Novel, Selective, and Bioavailable 5-HT<sub>2A</sub> Receptor Antagonists. *Journal of Medicinal Chemistry* **2002**, *45* (2), 492-503.
66. Alsenz, J.; Kansy, M., High throughput solubility measurement in drug discovery and development. *Adv Drug Deliv Rev* **2007**, *59* (7), 546-67.
67. Di, L.; Kerns, E. H.; Hong, Y.; Kleintop, T. A.; McConnell, O. J.; Huryn, D. M., Optimization of a higher throughput microsomal stability screening assay for profiling drug discovery candidates. *Journal of biomolecular screening* **2003**, *8* (4), 453-62.
68. Wang, Q.; Rager, J. D.; Weinstein, K.; Kardos, P. S.; Dobson, G. L.; Li, J.; Hidalgo, I. J., Evaluation of the MDR-MDCK cell line as a permeability screen for the blood-brain barrier. *International journal of pharmaceutics* **2005**, *288* (2), 349-59.
69. Bendayan, R.; Lee, G.; Bendayan, M., Functional expression and localization of P-glycoprotein at the blood brain barrier. *Microscopy Research and Technique* **2002**, *57* (5), 365-380.
70. Stuhr-Hansen, N.; Sørensen, J. K.; Moth-Poulsen, K.; Christensen, J. B.; Bjørnholm, T.; Nielsen, M. B., Synthetic protocols and building blocks for molecular electronics. *Tetrahedron* **2005**, *61* (52), 12288-12295.
71. Wang, X.; Xu, Y.; Mo, F.; Ji, G.; Qiu, D.; Feng, J.; Ye, Y.; Zhang, S.; Zhang, Y.; Wang, J., Silver-mediated trifluoromethylation of aryldiazonium salts: conversion of amino group into trifluoromethyl group. *Journal of the American Chemical Society* **2013**, *135* (28), 10330-3.